A 13 MHz SPIN ECHO NUCLEAR MAGNETIC RESONANCE SPECTROMETER

A Thesis Submitted
In Partial Fulfilment of the Requirements
for the Degree of
MASTER OF TECHNOLOGY

BY
RANJIT SINGH

to the

DEPARTMENT OF ELECTRICAL ENGINEERING
INDIAN INSTITUTE OF TECHNOLOGY KANPUR
SEPTEMBER 1971

Dedicated to

all those persistent men and women who spent many a mealless days and sleepless nights in pursuit of their scientific research.

CERTIFICATE

Certified that this work on "A 13 MHz SPIN ECHO NUCLEAR MAGNETIC RESONANCE SPECTROMETER" by Mr. Ranjit Singh has been carried out under my supervision and that this has not been submitted elsewhere for a degree.

Dr. R. Sharan
Assistant Professor
Department of Electrical Engineering
Indian Institute of Technology
KANPUR

ACKNOWLEDGEMENTS

The author expresses his deep sense of gratitude and appreciation to Dr. T.R. Viswanathan and Dr. R. Sharan for their meticulous supervision and constant encouragement during the various phases of this work. Conversations and associations with Dr. C.V. Seshadri and Mr. S.C. Raisinghani were of immense help in performing the work described here. The author is deeply indebted to Prof. B.D.N. Rao and Miss Anup Kitchlew for their continued interest and stimulating discussions. The author was profoundly benefitted by revealing criticisms from Prof. S. Venkateswaran and Dr. R.N. Biswas.

The valuable assistance extended by Mr.S.N. Sikdar, Mr. V.N. Shukla, Mr.A.K. Dhingra and Mr. Deepak Kapoor is gratefully acknowledged. Thanks are due to Mr. Yogendra Chandra for doing a neat job of typing this thesis.

Author is grateful to Burmah Shell Oil Corporation of India (Pvt. Ltd.) for the financial support during the tenure of the work.

SYNOPSIS

Ranjit Singh, M.Tech.
Department of Electrical Engineering
Indian Institute of Technology, Kanpur
September, 1971

A 13 MHz Spin Echo Nuclear Magnetic Resonance Spectrometer

Design and fabrication of "A 13 MHz Spin-Echo NMR Spectrometer" using incoherent detection technique is described. The 'pulse programmer' gives $\pi/2$ and π pulses with independent control of the widths, repetition period and delay. The pulsed RF source consists of a new solid-state, crystal controlled 'gated - oscillator' configuration yielding thereby an infinite 'Carrier Suppression Ratio' at the output of the 'transmitter'.

Measures have been taken to circumvent the difficulties inherent in the 'single-coil technique' and for achievement of acceptable output signal to noise ratio.

A new circuit for the solid state power amplifier using a recent semiconductor device, the "overlay-transistor" is proposed.

The instrument has been made self-contained by incorporating the necessary power supplies.

———— o ————

CONTENTS

	ACKNOWLEDGEMENTS	-(iv)
	SYNOPSIS	(v)
I	INTRODUCTION	1
II	SYSTEM STUDY	6
	2.1 Design Specifications	6
	2.2 Block Diagram	7
III	SAMPLE COIL DESIGN CONSIDERATIONS	10
	3.1 Introduction	10
	3.2 Transmitter Coil Requirements	10
	3.2.1. Geometry	10
	3.2.2. Q Requirements	11
	3.3 Receiver Coil Requirements	13
	3.3.1. Noise Considerations	13
IV	DESIGN OF TRANSMITTER	16
	4.1 Pulse Programmer	16
	4.2 Gated Oscillator	20
	4.3 Booster & Buffer	27
	4.4 DriverStage	29
	4.5 Power Amplifier	33
	4.5.1. Discussion	33
	4.5.2. Calculations	35
	4.5.3. Circuit Description	37
	4.5.4. Tank Circuit Design	39
	4.5.5. Stabilization	41

	4.5.6. Grid Bias Scheme	41
	4.6 Proposed Solid State Power Amplifier	42
V	DESIGN OF RECEIVER	47
	5.1 Tube Receiver	47
	5.1.1. Input Network	47
	5.1.2. RF Amplifier	49
	5.1.3. Detector	51
	5.1.4. Audio Amplifier	51
	5.1.5. Display	52
	5.2 Solid State Receiver Design	53
	5.2.1. Input Network	53
	5.2.2. Preamplifier	56
	5.2.2.1. Neutralization	56
	5.2.2.2. Tank Circuit Design	57
	5.2.3. Wideband Amplifier	58
	5.2.3.1. Buffer	58
	5.2.3.2. CA 3023 Unit	61
	5.2.4. Detector	61
	5.2.5. Audio Amplifier	61
VI	DESIGN OF POWER SUPPLIES	62
	6.1 General Discussion	63
	6.1.1. +6 VDC & - 6 VDC supplies	63
	6.1.2. + 230 VDC & + 180 VDC Supplies	63
	6.1.3. Current Supply (1.3 ADC)	63
	6.1.4. Filament Supply (6.3 VAC)	68
	6.1.5. Grid Supply (-20 VDC)	68

	6.1.6. Driver Stage Supply (+15 & +45 VDC)	68
	6.2 Detailed Design of + 180 VDC Supply	68
VII	EXPERIMENTAL	76
	7.1 Procedure	76
	7.2 Simulation	78
	7.3 RF Monitoring	78
VIII	CONCLUSIONS	80
	BIBLIOGRAPHY	82
	GENERAL REFRENCES	84

APPENDICES

A	RELATION BETWEEN PEAK INDUCED OSCILLATING MAGNETIC FIELD & PEAK TO PEAK RF VOLTAGE	86
B	USEFUL CHARACTERISTICS	
	B.1 5763 Tube	88
	B.2 6AK5 Tube	89
	B.3 TIS 59 FET	90
	B.4 CA3023 IC	91
C	TRANSFORMER DESIGN	92
D	SHORT NOTES	
	D.1 Pulsed Response of Tuned Circuits	94
	D.2 On The Use of Crystal In A Pulsed Oscillator	96
	D.3 Oscillator Build Up Analysis	98
E	SOME CONCLUSIONS ON RF CHOKE DESIGN	100
F	FET PREAMPLIFIER ANALYSIS	103
G	HARDWARE CONSIDERATIONS	
	G.1 Components Used At High Frequencies	105
	G.2 Chasis Layout & Other Fabrication Aspects	109
	G.3 Complete Circuit Diagram	111

LIST OF FIGURES

1.1	Explanation of various terms	2
1.2	Schematic diagram of NMR Apparatus	2
2.1	Detailed Block diagram of the instrument	8
4.1	Synthesis of $\pi/2 - \pi$ sequence	17
4.2	Block diagram of Pulse generator	17
4.3	Clock and Delay	18
4.4	$\pi/2$ pulse and π pulse	19
4.5	Gated astable multivibrator	22
4.6	Development of Gated Oscillator configuration	22
4.7	Gated Oscillator	24
4.8	Booster and Driver stages	28
4.9	Base voltage waveform for Class C transistor stage	31
4.10	Output waveform of Class C stage	31
4.11	Efficiency vs. Conduction angle	31
4.12	Power Amplifier	38
4.13 (a)	Overlay Transistor Geometry	43
4.13 (b)	Family of RCA overlay transistors	43
4.14	Proposed Design Of Solid State Power Amplifier	46
5.1	Tube-Receiver	48
5.2	Block diagram of the semiconductor receiver	54
5.3	Basic coupling network	54
5.4	Neutralization Scheme for the FET	54
5.5	FET Preamplifier	59
5.6	Wideband Amplifier	60
5.7	Detector & Audio Amplifier	60
6.1	+ 6 VDC power supply	64

6.3	+ 230 VDC supply	66
6.4	1.3 Amp DC Current Supply	67
6.5	Driver stage power supply	69
6.6	Regulator Circuit	71
6.7	Heat Sink Design	71
6.8	+ 1 80 VDC power supply	73
	Photographs	79
A.1	Coil gemometry	86
A.2	Series-parallel resonant circuits equivalence	86
B.1	Plate characteristics+Pin Connections (5763)	88
B.2	Pin Connections (6AK5)	89
B.3	Plate characteristics (6AK5)	89
B.4	Transfer characteristics (6AK5)	89
B.5	Outline TIS 59	90
B.6	Voltage gain set up of CA 3023	91
B.7	Frequency Response of CA3023	91
B.8	CA3023 outline	91
C.1	Window area and stack depth of a transformer core	93
D.1	Parallel tuned circuit excited by a pulse	94
D.2	Crystal Equivalent circuit and its impedance function	96
D.3	Model for oscillator build up analysis	98
D.4	Oscillator Build up phenomena	99
E.1	π winding	102
F.1	FET neutralization scheme	103
F.2	Equivalent Circuit for F.1	103
G.1	Front panel design	110

LIST OF TABLES

1.1	Useful Data At 13 MHz	5
4.1	Class C Amplifier Design: K_1-K_5 vs θ_p	33
4.2	Class C Amplifier Design: K_6 vs E_{c1}/E_{g1}	34
4.3	Selected List of Overlay Transistors	44
5.1	Bias Conditions For Receiver Tubes	51
6.1	Thermal Resistance of Several Transistor-Mounting Materials	70
6.2	+ 180 VDC Supply Data	75
7.1	Control of T_D, T_R & t_w	77
C.1	Copper wire Gauge Data	89
G.1	Coaxial Cable Data	108

CHAPTER I

INTRODUCTION

Nuclear magnetic resonance techniques have become the indispensable tools of research in the field of modern physics and chemistry. The investigations about the numerous molecular and nuclear phenomena have become possible by means of NMR spectroscopy. Since 1946 when Bloch observed the phenomena and gave a sound theoretical basis of this, about 2000 NMR spectrometers have sprung into use in the various research laboratories throughout the world. The incessant stream of the voluminous data on NMR speaks itself of the importance of this technique to the research worker in the pure sciences.

Basically, an NMR spectrometer (Fig.1.1) consists of a source of rf power applied to a coil, containing the sample to be investigated, mounted in a homogeneous magnetic field. An amplifier-detector system picks up the small nuclear signal which is produced when the rf frequency and magnetic field satisfy the resonance condition. From the nature of the observed signal, and on controlling the parameters of the spectrometer to emphasize one effect in relation to others, one can measure the pertinent property of interest.

NMR apparatus can be broadly classified into two types: "Steady State NMR" and "Pulsed Nuclear Resonance Apparatus".

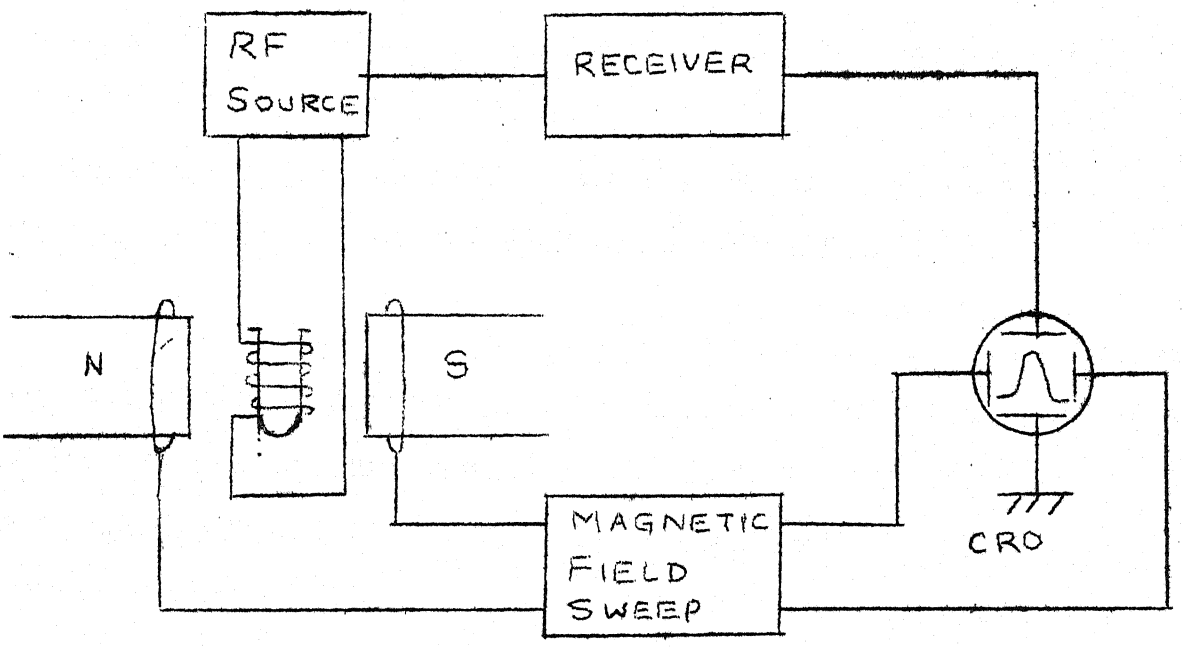

FIG. 1.1. SCHEMATIC DIAGRAM FOR NMR EXPERIMENT.

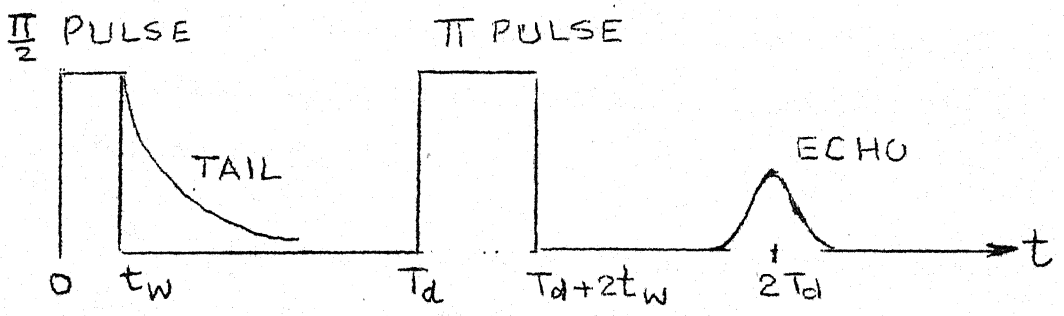

FIG. 1.2. EXPLANATION OF VARIOUS TERMS.

In the former, the rf is continuously applied to the sample whereas in latter the sample is subjected to intense bursts of rf lasting for short intervals of time and the resultant nuclear signal is observed after the pulses are removed. This method is called the SPIN-ECHO TECHNIQUE.

Fig.1.2 depicts the pulse sequence used and the nuclear induction signal induced in the coil. The two rf pulses of widths t_w and $2t_w$ are termed as $\pi/2$ and $\pi/$ pulses. The exponentially decaying signal is called as TAIL and the Gaussian shaped pulse is the SPIN-ECHO. The delay between the two pulses is denoted by T_d and appereance of the ECHO at $2T_d$, as shown, is characteristic of the Spin-Echo phenomena. The amplitude of the NMR signal is a fraction of a millivolt for proton resonance in water. The measurement of the NMR signals using Spin Echo technique has made possible the determination of the parameters like nuclear spin relaxation times, self-diffusion coefficients in fluids, chemical shift, indirect Spin-Spin coupling, etc.

In Fig.1.2, any leakage of rf during "off" periods is detrimental to the nuclear induction signal. In the past, major efforts have been to synthesize an rf gate with as high a carrier suppression ratio (CSR) as possible. For example, Blume's circuit (CSR = 10^9) employs an oscillator housed in a spun copper can where a planar grid tube couples the rf to power amplifier. The main purpose of the present investigation was to study the feasibility of a gated oscillator, thereby,

achieving an infinite CSR.

A usual crystal oscillator circuit will turn on (and off) very slowly because of extreme high Q of the circuit. However, if the relaxation mode with built-in high regenerativ feedback is employed, the oscillator can be turned on and off within times which are governed by rise and fall times of the incoming pulses and switching response of the active devic used. This design eliminates much of the trouble encountered in conventional spin echo spectrometers together with the economy of hardware, without compromising the flexibility of the instrument in terms of various feasible pulse sequences. Above all, the cost is cut down drastically because for most part of the design, the instrument becomes amenable to fabrication using indigenous components.

The radio frequency pulses are amplified to drive the power amplifier. The nonavailability of "overlay-transistors" has prevented the complete solid state design of the transmitte which in the present work employs power tubes in the last stage.

The receiver has the following two important features: first, a new type of input coupling network has been conceived in view of the compromises incurred upon by using a single coil technique. Second the audioamplifier design incorporates the measures for getting acceptable output signal to noise ratio. In the solid state version of the receiver the R.F. amplifier uses low noise features of the Field Effect Transistors at the input, followed by a wideband amplifier whic

employs an integrated circuit simplifying the design considerably.

It should be noted that the symbol H used throughout the literature for magnetic field (units gauss) has been replaced here by B. The symbol H is reserved for magneto-motive force in electrical engineering and hence has been avoided here to prevent any confusion. Also, the MKS units used here introduce the parameter μ_o - the permeability of vacuum into some of the design equations.

TABLE 1.1

USEFUL DATA AT 13 MHz

1. Magnetic field for resonance :

   $B_o = 3.06$ K gauss $= 0.306$ Wb/m^2

2. Radian frequency:

   $w_o = 2\pi f_o = 8.16 \times 10^7$ rad/sec.

   $\therefore \quad w_o^2 = 6.65 \times 10^{15}$ rad^2/sec^2

3. Tank Circuit:

   (i) $L(\mu H) \times C(pf) \doteq 150$

   (ii) $Q = R_p(K\Omega) \times C_p(pf)/12.25$

4. Impedance of

   (i) 1 μH coil $\doteq$ 80 Ω

   (ii) 0.1 μF capacitor $\doteq$ 0.1 Ω

   (iii) 100 pf capacitor $\doteq$ 100 Ω

———o———

CHAPTER II

SYSTEM STUDY

The pertinent design parameters of the Spin Echo Spectrometer to be fabricated are listed below. The symbols used are same as in fig.1.2.

2.1 DESIGN SPECIFICATIONS :

(a) Transmitter:

(i) Pulse sequence to be synthesized:

$\pi/2$, T_d, π ; $\pi/2$, T_d, π ; .....

where T_d is the delay.

(ii) Pulse width range:

$\pi/2$ pulse: $5 \leq t_w \leq 50$ μ sec.

π pulse: $10 \leq 2t_w \leq 100$ μ sec.

The widths are to be independently controllable.

(iii) Delay, T_d:

100 μ sec $\leq T_d \leq$ 200 m sec.

(iv) Pulse-Sequence Repetition Period, T_R:

100 m sec $\leq T_R \leq$ 10 sec.

(v) Rise time and fall time of rf pulses; t_r, t_f:

$t_r \leq 1/10\ (t_w)_{min}$

$t_f \leq 1/10\ (t_w)_{min}$

(vi) R.F. across the sample coil:

Peak to peak excursion $\doteq$ 250 volts.

(vii) Carrier Suppression Ratio (CSR):

CSR better than 10^{-8}.

(viii) Frequency Stability:

As large as possible.

(b) Receiver:

(i) Voltage gain $\doteq$ 40 dB.

(ii) Bandwidth:

Sufficient for distortionless reproduction of spin echo signal.

(iii) Signal to Noise Ratio:

Noise level in final displayed waveform not to exceed one tenth of the spin echo signal.

(iv) Recovery time:

As small as possible.

(v) Display:

Cathode Ray Oscilloscope.

(c) Sample Coil:

(i) Coil configuration:

Single coil technique.

(ii) Gradient coils to be installed. Regulated direct current upto 1.2 Amp. is required.

2.2 DETAILED BLOCK DIAGRAM

The basic block diagram of the NMR instrument is presented in greater detail in fig.2.1 to delineate the relationship between the various parts of the apparatus. The output waveforms of the three major sub-blocks, viz, the pulse programmer, the transmitter and the receiver are also sketched for comparison. The letter x denotes the buffer amplifiers which have been omitted for simplicity.

The pulse programmer synthesizes the required $\pi/2 - \pi$ pulses which turn "on" and "off" the gated oscillator. The

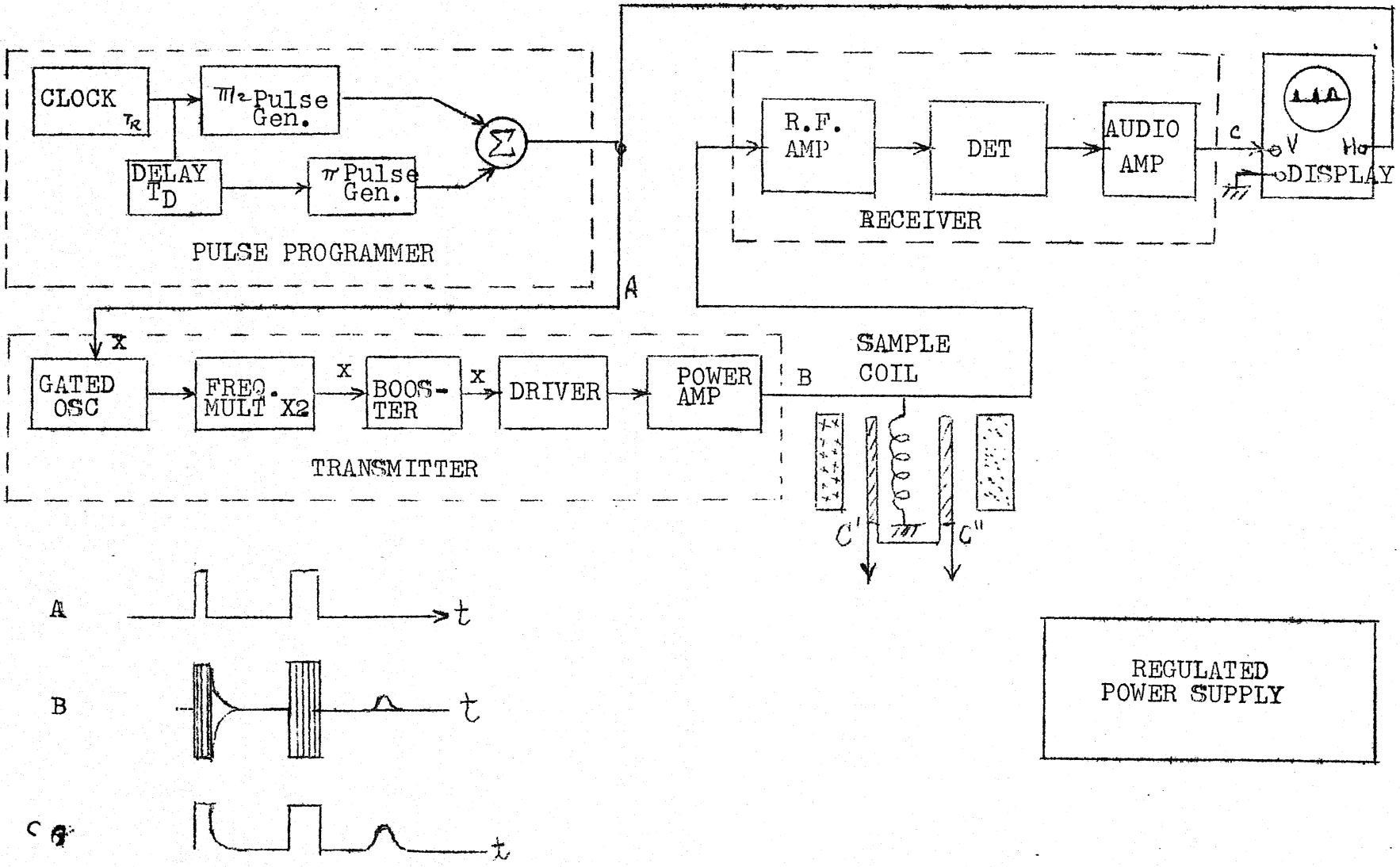

FIG. 2.1 DETAILED BLOCK DIAGRAM

gated oscillator produces rf pulses at 6.5 MHz. which are converted to 13 MHz yielding an output of 1.5 V peak to peak. The booster amplifies the rf pulses to feed the driver stage which yields enough voltage for the class C operation of the power amplifier.

The amplified rf pulses are applied to the sample coil housed inside the magnet. The gradient coils C', C'' carry regulated direct current. The nuclear induction signal corresponding to the Larmour frequency of precession is picked up by the amplifier-detector system and further processed by Audio-Amplifier for final display on the C.R.O.

The block designated 'Regulated Power Supply' comprises of the following power supplies: + 6 VDC, + 15 VDC, + 180 VDC, + 230 VDC, - 6 VDC, - 20 VDC, the current supply (1.3ADC) and 6.3 VAC filament supply.

The following chapters consider in detail the design of the individual sub-blocks. The special steps taken to meet the stipulated requirements have been emphasized with particular reference to the various compromises made. The level of performance has been mentioned alongwith the brief description of the circuit diagram. The fabrication aspects which are as important as the actual design have been described in Appendices together with some relevant derivations. The constant feedback between the theoretical design and the experimental performance would be evident throughout.

CHAPTER III

SAMPLE COIL DESIGN CONSIDERATIONS

3.1 INTRODUCTION:

Use of single sample coil imposes severe compromises to be made in the design of spin echo apparatus. This is because different electrical requirements are needed for the same coil to serve as a "transmitter-coil" as well as the receiver coil. This difference basically arises due to entirely different characteristics of the carrier signal during "on" and "off" periods e.g. during "on" periods R.F. amplitude is about 250 volts peak to peak with preferably as low rise and fall times as possible whereas during "off" periods the nuclear induction signal is a fraction of millivolt excursion modulated by a slowly varying component. The details are discussed here including the noise considerations as this aspect forms one of the most important design parameters.

3.2 TRANSMITTER COIL REQUIREMENTS:

3.2.1. Geometry:

The geometry selected is a single layer solenoid. The model chosen to represent the transmitter coil is a medium Q parallel RLC circuit resonating at the nuclear resonance frequency f_o. It is shown in the Appendix A that the peak amplitude of the induced oscillating rf magnetic field, $2B_1$ (gauss), is related to the peak to peak rf voltage

excursion, V_{pp} by the approximate relation:

$$2B_1 \approx \frac{2\,\mu_o\,V_{pp}}{14.2} \cdot \sqrt{y} \cdot \sqrt{\frac{C_p\ (pf)}{V\ (cc)}} \qquad \ldots(3.1)$$

where

μ_o = permeability of vacuum = $4\pi \times 10^{-7}$ h/m

y = a dimensionless parameter depending on coil geometry.

C_p = tank capacitance (pf)

V = volume of coil (cc)

Thus to maximize B_1 one should aim at maximizing V_{pp}, C_p and y, and minimizing V. It is to be noted that the effect of variation of V_{pp} is relatively more dominant, since all other quantities have square root dependence.

The dependence of coil design on B_1 occurs through y and V from Appendix A as :

$$\frac{y}{V} \propto \frac{(9+10\,c)}{(4+c^2)r^3} \qquad \ldots(3.2)$$

where r is the radius and c is the ratio of the length to radius of the coil. It can be readily shown that for fixed value of radius this ratio (3.2) has maxima at

$$c \doteq 1.3 \qquad \ldots(3.3)$$

3.2.2. Q Requirements:

Loaded Q of a parallel RLC circuit is given as

$$Q = w_o R_p C_p \qquad \ldots(3.4)$$

And the pulsed power P is related to peak to peak rf voltage by

$$P = V_{pp}^{\ 2} / 8R_p \qquad \ldots(3.5)$$

Using (3.4) and (3.5) in (3.1) one gets

$$B_1 \propto (PQ/f_oV)^{\frac{1}{2}} \qquad \ldots(3.6)$$

Thus in order to maximize B_1, Q should also be maximized. However, increasing Q reduces the bandwidth of the amplifier which in turn leads to the following three disadvantages:

(i) The 10% - 90% rise time of a tuned amplifier is given by the empirical relation[1]

$$t_r \doteq \frac{0.8}{B.W.} = \frac{0.8\ Q}{f_o} \doteq 5R_pC_p \qquad \ldots(3.7)$$

where B.W. = 3dB bandwidth.

Consequently, reduction in bandwidth results in increase of rise time (as well as fall time) of the rf pulses which is undesirable for spin echo technique.

(ii) The minimum pulse width[2] that can be supported across a tuned circuit is of the order of 1/B.W. . This imposes a severe restriction on the pulsed rf parameters.

(iii) Reduction in bandwidth increases the gain (and hence the loop gain) which makes the amplifier amenable to instability.

An approximate value of Q can be obtained from Eq(3.7), for, say $t_r < 0.5\ \mu$ sec, as

$$Q < f_o t_r/0.8 \doteq 8 \qquad \ldots(3.8)$$

From above discussion it is concluded that:

(a) Transmitter coil should be fabricated with smallest possible diameter, with length to radius ratio approximately equal to 1.3.

(b) Loaded Q of the transmitter coil should be less than 8.

3.3 RECEIVER COIL REQUIREMENTS:

3.3.1. Noise Considerations:

The requirements of the receiver coil are different from those of the transmitting coil. A receiver coil is designed to present the free induction signal with the highest possible signal to noise ratio. The model assumed is a parallel RLC circuit resonant at nuclear resonance frequency with quality factor Q. The signal to noise ratio has been calculated to be[3]

$$\frac{E_S}{E_N} = \frac{\alpha N A Q \phi}{(4k B(2\pi f_o Q D A^{\frac{1}{2}} N^2 T_C + R_{eq} T_{eq}))^{\frac{1}{2}}} \qquad \ldots(3.10)$$

where

α = parameter representing nuclear spin properties

N = number of turns of the receiver coil

A = cross sectional area of the coil

Q = quality factor of the coil

ϕ = filling factor of the coil

k = Boltzmann constant

B = 3dB bandwidth of the circuit

f_o = nuclear resonance frequency

D = a slowly varying function of the coil shape

T_C = Temperature of coil, °K

R_{eq} = equivalent short noise resistance of the receiver referred to input

T_{eq} = noise temperature corresponding to R_{eq}, °K

Thus the signal to noise ratio will be increased

as T_C, the temperature of the coil is reduced. At room temperature, the equation (3.10) simplifies to

$$\frac{E_S}{E_N} \doteq \alpha \phi (AQ/8\pi k f_o DB T_C)^{\frac{1}{2}} \qquad \ldots (3.11)$$

because $R_{eq} T_{eq} \ll R_p T_C$.

Consequently SNR is maximized by:

(i) high filling factor, which implies that the coil fits closely on the sample and is shorter than the sample.

(ii) having A large suggests a large sample.

(iii) selecting large Q.

(iv) small bandwidth B.

The parameter α is not amenable to external control once the sample is fixed but for various samples, α will differ e.g. for glycerine α is larger than that for water.

Now, the coil parameters Q, N, A, ϕ, D are complicated functions of each other[4] and at best one can give the qualitative statements. In practice, to maximize E_S/E_N one starts with the largest sample possible and winds as close to the sample as possible, the highest Q coil, that can be made to resonate with the receiver.

In summary, the optimum transmitter coil design calls for low Q and small volume of the sample whereas the optimum receiver coil design calls for high Q and large volume of the sample. In the former case one is trying to achieve as small rise and fall times as possible whereas in latter, one

is striving to maximize signal to noise ratio. It is obvious that performing these two functions with a single coil involves the ultimate compromise between rise time and signal to noise ratio.

It is pointed out here for design considerations that the signal to noise ratio also depends on the noise contributed by the transmitter tubes. This important fact is particularly emphasized again in the design of the power amplifier where quiescent current during "off" periods is kept small to reduce the shot noise as far as possible. It is evident that class A amplifier configuration is unsuitable for this application.

———— o ————

CHAPTER IV

DESIGN OF TRANSMITTER

The transmitter consists of Pulse-programmer, Gated Oscillator, Booster, Driver and Power amplifier. The detailed design of these stages is described in this section. In the end, the design of the solid state power amplifier is proposed.

4.1 PULSE PROGRAMMER

The desired waveform which actuates the "Gated Oscillator" is depicted in fig.4.1. The t_w and $2t_w$ are the widths of $\pi/2$ and π pulses respectively with T_D the delay between them. This sequence is repeated at intervals of T_R. All the four parameters are independently controllable by the respective knobs. The amplitude V_p is as fixed quantity. The rise and fall times are not of much concern here.

The synthesis procedure[5] for this rather unfamiliar waveform is explained in fig.4.1. The clock (fig.4.2) generates a square waveform $v_1(t)$ with repetition rate equal to T_R. This is differentiated and clipped to drive the one shot I, yielding the $\pi/2$ pulse ($v'(t)$). Simultaneously, the square wave initiates a "delay" unit which yields a rectangular train $v_3(t)$. This is differentiated and clipped & fed to the one shot II giving the π pulse ($v''(t)$).

The circuit realization (fig.4.3) of the block diagram (fig.4.2) is str ight forward. Q_1 and Q_2 constitute an

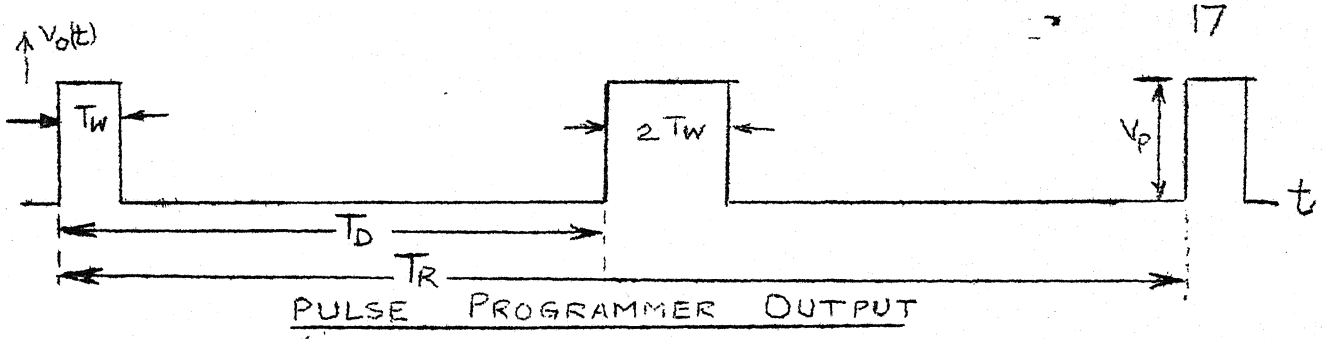

PULSE PROGRAMMER OUTPUT

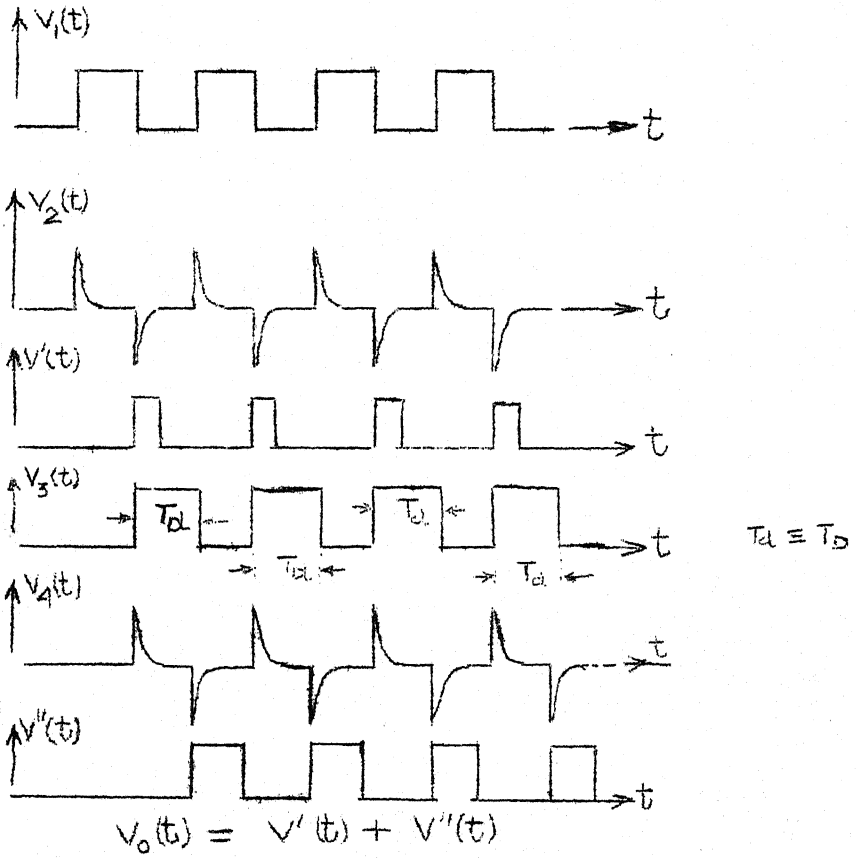

FIG 4-1 SYNTHESIS PROCEDURE FOR $V_o(t)$

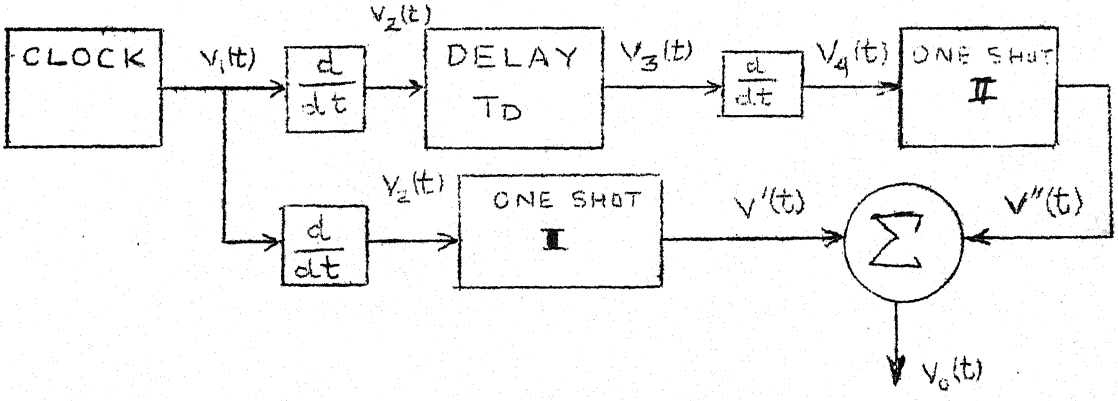

FIG 4.2: BLOCK DIAGRAM OF PULSE PROGRAMMER

CLOCK AND DELAY

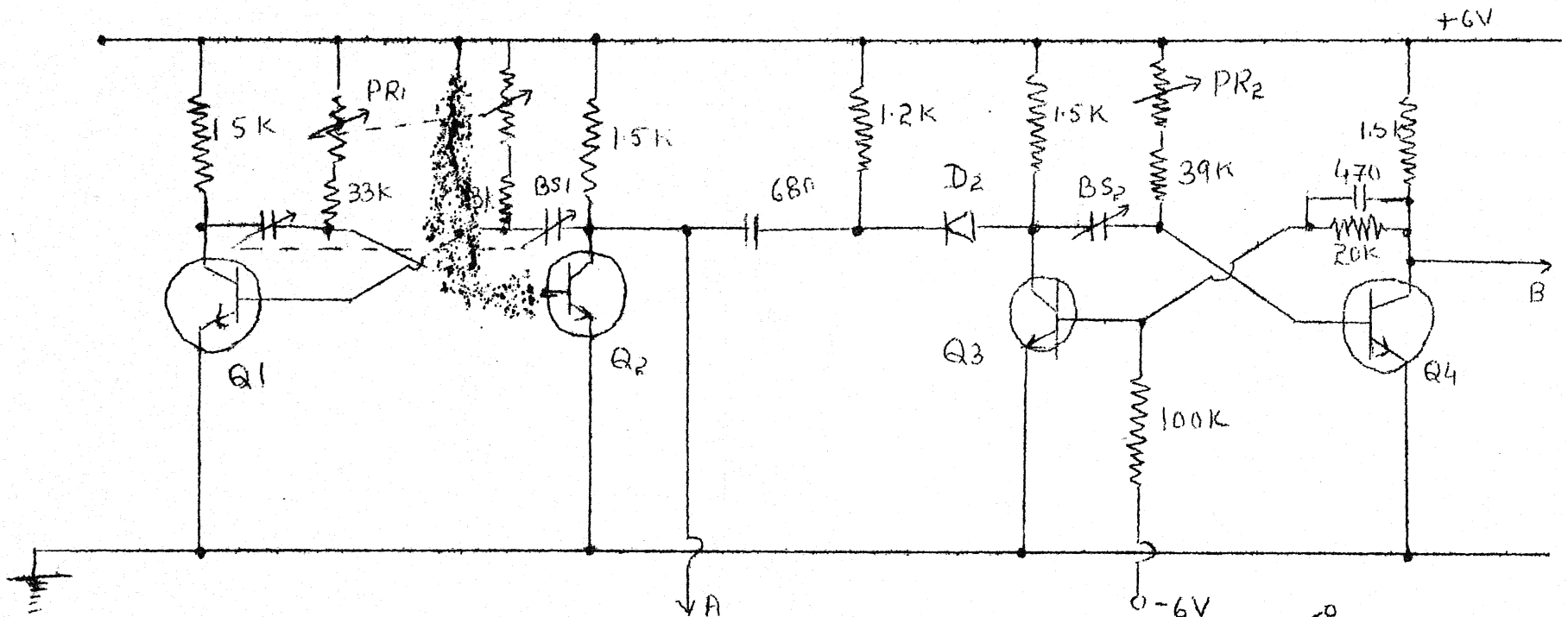

Q_1, Q_2, Q_3, Q_4 : CIL523

D_2 :

FIG 4·3

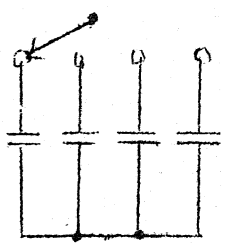

DETAIL OF BS1

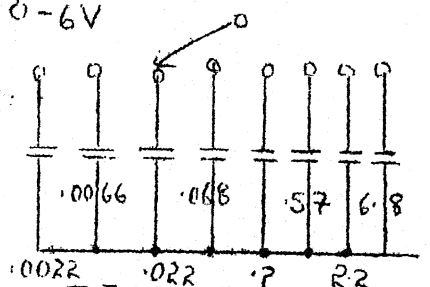

DETAIL OF BS2

π/2 PULSE AND π PULSE

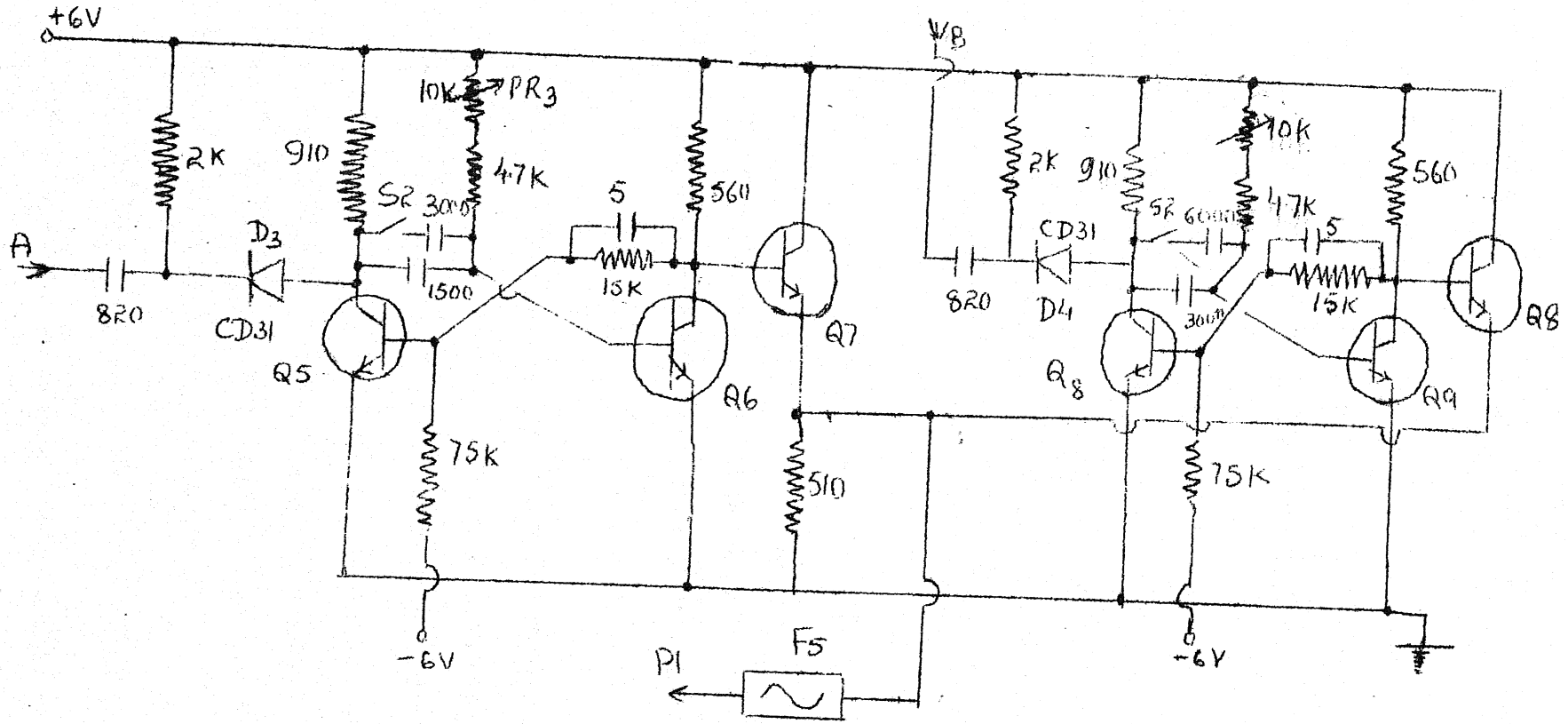

Q5, Q6, Q7, Q8, Q9, Q10 : CIL 732

F5 : 100 ma

FIG. 4.4

astable multivibrator using high gain silicon transistors CIL 523 (h_{FE} = 250) for stability. The ganged potentiometer PR1 simultaneously varies conduction times of both the transistors. The very wide variation in T_R necessitates variation of the capacitor also. This is accomplished by bandswitch BS 1.

The two pulse generators and the delay unit are synthesized by means of monostable multivibrators. The required timings are properly achieved by hand-picking the components. This means that several units were taken and measured to give the matched values, e.g. the timing capacitors 1500 pf and 3000 pf must be exactly in the ratio 1:2. The switch S_2 is SPDT type and determines the two "windows" in the pulse widths, viz. when S_2 is open, the timing capacitors in the pulse generators are 1500 and 3000 pf whereas, when S_2 is closed, the respective values are 3000 and 6000 pf. This gives the two windows in π pulse as: 10 - 50 μ sec and 50 - 100 μ sec.

The diodes D_2, D_3, D_4 are silicon diodes CD31 whose PIV is not of concern here. The other transistors Q 5 through Q 10 are CIL 732. The "adding" is simply accomplished by lowering down the two generator impedance levels by means of emitter follower and taking output across the common 510 Ω resistor. The fuse F_5 (100 mA) is connected at the output of $v_o(t)$. The output amplitude is 4.5 volts.

4.2 GATED OSCILLATOR

Design of gated oscillator is heart of the whole investigation. The final circuit though simple, was evolved after the

extensive experimentation with conventional oscillator circuits did not yield the desired results. The fundamental problem is as follows: the oscillator must be capable of starting and quitting oscillations in times $\simeq$ 0.1 x (Minimum pulse width) i.e. about 0.5 μ sec. The requirements of high frequency-stability dictate the choice of crystal as the basic element in the tank circuit. Now, it can be proved easily (App. D.1) that number of cycles required for an oscillating circuit to reduce the RF amplitude to P% of the steady state value is given by:

$$N' = \frac{P\ Q}{100} \qquad \ldots (4.1)$$

Since Q for a crystal is of the order of 10^4, it will require exhorbitantly large number of cycles to elapse for a crystal oscillator used in conventional circuits like Hartley, Colpitts, Pierce etc. This fact has been experimentally verified with several oscillator configurations.

These difficulties arise because the loop gain of the basic amplifier varies slowly to reach a value more (or less) than unity. Conceptually, then an oscillator configuration with large amount of feedback such as is possible in switching mode may be the answer to this problem. Hence, the basic astable multivibrator was investigated in this respect.

Fig.4.5 shows the basic astable multivibrator with the following modifications:-

(i) two crystals are inserted in place of the timing

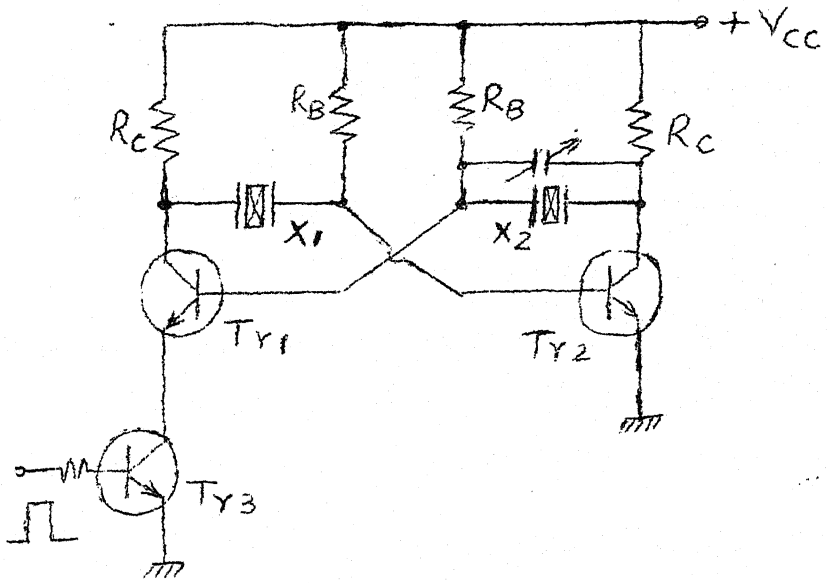

FIG 4.5: GATED ASTABLE MULTIVIBRATOR

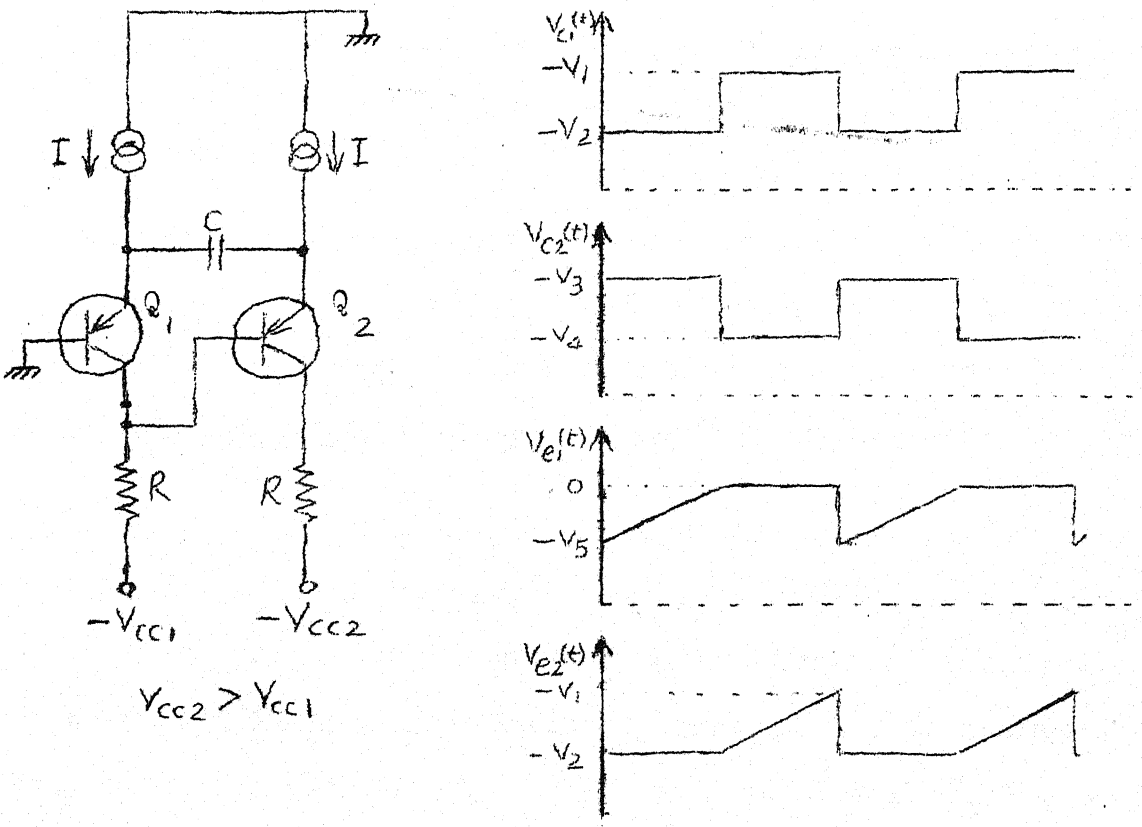

FIG 4.6: DEVELOPMENT OF GATED OSCILLATOR CONFIGURATION

capacitors. A variable capacitor is connected across X_2.

(ii) a means for starting and stopping the A.M.V. is incorporated in emitter leg of Tr_1 by the third transistor. It was proved experimentally that such an oscillator can be gated in times that are not governed by Q of the crystal but by the charging and discharging mechanisms inherent in the transistors. Thus one has to choose fast transistors to achieve small rise & fall times. This is a very significant result as it made possible further refinement of this circuit to that shown in fig.4.7.

Working of this circuit will be explained by the model in fig.4.6. The emitters of Q_1 and Q_2 are supplied by identical constant current sources. Base of Q_1 is grounded and its collector is directly returned to base of Q_2. The emitters are tied up through the capacitor C. The collectors contain equal loads but are returned to different power supplies - V_{CC_1} and - V_{CC_2}. Alternatively, as will be evident soon, the collector supply could be same with unequal collector resistances. However, this circuit will not work if both $R_{C_1} = R_{C_2}$ and $V_{CC_1} = V_{CC_2}$.

By virtue of above configuration any change in collector voltage of Q_1 is transmitted immediately to base of Q_2. (This is in contrast to conventional multivibrator circuits). Due to this full positive feedback, none of the transistors can remain in active region. Little thought will reveal that it is also impossible for both transistors to be cut off or both to be in saturation. This leaves the only two remaining possibilities:

FIG 4·7 GATED OSCILLATOR

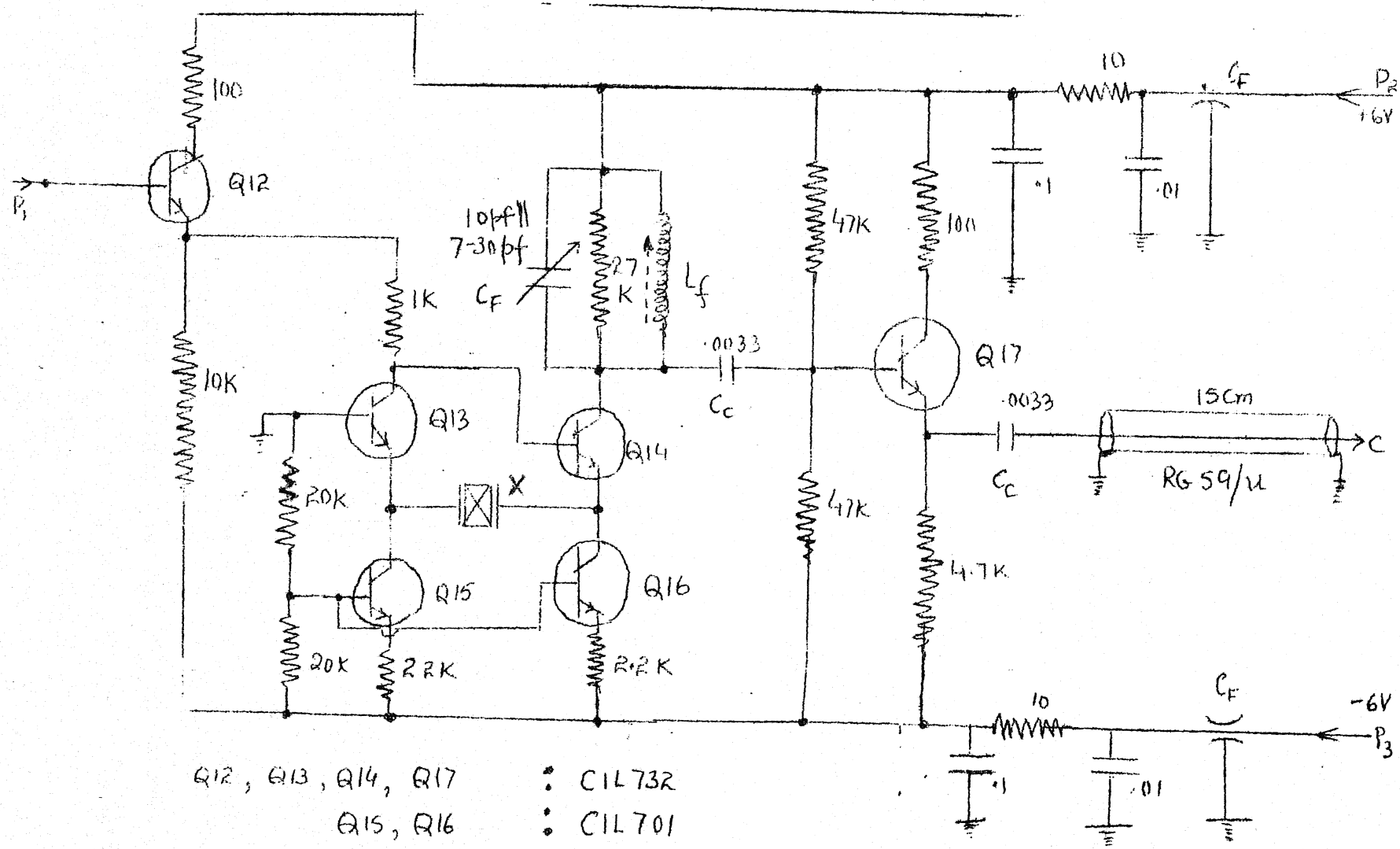

Q12, Q13, Q14, Q17 : CIL732

Q15, Q16 : CIL701

C_F : 2300 pf

X : 6497·9 KHz. Crystal

COIL DATA

	VALUE	Q	REMARKS
L_f :	28-5 μH	60	MILLER #4504

(i) Q_1 off Q_2 on

(ii) Q_1 on Q_2 off.

Now it will be proved that these states will follow one another i.e. the circuit performs the function of an astable multivibrator. Assume for the moment that Q_1 is initially off and Q_2 is on. Then $I_{e_1} = 0$ and the current flows through the capacitor, C from left to right. Therefore, $I_{e_2} = 2\ I$. The constant current I charges the capacitor linearly, causing V_{e_1} to rise linearly as shown in fig.4.6. The collector voltages are held constant during this interval at values:

$$v_{C_1} = - V_{CC_1} = - V_2 \qquad \ldots(4.2)$$

and

$$v_{C_2} = - V_{CC_2} + 2\ I\ R = - V_3 \qquad \ldots(4.3)$$

As soon as $V_{e_1} > 0$ (neglect diode drops for simplicity) the transistors switch the states through the regenerative feedback and collector voltages become

$$v_{C_1} = - V_{CC_1} + 2\ I\ R = - V_1 \qquad \ldots(4.4)$$

and

$$v_{C_2} = - V_{CC_2} = - V_4 \qquad \ldots(4.5)$$

Now, the current has reversed its direction in the capacitor and it charges linearly causing V_{e_2} to increase at the same rate. As soon as V_{e_2} becomes equal to $-V_1$ the transistor Q_2 no longer remains off. Thus the system is in the same state as before and the circuit is self perpetuating. Hence, the collector waveforms are square waves. The frequency of this waveform is determined as follows:

The capacitor charging equation is:

$$1/C \int_0^{T/2} I \, dt = V_1 - V_2 \qquad \ldots(4.6)$$

But from (4.2) and (4.4) one gets

$$V_1 - V_2 = 2 \, I \, R \qquad \ldots(4.7)$$

Therefore

$$T/2 = 2 \, R \, C$$

or

$$f = 1/4 \, R \, C \qquad \ldots(4.8)$$

Note that actual value of current generators is of no significance. In fig.4.7, the crystal decides the period of switching of the multivibrator. Crystal frequency is 6.5 MHz. The 2nd harmonic is extracted by means of parallel tuned circuit consisting of:

(i) Inductance L_f, miller coil 4504 with value adjustable from 2.8 to 5 μ H. The unloaded Q at 7.9 MHz is 60.

(ii) Trimmer, C_f : 7 - 30 pf.

(iii) A resistor whose value decides the loaded Q and hence the bandwidth. Since the rise and fall times of final RF output are decided by the sample coil, the design of this network is not critical from the bandwidth point of view. A low value of loaded Q is desirable to avoid ringing. Hence, a loaded Q of 5 with 30 pf capacitor at 13 MHz gives

$$R_P = Q/w_o C_P \doteq 2 \text{ k}. \qquad \ldots(4.9)$$

In fig.4.7, Q_{13}, Q_{14} form the basic multivibrator supplied by constant current generators Q_{15} and Q_{16} having thermal stability factor $\doteq$ 6. The gating pulses are applied as one of the collector supplies through the isolating transistor Q_{12}.

The output is capacitively coupled to the emitter follower Q_{17} biased at 1 m A with thermal stability factor = 6. Then the signal is applied to the "booster" through a 15 cm long RG59/U coaxial cable. The capacitance contributed by the cable is of no concern here since source impedance is quite low.

Since Q_{15} & Q_{16} carry constant currents these need not be fast switching transistors. Hence CIL 701 silicon NPN were selected. However, Q_{12}, Q_{13}, Q_{14} & Q_{17} are CIL 732 which is of fast switching type.

The + 6 vdc and - 6vdc supplies enter the chasis through 2300 pf feed through capacitors and π type decoupling filter networks.

4.3 BOOSTER & BUFFER DESIGN

The gated oscillator output of $\doteq$ 1.5 v.p.p. is insufficient for providing excitation to the driver stage. A Class-A amplifier of moderate gain is suitable to boost its value for adequate drive. An RF amplitude of 6 v.p.p. is suitable for the driver. With V_{CC} = 6 v., the V_{CE} required is 3 volts because of inductor action. For 3 mA quiescent current the emitter resistance, R_E = 1 K. For thermal stability factor S = 15, this gives $R_{B_1} \parallel R_{B_2} \doteq$ 14 K. The tank circuit is composed of :

(i) Inductor L_1 = 1.58 μ H of unloaded Q = 200 at 7.9 MHz. It is wound on a plastic former 2 cm dia using 11 turns of 18 gauge enamelled copper wire.

(iii Parallel combination of a fixed 56 pf disc ceramic capacitor and trimmer of value 7 - 30 pf.

DRIVER STAGE

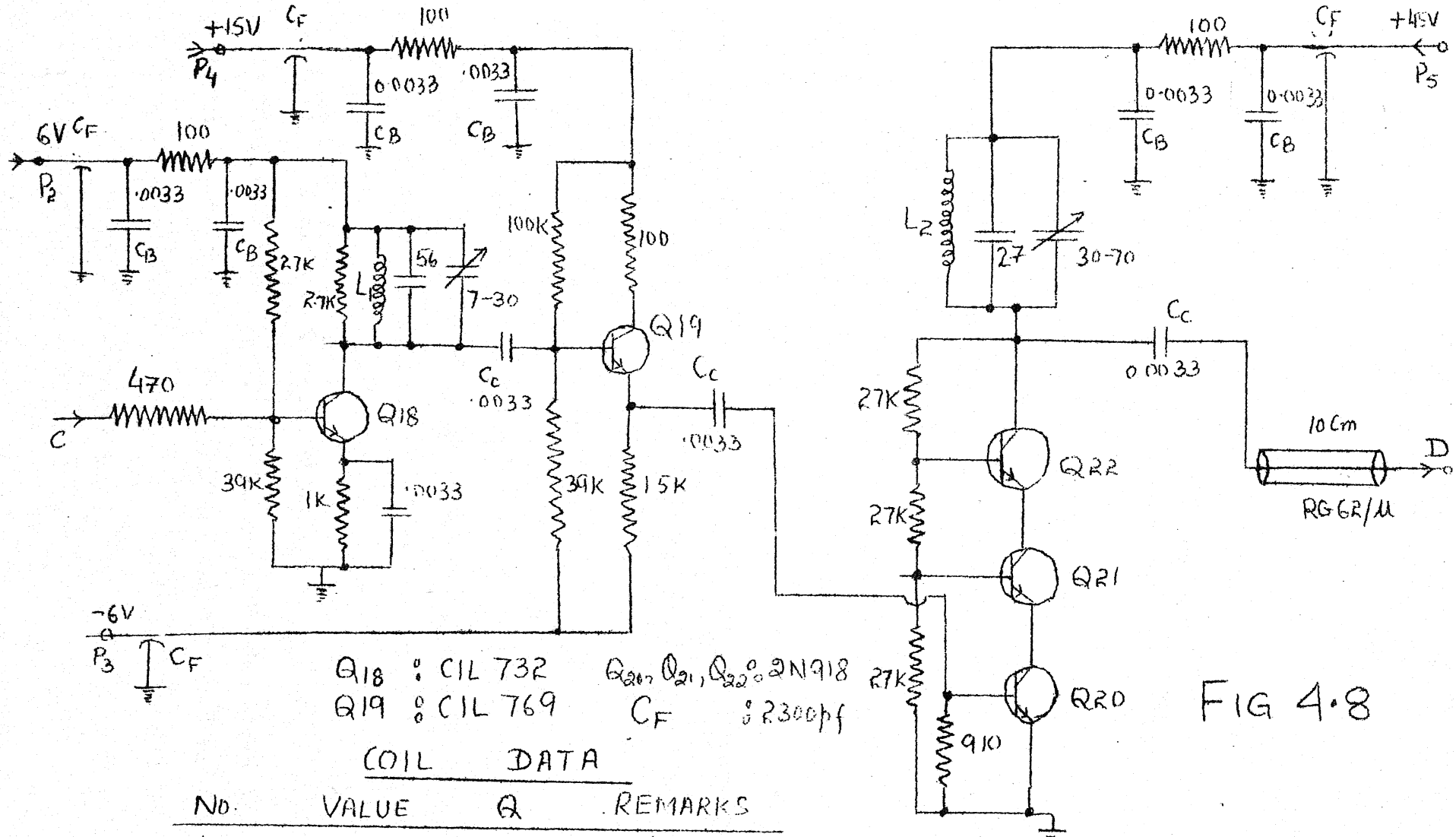

Q_{18} : CIL 732 Q_{20}, Q_{21}, Q_{22} : 2N918

Q_{19} : CIL 769 C_F : 2300pf

FIG 4·8

COIL DATA

NO.	VALUE	Q	REMARKS
L_1	1·58 μH	200	11 turns
L_2	1·78 μH	210	12 turns

C : FROM GATED OSCILLATOR.

D : TO POWER AMPLIFIER.

(iii) Shunt resistance of 2.7 K $\frac{1}{4}$ W resistor.

The bypass capacitor (3.3 nF) has reactance of $\doteq$ 3 ohms at 13 MHz. The resistance at the input serves to avoid undesirable oscillatins. Its value determined expermentally is = 470 ohms. The transistor Q_{18} is CIL 732 with BVCBO = 12 V.

The amplified signal is coupled through a 3.3 nF capacitor and applied to driver stage through the buffer amplifier Q_{19}. It is an emitter follower with 100 ohms in collector circuit for protection. The quiescent base voltage is $\doteq$ 0 VDC and current of 4 mA gives sufficiently low output impedance. The power supplies used are (i) + 15 VDC collector supply and (ii) - 6 VDC emitter supply. The former is derived from + 230 VDC. The feedthrough capacitors and decoupling networks have been added. For buffer, the transistor used is silicon NPN CIL 769 with BVCBO = 32 V.

4.4 DRIVER STAGE DESIGN

The driver stage must give about 70 v.p.p. RF to the power amplifier stage (vide sec.4.5). This can be conveniently obtained from a single tube. Instead, it was envisaged to make the solid state design. It is difficult to achieve this by means of a single transistor stage because high BVCBO transistor with high f_T and power dissipation rating was not available. The desired RF amplitude was obtained from the three transistor circuit shown in fig.4.8. The transistors are silicon NPN each with f_T = 600 MHz, BVCBO = 30 V and collector dissipation = 200 mW at 25°C (Q_{20} - Q_{22}).

The three 27K resistors equalize the dc voltage as well as signal excursions across the three transistors. The bias is provided by a method similar to grid leak. If V_B is the quiescent base voltage and I_B the average value of base current, then[6]

$$R_b = V_B/I_B \qquad \ldots (4.9)$$

Also R_b must be large enough so that capacitor holds the charge for sufficient amount of time during the discharge period. Thus,

$$R_b \gg 10\, X_c \qquad \ldots (4.10)$$

It will be noticed that for a transistor class C stage, this method needs no protective device as in tube, in absence of drive.

Now, the bias value V_B depends on the conduction angle choosen. Fig.4.9 depicts the base voltage $V_b(t)$[6]. The top portions are compressed due to conduction and hence cause reduced input impedance. It is clear that (Fig.4.9)

$$\text{Cos}\ (\theta/2) = (V_B + V_d)/(V_p/2) \qquad \ldots(4.11)$$

The values of the components used to produce the required bias are estimated as follows. Suppose 10mA of average collector current flows. If average $h_{FE} = 40$ then average base current needed is $\frac{1}{4}$ mA. For $V_p/2 = 2$ volts and $\theta = 120°$, one gets from (4.11): $V_B + V_d = 1$ volts. Hence $V_B = 0.4$ V and therefore $R_b = 1600$ ohms. From 4.10 the capacitor should be more than 8 pf at 13 MHz. The optimum value of R_b is experimentally determined to be 910 ohms.

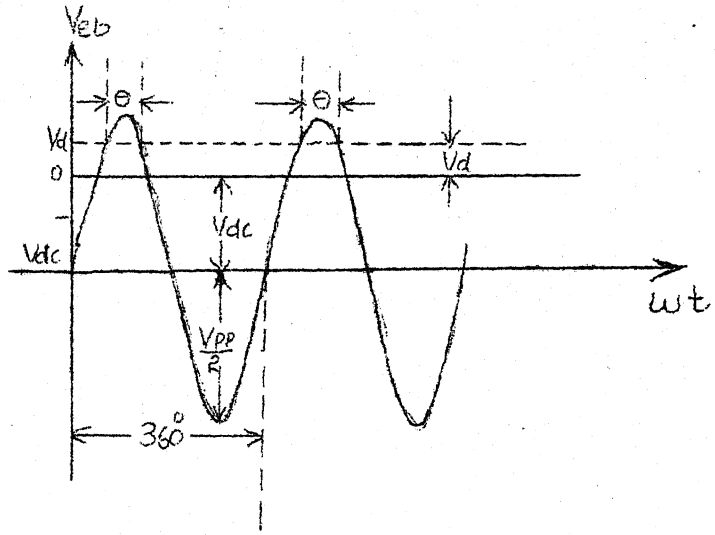

Fig. 4.9 : Base Voltage Waveform of a Class C Transistor Amplifier.

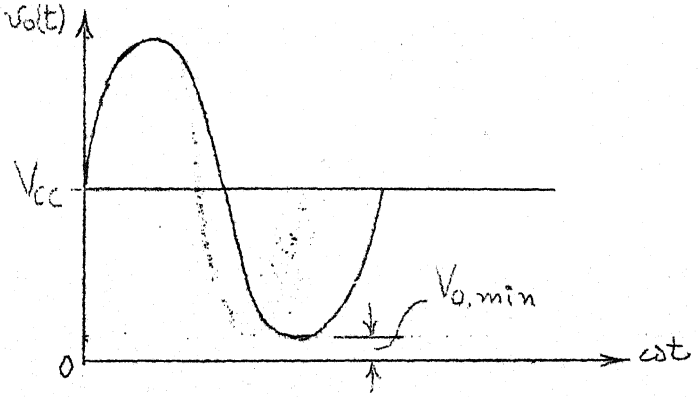

Fig. 4.10: Output Waveform of a Class C amplifier ~~Theoretical~~.

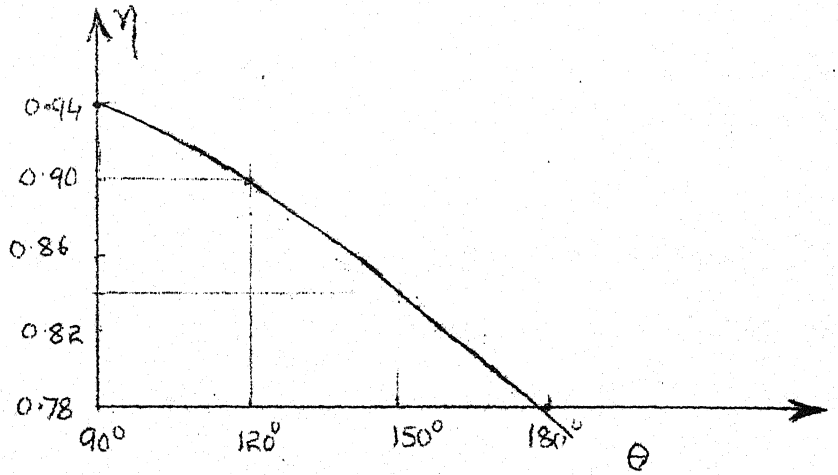

Fig.4.11: Efficiency vs. conduction angle.

The efficiency of a class C amplifier is theoretically given by[7]

$$\eta_{max} = \frac{\theta - \sin\theta}{4 \sin(\frac{1}{2}\theta) - 2\theta\cos(\frac{1}{2}\theta)} \qquad \ldots (4.12)$$

This result checks for $\theta = 180°$, when $\eta = 78.5\%$ for class B amplifier. Experimentally it is also possible to determine efficiency by[8]

$$\eta \doteq 1 - (V_{o\ min}/V_{CC}) \qquad \ldots (4.13)$$

where symbols are explained in fig.4.10. Fig.4.11 shows the graph between efficiency and conduction angle determined from (4.12) numerically using the digital computer.

The voltages at the base of Q_{21} and Q_{22} and collectors of Q_{20}, Q_{21} & Q_{22} are all in phase. Neglecting the storage delay, these voltages are in opposite phase to the base voltage of Q_{20}.

The tank circuit consists of:

(i) L_2 = 1.78 μH coil with unloaded Q = 210 at 7.9 MHz. It is hand - wound using 12 turns of 18 gauge enamelled Copper wire on plastic former of 2 cm diameter.

(ii) A condensor consisting of parallel combination of 27 pf ceramic disc capacitor, and a 30 - 70 pf trimmer. The 10 cm length of RG 62/U cable adds about 4.5pf and tubes of power amplifier furnish another 10 pf. At 13 MHz, $\frac{1}{4}$(wavelength) $\doteq$ 5.8 meters. Since cable lengths are much less than $\frac{1}{4}\lambda$, they essentially act as capacitive load to the tank circuit.

(iii) The 20 K grid resistor of power amplifier is in parallel with L_2. The parallel resistance can not be made as low as in gated oscillator tank circuit because this will reduce the resonance tank impedance and hence the voltage swing of the output.

Also, base resistances of the transistors must obey the following relation for avoiding too much of ac signal feedback[9]:

$$R_B \gg \tfrac{1}{5} R_C \qquad \ldots (4.14)$$

However, the upper bound on base resistance is restricted by thermal stability considerations.

Power supply is + 45 V.D.C. derived from + 230 VDC by means of zener diodes (fig.6.5). The feedthrough capacitor and π type RC decoupling network have been incorporated for proper R.F isolation. However, RF choke is not necessary in this circuit.

4.5 POWER AMPLIFIER DESIGN

This section describes the power amplifier made using the vacuum tubes.

4.5.1. Discussion

From specifications the order of RF voltage required is 250 V.P.P. across the sample coil. This is conveniently obtained by vacuum tubes instead of transistors. The class C configuration is employed because of:

(i) High efficiency

(ii) Low average current yields low tube noise.

(iii) Relative immunity to parasitic oscillations.

The pentode is chosen instead of triode because of former's negligible Miller effect and larger gain-bandwidth product. Grounded-cathode is the most suitable configuration. Simplified calculations are outlined here for determination of the operating conditions. The pertinent tube characteristics are listed in Appendix B.1

The conventional method for class C RF amplifier design is very tedious involving graphical integration of the plate current characteristics. The step-by-step design procedure given in reference (10) will be followed. Table 4.1 will be referred to for this method: The various symbols K_1 to K_5 cannot be defined as such but their meaning will evident from the equations used for design. An another factor, K_6 which is a function of grid bias and driving voltage is given in table 4.2. These factors K_1 to K_6 are calculated by assuming sinusoidal drive.

TABLE 4.1

θ_p	K_1	K_2	K_3	K_4	K_5
210	2.75	0.723	0.205	0.795	0.284
200	2.87	0.745	0.148	0.852	0.273
190	3.00	0.765	0.081	0.919	0.262
180	3.14	0.785	0.000	1.000	0.250
170	3.32	0.805	0.095	1.095	0.237
160	3.50	0.825	0.210	1.210	0.224
150	3.75	0.844	0.350	1.350	0.213
140	4.00	0.862	0.520	1.520	0.200
130	4.25	0.880	0.732	1.732	0.187
120	4.60	0.897	1.000	2.000	0.174
110	5.00	0.913	1.345	2.345	0.160
100	5.50	0.927	1.800	2.800	0.145
90	6.10	0.940	2.410	3.410	0.130

The choice of conduction angle is a compromise between the following factors:

(i) Large conduction angle which reduces drive power but results in reduced efficiency.

(ii) Small conduction angle which increases plate circuit efficiency but requires higher driving power.

Most satisfactory results are obtained for conduction angle equal to 140°.

4.5.2. Calculations:

Let E_b = 220 V , E_{c_2} = 220 V and plate input = 15 W.

The calculations proceed as follows:

(i) DC plate current, $I_b = (15/220)10^3 = 68$ mA

(ii) Peak plate current, $i_{b\ max} = K_1 \times I_b$.

$K_1 = 4$ for $\theta_p = 140°$, therefore $i_{b\ max} = 272$ mA.

(iii) From characteris (Appendix B.1) the effective minimum place voltage $e_{b(min)}$ and peak positive control grid voltage $e_{c_1,max}$ are found for E_{c_2} = 220 V and the calculated value of $i_{b\ max}$. For maximum plate circuit efficiency and maximum power gain, both $e_{b,max}$ and e_{c1max} should be as small as possible but choice of these values below the knee causes excessive control grid and screen grid currents. The use of values too far to the

TABLE 4.2

E_{c_1}/E_{g_1}	K_6	E_{c_1}/E_{g_1}	K_6
0.25	4.67	0.65	6.95
0.30	4.84	0.70	7.52
0.35	5.04	0.75	8.25
0.40	5.26	0.80	9.25
0.45	5.50	0.85	10.70
0.50	5.78	0.90	13.12
0.55	6.10	0.95	18.63
0.60	6.49		

right of the knee reduces power output and may result in excessive plate dissipation. In this case:

$$e_{b,\,min} = 70\ V,\ e_{c_1 max} = 14\ V.$$

(iv) Power Output = $P_o = K_2(E_b - e_{b\,min}) \times I_b$

$$= .862(220-70)\times 68\times 10^{-3} = 8.8\ W.$$

(v) Plate Dissipation $P_p = (E_b \times I_b) - P_o = 15 - 8.8 = 6.2W.$ which is within the maximum plate dissipation rating.

(vi) Control grid bias, $E_{c_1} = -(K_3 \times e_{c_1 max}) - \dfrac{K_4 E_{c_2}}{\mu_{g2g1}}$

The mu-factor = 16. Hence

$$E_{c_1} = -(.52 \times 14) - \frac{1.52 \times 220}{16} = -7.3 - 21 = -28.3\ V$$

(vii) Peak rf control grid voltage E_{g_1} required to drive the tube to full output is $E_{g_1} = -E_{c_1} + e_{c_1 max}$

$$= +28.3 + 14 = 42.3\ V$$

(viii) The peak control grid current from grid-current characteristic curves is, $i_{c_1 max} = 10$ mA. Then dc grid current is given by:

$$I_{c_1} = i_{c_1 max}/K_6$$

For $E_{c_1}/E_{g_1} = 28.3/42.3 = \frac{2}{3}$, $K_6 = 7$ from table 4.2.
Thus, $I_{c_1} = 10/7 = 1.4$ mA.

(ix) The approximate driving power required by the grid-cathode circuit of the tube is given by:

$$P_d = 0.9\ E_{g_1}\ I_{c_1}$$

$$= (0.9)(42.3)(1.4)\ mW = 53.4\ mW.$$

The above design requires very large rf swing at the input which will necessitate a tube for the driver stage also.

Hence the following modified design has been used in actual circuit which requires less rf drive voltage and no grid power.

Let Plate Input = 10 W. The other calculations are summarized below:

(i) E_b = 220 V, E_{c_2} = 220 V. $I_b = 10 \times 10^3/220 = 45.5$ mA

$\theta_p = 140°$

(ii) $i_{bmax} = K_1 I_b = 182$ mA (Table 4.1)

(iii) $e_{bmin} = 50$ V, $e_{c_1max} = 9.5$ V.

(iv) $P_o = 0.862(220 - 50) \times 45.5 \times 10^{-3} = 6.65$ W

(v) $P_p = 10 - 6.65 = 3.35$ W

(vi) $E_{c_1} = - .52 \times 9.5 - 21 = - 26$ V

(vii) $E_{g_1} = 26 + 9.5 = 35.5$ volts.

(viii) $i_{c_1max} = 0$ $\therefore$ grid driving power = 0

The above design fairly well meets the requirements. The experimental values are as under:

Plate voltage = 230 VDC

Screen grid voltage = 230 VDC

Control grid bias = - 20 VDC

Plate current drawn by a single tube in absence of drive is 1 mA

plate current drawn for <u>continuous</u> sine wave drive = 26 mA for one tube.

4.5.3. Circuit Description:

Fig. 4.12 depicts the power amplifier employing two tubes (5763) in parallel. The factors necessitating use of two tubes will be discussed in the "tube-receiver" design. The suppressor grid is connected to the cathode by a copper

FIG 4.12. POWER AMPLIFIER

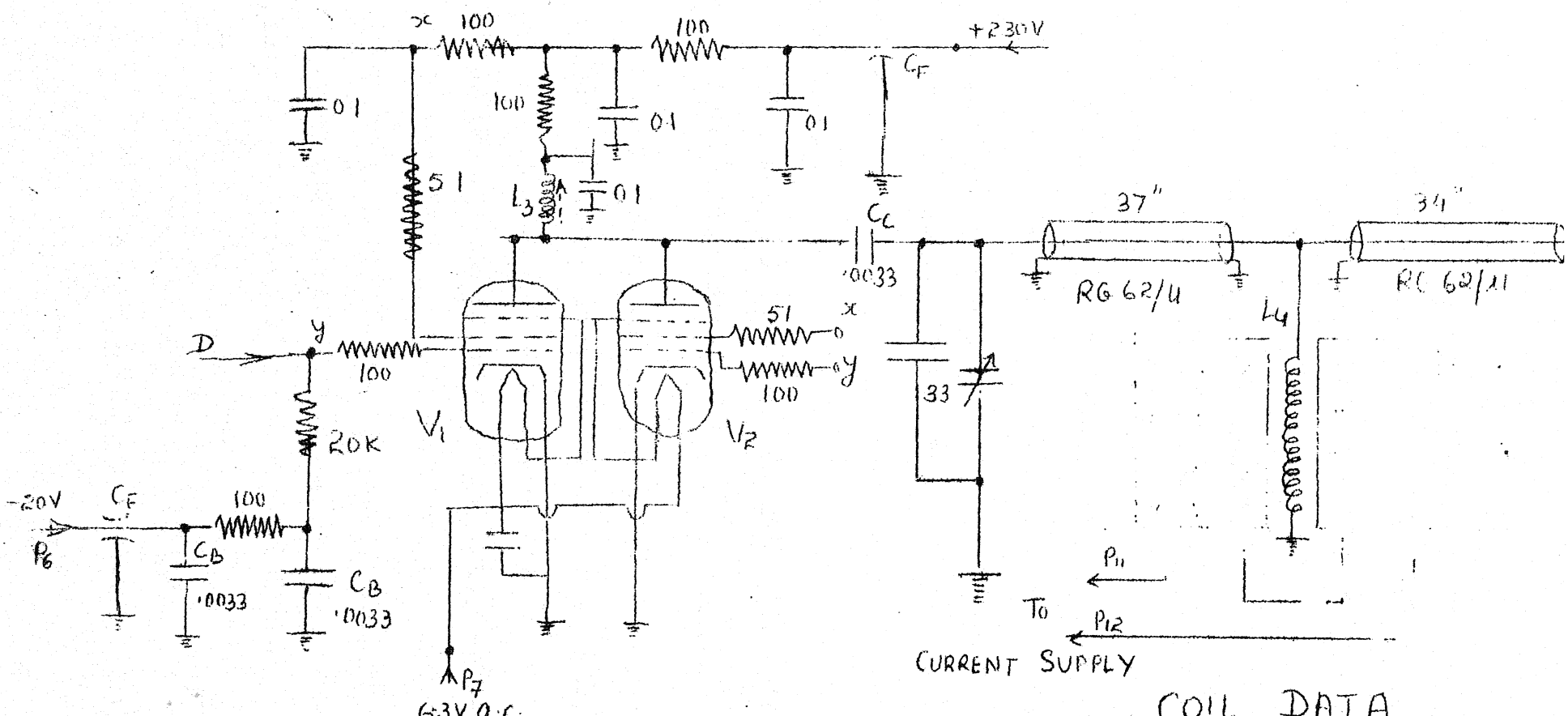

C_F : 2300 PF

V_1 : 6A

V_2 : 5763

COIL DATA

NO.	VALUE	Q	REMARKS
L_3	14.1 μH	33	RFC
L_4	1.0 μH	200	8 turns.

wire (gauge 16). The major difficulty experienced was due to the undesired oscillations which used to occur during off periods. This difficulty was circumvented by the following techniques:

(1) addition of 100 ohms resistors at the control grid of each tube, soldered at the socket.

(2) addition of 51 ohms resistors at the screen grid of each tube, soldered at the socket.

(3) addition of RFC (L_3) in the plate circuit.

(4) cascade of decoupling networks for the plate, control grid and screen grid voltage supplies.

(5) feed through capacitors of value 2300 pf affixed right at the entering points for the plate and control grid supply leads.

(6) using shortest possible leads of thick Copper wire for all interconnections.

The rf driving signal is coupled through 3.3 nF capacitor from the driver stage and applied to control grid by means of 10 cm long RG62/U coaxial cable grounded at both the ends. Of the various types of interstage couplings possible e.g. inductive coupling, link coupling and capacitive coupling; the last one is the simplest and most economical. Since driver power requirement is nil, the maximum power transfer afforded by other method is not required here.

4.5.4. Tank Circuit Design:

The various compromises in the design of sample coil have been explained already (Chapter 3). The sample coil inductance value is determined by the tank capacitance which

depends on the length of the cables used to transmit the signal to and from the coil. This in turn depends on the physical location of the coil and the magnet with respect to the transmitter and the receiver. Assuming 1 yard of RG62/U cable length for each side, the absolute minimum value of tank capacitor is = 13.5 x 6 = 81 pf (Table 6.1). The sum of power - amplifier tube output capacitances and the receiver tube input capacitance $\doteq$ 15 pf. Assuming 30 pf to be put as an external capacitor, the approximate value of tank capacitor is then 126 pf. In actual circuit, the sample coil inductance is 1 μH requiring capacitance of about 150 pf at 13 MHz. The rest of the capacitance is provided by parallel connection of 33 pf fixed ceramic disc capacitor and a variable condenser. The measured lengths of the coaxial cables are 37" and 34" respectively.

The choice of the cable type is very critical in this tank circuit e.g. two yds of RG58/U cable (Z_o = 53 ohms) which is mostly used in ordinary laboratory work will have shunting capacitor of value about 170 pf. This will make the tank inductance small enough to make resonance impedance undesirably low.

Since the rf voltage levels are the highest in this circuit, the proper decoupling circuits and the actual circuit layout are very important for the final success of the amplifier operation. Ceramic capacitors have been used throughout.

4.5.5. Stabilization:

The high frequency high voltage amplifiers are always prone to undesired oscillations at the signal frequency or other parasitics. The various techniques described earlier (Page 39) are mostly empirical, cut and try methods. Since these have succeeded, one need not design the relatively complicated neutralizing circuits. However, the class A configuration which was extensively experimented upon also, could not be made free of oscillations without neutralization. The final class C design is stable as well as less noisy because of very small average direct current.

The shielding aspect is discussed separately in the chasis layout (Appendix G.2).

4.5.6. Grid Bias Scheme:

Of the three methods viz, the fixed bias, the grid leak bias and the self bias; fixed bias is the most suitable. The grid-leak bias can not obviously be used alone because the pulsed operation will increase plate current enormously during the off periods. The self bias is not as stable as the fixed bias. The fixed bias is obtained from a negative supply (- 20VDC) through a 20K grid resistor. No RF choke is needed in the grid circuit since adequate decoupling is achieved by π type RC filters.

4.6 PROPOSED POWER AMPLIFIER DESIGN USING SEMICONDUCTORS

The high value of RF amplitude led to the choice of tube in the power amplifier design. This choice though convenient and economical is not however indispensable. It is the purpose of this article to envisage a solid state design for this unit also.

Upon surveying the transistor data sheets it is evident that most high frequency, high power transistors have maximum collector breakdown voltage as 60 V. Thus, we have to use the same concept as in the design of driver stage (sec.4.4) to circumvent this voltage breakdown limitation. It was obvious there, that due to signal feedback the excursion of output signal was less than the otherwise possible value of 2 V_{CC} in the tuned circuits, This feedback cannot be reduced below a certain limit because of thermal stability considerations.

The ability of a transistor to operate satisfactorily as a class C power amplifier at high frequencies depends on its ability to handle large peak currents at these frequencies. The "overlay transistor "[11] makes this design possible wherein a large number of separate emitters are tied together by diffused and metallized aluminium regions (fig.4.13 a). The advantages of this construction are high power output at high frequency, high gain and efficiency, and low input and output capacitances. Fig.4.13 (b) depicts some overlay transistors with their useful power output as a function of frequency. Table 4.3 (Page 44) lists their collector dissipation, BVCBO and f_T.

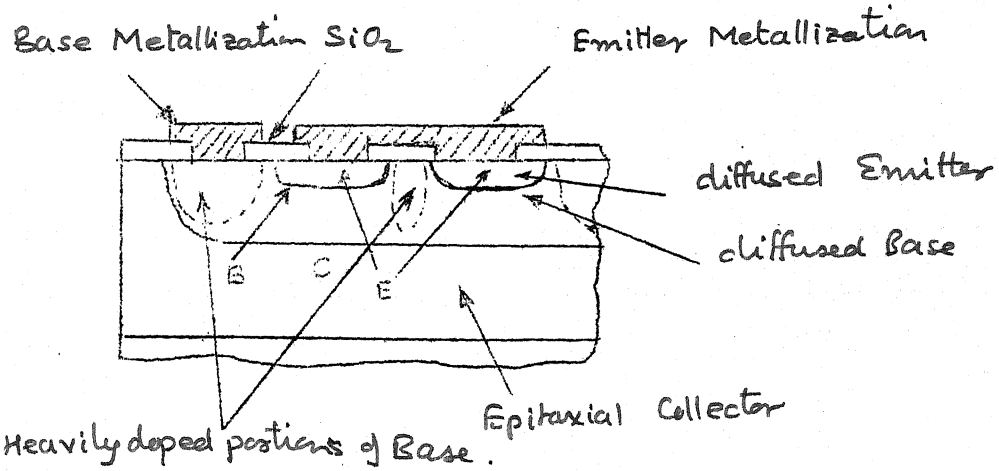

Fig. 4.13 (a) : Geometry of the "Overlay Transistor".

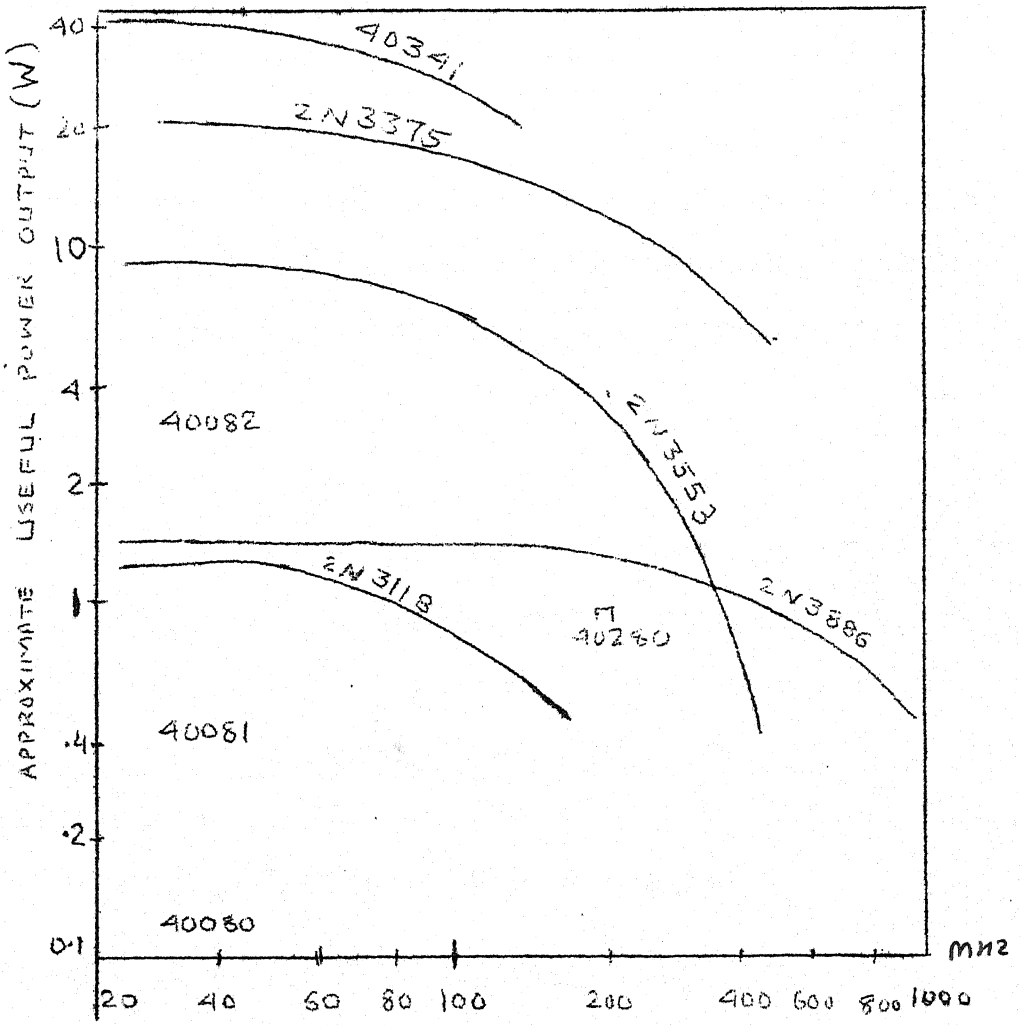

Fig. 4.13 (b) : Some R.C.A. Overlay Transistors, Useful Power Output vs Frequency.

TABLE 4.3

R.C.A. OVERLAY TRANSISTOR TYPES

Type	P_C(W)	BVCBO (V)	f_T (MHz)
40082	5.0	60	27
40292	23.0	50	30
2N3375	11.6	65	?
2N3553	7.0	65	500
2N3866	5.0	55	800
2N4012	11.6	65	500
2N3632	23.0	65	400
2N3773	23.0	65	400
40340	70.0	60	class C Amplr. at 100 MHz.
40341	30.0	80	

It is evident from these data that class C amplifier at frequencies as high as 100 MHz delivering 70 watts of power are feasible. In the present problem a set of 2N3553 transistors will be considered for design since a single transistor can not be used here due to low BVCBO.

For 250 volts peak to peak RF output the minimum number of transistors needed will be four. Choice of 5 transistors will be imperative due to reasons mentioned earlier (Page 42). The input and output powers for a single stage class C amplifier are related to conduction angle[7] as follows:

$$P_{in} = V_{CC}\, I/\pi\, (\sin \tfrac{1}{2}\theta - \tfrac{1}{2}\theta \cos \tfrac{1}{2}\theta) \qquad \ldots(4.15)$$

$$P_{out} = V_{CC}\, I/\, 4\pi\, (\theta - \sin \theta) \qquad \ldots(4.16)$$

The optimum conduction angle for transistor class C amplifier is about 120°[6]. The supply voltage is decided as

follows: The efficiency for $\theta = 120°$, from (4.12) is 0.897. Also the efficiency is related to output swing through the (4.13). Since RF output swing = 2 $(V_{CC} - V_{omin})$ one gets: output voltage swing = 2 η V_{CC}.

$$\text{So } V_{CC} = \frac{(\text{RF swing})}{2\,\eta} \qquad \ldots\ (4.17)$$

Hence

$$V_{CC} = 250/2(0.897) = 139 \text{ V.}$$

So, V_{CC} = 150 V will be selected. Then from (4.16) the average collector current is:

$$I = (P_{out}\ 4\pi)/(V_{CC}\ \pi(\theta - \sin\theta))$$

$$\doteq (6.6/5)(4\pi)\ 1000/150(2.1 - 0.87) = 40 \text{ mA.}$$

$\therefore$ $V_{CC}/5$ x I = 30 x 40 = 1200 mW which is well under each transistor's collector dissipation rating.

The tank circuit design poses no new problems and will be considered to be the same as that in tube-version (sec 4.5). The input bias circuit design has been explained earlier in the design of driver stage (sec 4.4). Following the same arguments, the other values are listed:

Let input drive peak value = 3 volts. = $V_p/2$

$\therefore$ $V_B + V_{rl} = 1.5$ volts for $\theta = 120°$.

Hence $I_B R_B = 0.9$ volts. For $h_{FE} = 40$, $I_B = 1$ mA.

Hence R_B = 900 ohms.

The optimum value of R_b must be determined experimentally as was done in the driver stage design. The final circuit is shown in fig.4.14. The voltage equalizing resistors $R \gg R_L/5$ in this case. Therefore, R = 12 K is satisfactory.

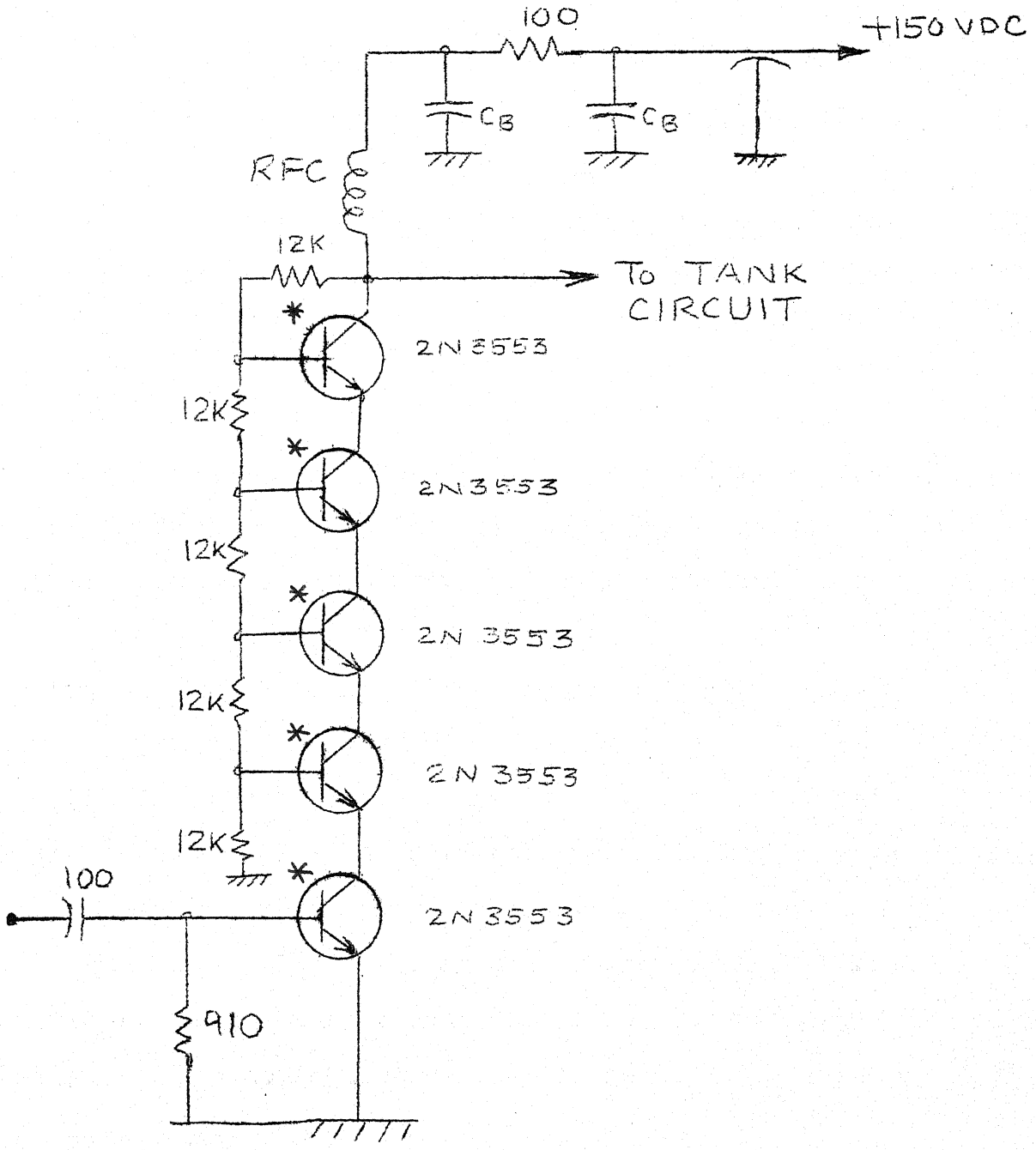

FIG 4.14: THE PROPOSED DESIGN OF SOLID STATE POWER AMPLIFIER.

CHAPTER V

DESIGN OF RECEIVER

The receiver picks up the nuclear induction signal induced in the sample coil (fig.2.1) and processes it for final display on the Cathode Ray Oscilloscope. It consists of the input network, RF Amplifier, Detector and the Audio Amplifier. The design of these stages is considered next.

5.1 TUBE-RECEIVER

5.1.1. Input Network:[12]

The design of this network is very crucial because of various compromises to be made as explained in sample coil design considerations (Chapter III). The coupling from sample coil to the receiver is chosen to be capacitive for simplicity. Choice of the grid resistor is influenced by following considerations:

(i) During "on" periods the tube V_3 gets saturated because of very high input grid voltage. So, small value of R_g is desired for reduction of recovery time of the receiver.

(ii) Too small a value of grid resistor will reduce the loaded Q of the tank circuit and hence the resonance impedance. This consequently reduces the RF voltage swing also.

By connecting an inductor L_5 (Fig.5.1) of inductance $\gg$ sample coil L_4, in series with grid resistor one reduction

FIG 5.1 : RECEIVER

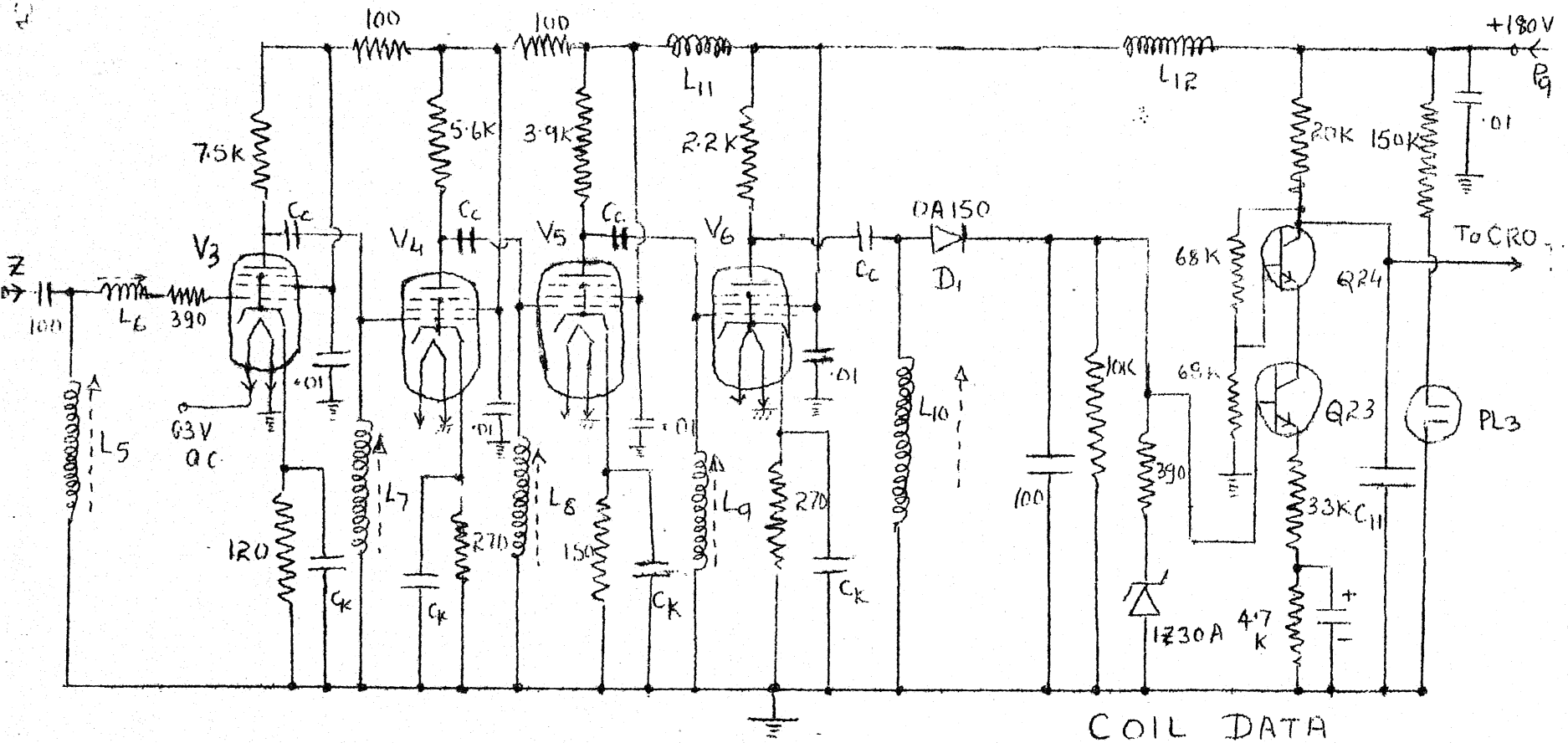

Q23, Q24 : 2N1990

C_c : .0033μF

PL3 : 65V NEON LAMP

Z : From Sample Coil.

COIL DATA

S.NO.	VALUE	Q	REMARKS
L_5	65	55	---
L_6	75	55	---
L_7, L_8, L_9, L_{10}	9.5	60	Nominal Value
L_{11}, L_{12}	RFC	---	MILLER # 4505

in loaded Q can be avoided. Also, when the tube gets saturated its low input impedance directly comes across the tank circuit which again is undesirable. Connecting another inductor L_6 in series with control grid avoids this difficulty also. However, the value of L_6 cannot be arbitrarily large to remove this undesirable effect because inductance is in series with the input impedance of the tube which may became comparable to impedance of L_6 and thus effectively reduce the NMR signal at the input.

The 390 ohms resistor in series with grid is for avoiding oscillations in the receiver. Its value is determined experimentally. (This however increases the equivalent input noise resistance of the receiver).

Now, sufficiently large values of L_5 and L_6 will avoid the reduction in loaded Q but they simultaneously impair the transient response of the envelope of RF pulses. Hence, the inductance values are only kept moderately high and two tubes in parallel are put instead of a single tube in the "power-Amplifier" to increase its output power. The exact values of L_5, L_6 were determined experimentally, keeping these compromises in view.

5.1.2. R.F. Amplifier:

The order of NMR signal induced in the sample coil is estimated to be about 1 mV peak to peak. A gain of 10^4 will be adequate. This is achieved by four stage tube amplifier. Gain of the first stage is kept largest to have

low noise figure of the amplifier. Bandwidth is decided by three factors:

(i) signal: NMR signal is a slowly varying signal, the width of the echo depending on the sample itself. The minimum width is estimated to be 1 ms.

(ii) stability: Small bandwidth means high loaded Q and consequent problems of oscillations. Hence, instead of small number of high Q stages, a four stage, tuned amplifier with low Q tank circuit was constructed.

(iii) Noise: Smaller the bandwidth less the noise at the output.

The tank circuit comprises of single layer coils of nominal value 9.5 μH and unloaded Q = 60 (at 7.9 MHz) resonating with tube capacitances. Then tapering of the four plate resistors as shown (fig.5.1) allows tuning to be easily affected by the first two stages. Thus the last two stages have less effect on the tuning. The interstage coupling is again, for sake of simplicity, consists of disc ceramic capacitor of value 3.3 nF. The decoupling networks have been used to avoid undesirable signal feedback. The tubes have been shielded and laid in four compartments in the chasis. (See plate I, page 79).

The self bias has been utilized here for simplicity. Table 5.1 shows various dc voltages and the calculated current values for reference. (Page 51). The vertical line inside the tube (P. 48) indicates the internal connection of suppressor grid to the cathode.

TABLE 5.1

Bias Conditions For Receiver Tubes

	V_3	V_4	V_5	V_6
R_p K ohms	7.5	5.6	3.9	2.2
R_K K ohms	120	270	150	270
V_p Volts	87	125	135	120
V_K Volts	2.2	3.5	3.8	12
I_K mA	18.3	13	25.3	44.5
I_p mA	13.3	10.7	12.8	29.5
I_{c2} mA	5	2.3	12.5	15.0

The tubes are sharp cut off pentodes (App.B.2) 6AK5 with + 180 VDC supply voltage.

5.1.3. Detector:

This is the usual linear detector (envelope detector) suitable for extracting amplitude modulated NMR signals. Diode D 1 in combination with 10 K & 100 pf constitute this network. The direction of diode is suitable for transistor audio amplifier shown here using NPN units. This direction must be reversed for tube audio amplifier (or PNP transistors in audio amplifier) to give proper bias.

5.1.4. Audio Amplifier:

The NMR signal is large enough after the detector stage to be conveniently observed on CRO. But SNR of the detected signal is not satisfactory. To achieve higher SNR a high pass filter is connected after the audio amplifier. (This

obviously can not be done just after the detector, hence the need for an amplifier). This simple technique of improvement of SNR is feasible here only because of bandlimited nature of NMR signal as compared to noise. The circuit design uses the same concept as in the driver stage excepting the output circuit. Instead of two transistors connected in this fashion, one can also use an appropriate zener to bring down the voltage supply. The input is direct coupled to the detector. The zener diode at the input of the amplifier is to clip off voltages in excess of 30 V. Q23 & Q24 are 2N1990 Silicon NPN transistors with BVCBO = 100 V and P_c = 600 mW at 25° C.

The capacitor C_H at the output serves as the high pass filter to the audio amplifier whose output impedance is 20 K ohms. Nominal value of C_H is 1 nF but varying this, one can achieve any desired degree of improvement in SNR keeping in mind the upper cut off frequency of the signal.

5.1.5. Display:

The output of the audio amplifier is fed to the vertical plates of the CRO and the horizontal plates are excited with the pulse output from the pulse programmer. The latter measure is necessary for stable display of a waveform which is repetitive at very low frequencies. Hence, any low frequency oscilloscope is suitable for the spin-echo display. However for observing the transmitter output, a high frequency oscilloscope like Tek 516 or 454 is necessary.

In fig.5.1 the pilot lamp PL3 is 65 V neon bulb & carries a current af about 0.6 mA indicating the + 180 VDC

connection to the receiver circuit.

5.2 SOLID-STATE RECEIVER DESIGN:

The detailed block diagram of the semiconductor version of the receiver is shown in fig.5.2. A voltage gain of 10000 (80dB) will be adequate. The center frequency is 13 MHz. It will be recalled that bandwidth of the tube receiver was compromised for stability since smaller bandwidth imply large loaded value of Q and consequent possibility of oscillations in the tube circuit. Here, this aspect does not impose limitations since the neutralization is envisaged for the amplifier stages. The detailed design follows:

5.2.1. Input Network:

Synthesis of this network involves careful consideration of the incoming signal. The RF excursion of 250 v.p.p should be prevented from being applied directly to the semiconductor amplifiers. Also the NMR signal appearing during the off periods is of a small magnitude and the input network should not attenuate this signal. Thus, the transfer characteristics of the coupling network should be:

(i) Zero transmission when RF is on.
(ii) full transmission when RF is off.

...(5.1)

This immediately suggests the use of a switch synchronously operated with the gated oscillator wave-form. But it is to be kept in mind that this device has to switch in and out a 250 v.p.p. signal having excursions from - 125 V to + 125 V i.e. it is a bipolar signal with enormously large amplitude.

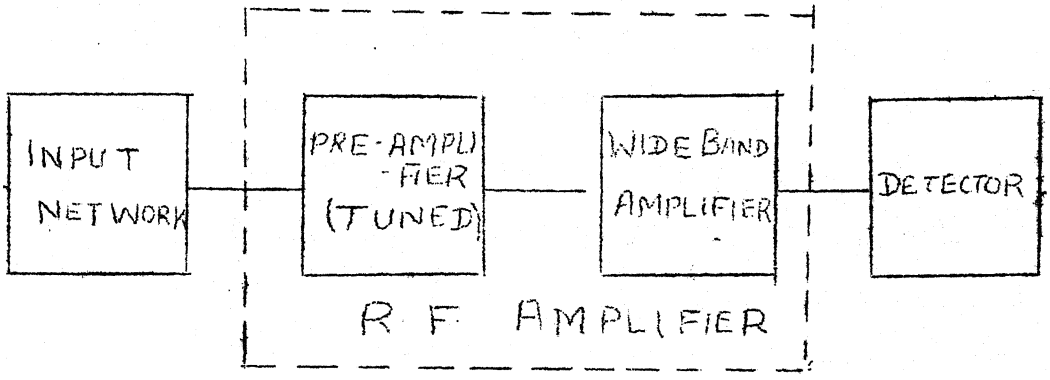

FIG. 5.2 BLOCK DIAGRAM OF SEMICONDUCTOR RECEIVER.

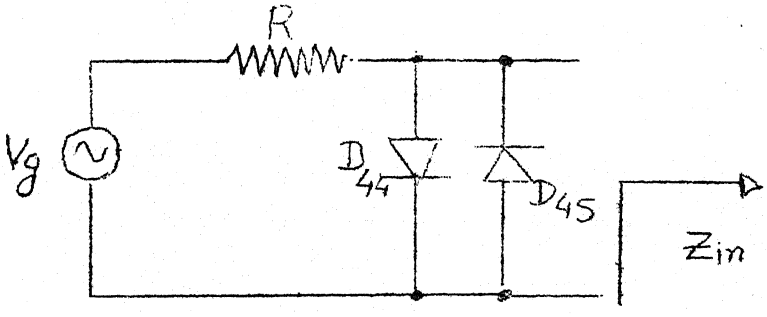

FIG. 5.3 BASIC INPUT COUPLING NETWORK

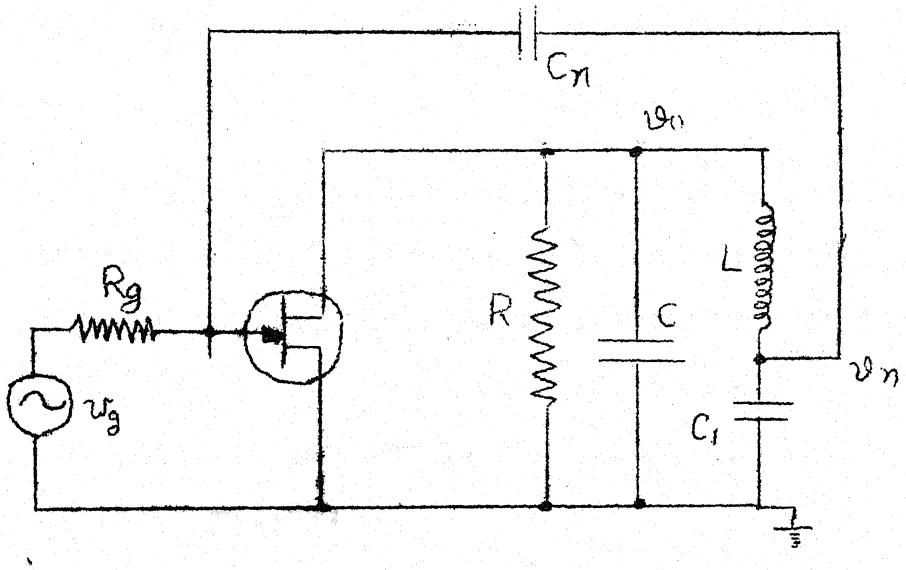

FIG. 5.4 NEUTRALIZING SCHEME FOR F.E.T.

A simple circuit that exhibits the stipulated nonlinear behaviour is shown in fig.5.3. Suppose, for the moment that R is replaced by a short circuit. Then the output of the circuit during RF on periods is limited to $\pm V_d$ and during RF off periods, the NMR signal passes through unaffected since its amplitude (<1 mV) is insufficient to forward bias the diodes and hence the impedance is infinite. The two diodes are necessary because input signal is bipolar.

The resistance R is necessary to limit the current through the diodes in RF "on" periods. The factors governing its value are:

(i) R should be large enough to effectively limit the peak diode current.

(ii) R should not be too large to attenuate the NMR signal during the RF "off" periods. i.e. $R \ll Z_{in}$.

(iii) Recovery time: The diode junction capacitances must discharge for the effective impedance to change its value. This discharge path is to be through resistance R (and the coil itself which is direct coupled in this case). Hence making R large will yield in large recovery times.

This leads to the choice of diodes with as large current capability as possible and as small junction capacitance as feasible. Another factor which is to be considered is PIV of the diode. (Here, PIV $>$ 125 V). These three parameters are too restrictive. Hence, two possibilities may be:

(a) A series of diodes to be substituted for each D_1, D_2. This will take care of PIV problem. Also the net capacity to the ground will be a series combination of the diode capacities in the diode stack. This is also desirable from "recovery-time" point of view.

(b) The diode connected transistor may be used if the parameters of the transistor collector-base junction meet the above requirements.

The RF Amplifier consists of two sub-blocks: "preamplifier" and "wide-band amplifier". A total gain of 10,000 is to be supplied by these amplifiers.

5.2.2. Preamplifier:

The preamplifier design has the following salient features:

(i) It must be low noise amplifier since the noise figure of the preamplifier governs the noise figure of the whole receiver provided the gain of the amplifier is moderately large.

(ii) This unit controls the bandwidth since tuned circuits will invariably be required.

The semiconductor device selected for preamplifier is the junction field effect transistor for low noise figure and high input impedance. Due to large Miller effect present in an F.E.T., neutralization is indispensable.

5.2.2.1. Neutralization:[13,14]

Of the various neutralization schemes the simplest chosen is shown in fig.5.4. Here, C and L are tank compo-

nents deciding frequency of operation and R determines the bandwidth. The capacitor C_1 develops a voltage v_n whose component is opposite in phase to the output voltage. This out-of-phase voltage is made to feed a current through capacitor C_n to cancel the effect of Miller feedback.

The value of capacitor C_1 can be shown to lie in the range[15]

$$1/w_o^2 L \ll C_1 < g_m/2\pi (B.W) \quad \ldots\ldots (5.2)$$

The first inequality stems from the fact that at resonance, the impedance of C_1 should be much smaller than impedance of series inductor for tank circuit action to take place. The second inequality shows the limitation due to trans-conductance of the device itself. The derivation is outlined in App. F.

Once C_1 is determined, C_n can be calculated from (F.15):

$$C_n \doteq (w_o^2 L C_1 C_{gd}) / (1 - (w_o^2 L C_1/g_m R)) \quad \ldots (5.3)$$

where, C_{gd} is drain to gate capacitance.

5.2.2.2. Tank Circuit Design:

The resonance impedance is decided by the voltage gain. Two stages will be necessary for gain of 100. (The rest of the gain will be provided by the wideband amplifier). Since nominal value of g_m = 2 m$\mho$ (App. B.3), a gain of 10 implies $R \doteq 5$ K. The bandwidth will be fixed by loaded Q:

$$f_o/\Delta f = Q = w_o CR \quad \ldots (5.4)$$

where, Δf is the 3 dB bandwidth. $\equiv$ B.W.

Thus, C is calculated since all other quantities are known. Hence inductance value is also determined.

For bandwidth = 0.5 MHz, Q = 26 at 13 MHz, C = 64 pf and L = 2.3 μH. Hence (5.2) yields:

$$64 \ll C_1 < 640 \text{ pf} \qquad \ldots(5.5)$$

So, choose C_1 = 330 pf. From (5.3) the value of neutralization condenser is equal to 30 pf.

The final circuit diagram of the two stage FET preamplifier is shown in fig.5.5. Transistors Q44, Q45 are n channel junction FET's : TIS 59 (see Appendix B.3 for pertinent characteristics). L_{14}, L_{15} are Miller 4404 coils of unloaded Q of 60 at 7.9 MHz. L_{16}, L_{17} are RF chokes (Miller 4408 coils). The + 6 VDC power supply is applied through the Π type decoupling filter.

5.2.3. Wideband Amplifier:

This unit has been synthesized using RCA 3023 integrated circuit[16] which exhibits useful frequency range upto 40 MHz. (vide App. B.4 for relevant parameters). A buffer amplifier is necessary between the preamplifier and the I.C. chip because of different impedance levels. (see fig.5.6).

5.2.3.1. Buffer (fig.5.6):

This utilizes CIL911 transistor with f_T = 350 MHz. Since, frequency response of a transistor is better at higher bias currents, a collector supply voltage of + 18 VDC was chosen. The bias point selected is V_{CE} = 5 V. & I_E = 5 mA. The thermal stability factor, $S \doteq 8$. A smaller supply voltage like + 6 VDC will reduce the emitter resistor and hence make thermal stability correspondingly poor.

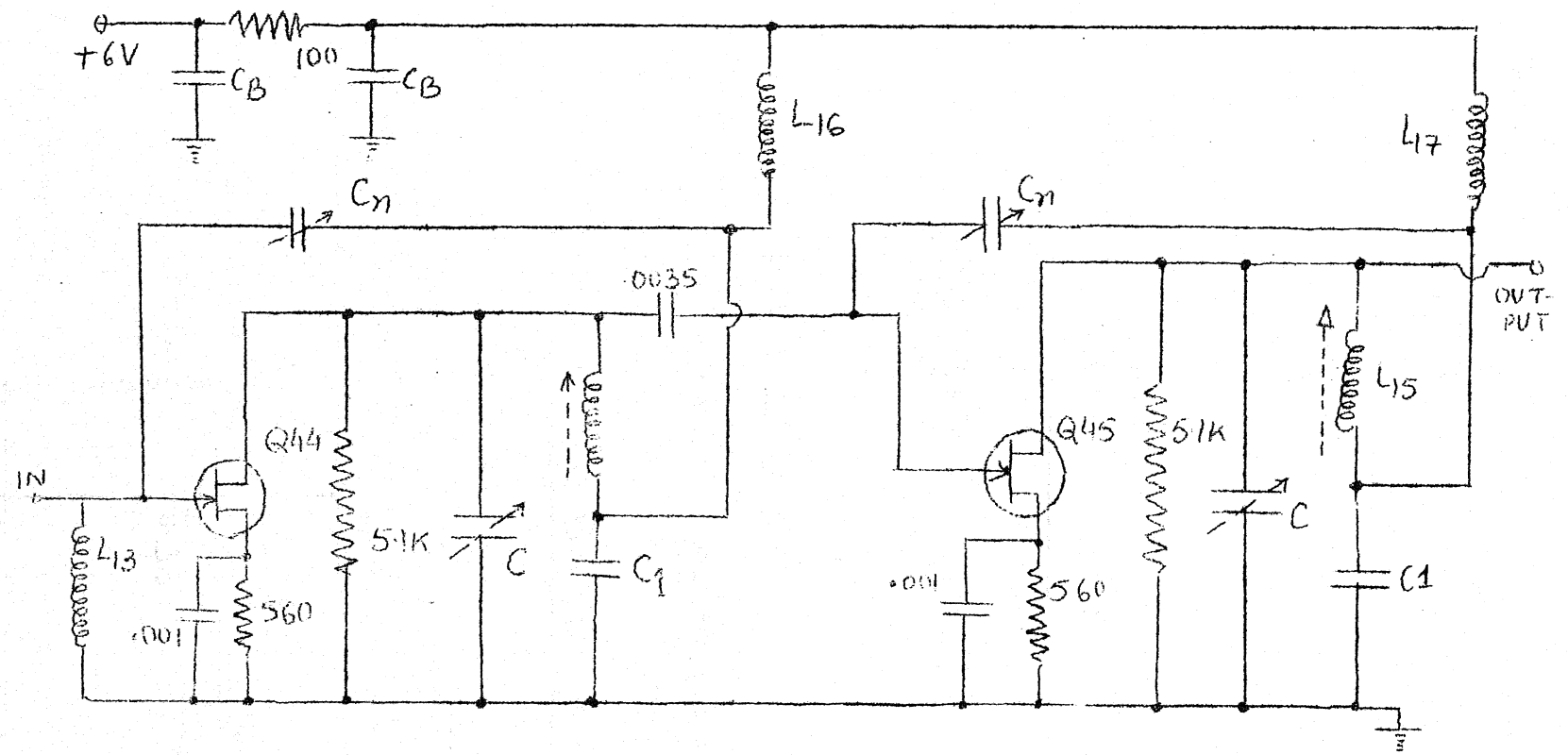

Q44, Q45	:	TIS 59	C	:	10–70 pf trimmer
C1	:	330 pf	C_n	:	7–30 pf parallel with 18 pf
C_B	:	3·3 nf	L_{13}, L_{14}, L_{15}	:	2·5 µH
			$L_{16}, 17$	:	RFC.

FIG. 5·5: FET PREAMPLIFIER.

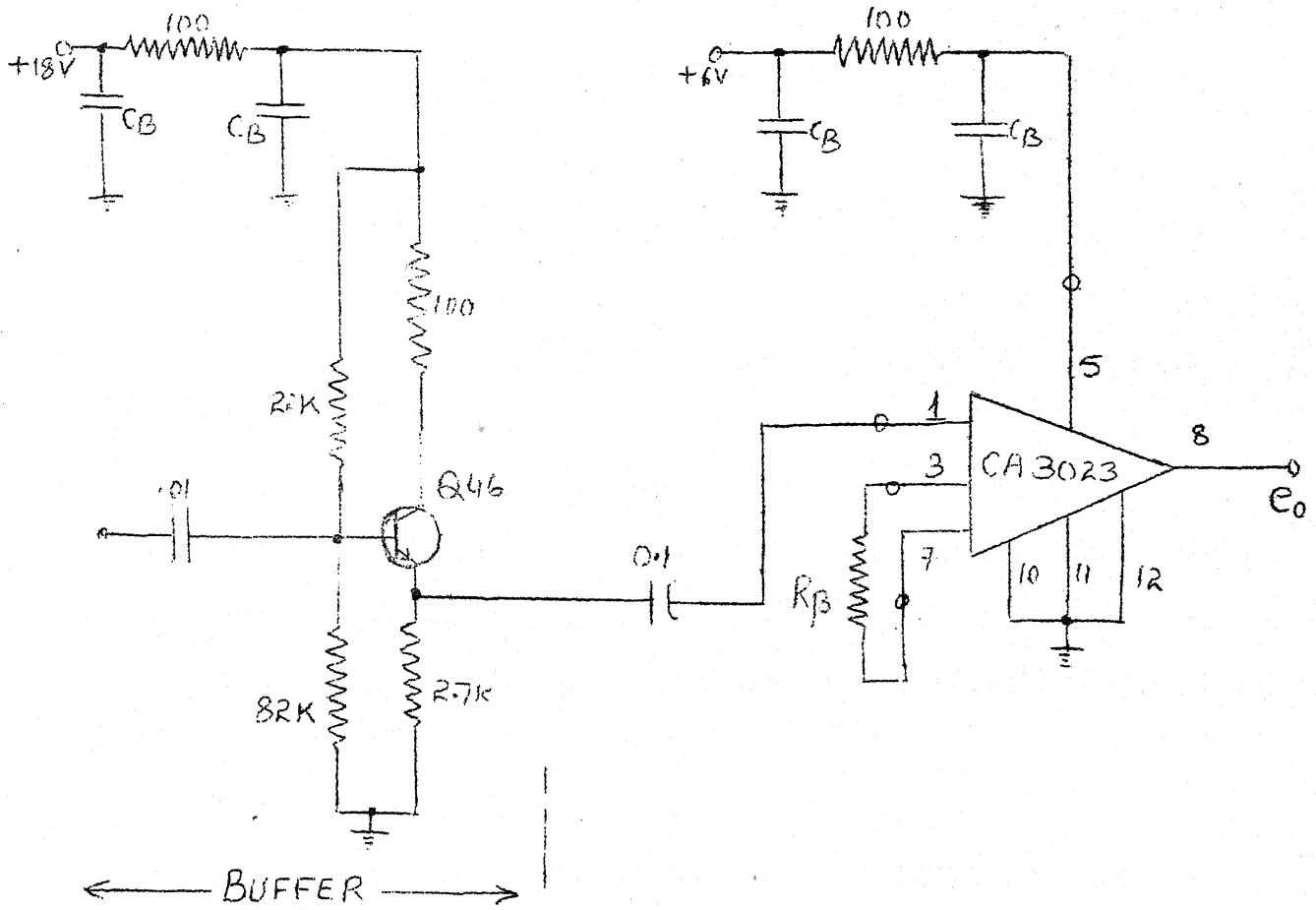

Q46 : CIL 911 C_B = 3·3 nf R_B = 2·7K, ¼ W

FIG 5·6: WIDEBAND AMPLIFIER

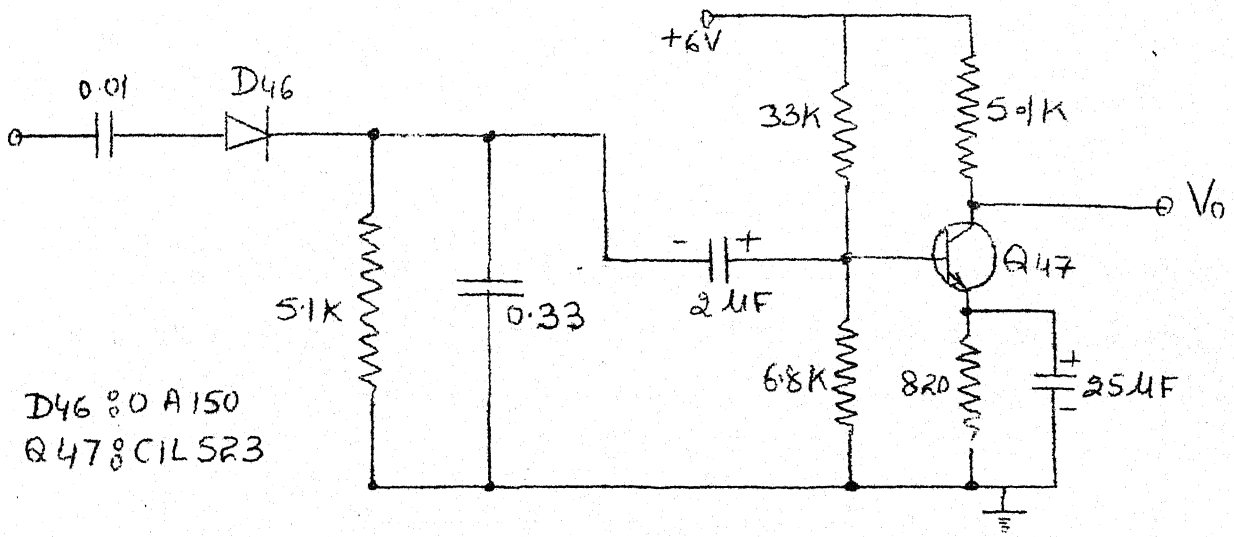

FIG 5·7: DETECTOR & AUDIO AMPLIFIER.

5.2.3.2. CA 3023 Unit:(fig.5.6)

Use of integrated circuit has simplified the design in this portion of the circuit. The value of R_F is decided by 2 factors:

(i) high value of R_β yields higher gain which may cause undesired oscillations.

(ii) low value of R_β causes reduction in gain because of feedback e.g. for R_β = 2.7 K gain at 13 MHz is 0.9 of the midband value. Voltage gain of wideband amplifier ≐ 40 dB.

Both the preamplifier and wideband amplifier are mounted on the printed circuit cards.

5.2.4. Detector: (fig.5.7)

A simple linear envelope detector is required. The diode D46 is OA150 (C_j = 2 pf, PIV = 50 V). The load resistor R_L = 5.1 K. The filter capacitor value is chosen according to[17]

$$R_L C \doteq (1 - m_a^2)^{\frac{1}{2}} / m_a w_m \qquad \ldots(5.6)$$

where, m_a = modulation index

w_m = maximum modulation frequency.

For, $m_a = \frac{1}{2}$ and w_m = 1 KHz, the value of capacitor needed is $\doteq \frac{1}{3}$ μF.

5.2.5. Audio Amplifier: (fig.5.7)

This stage uses a high gain transistor CIL523 (h_{FE} = 250) biased at $I_E = \frac{1}{2}$ mA & V_{CE} = 3 V with thermal stability factor, S ≐ 8. Collector power supply V_{CC} = + 6 VDC.

———— o ————

CHAPTER VI

DESIGN OF POWER SUPPLIES

The following regulated power supplies have been designed:

(i) + 6 VDC

(ii) - 6 VDC

(iii) + 230 VDC

(iv) + 180 VDC

(v) 1.3 Amp. DC

(vi) 6.3 VAC (unregulated)

(vii) - 20 VDC

(viii) + 15 VDC

(ix) + 45 VDC

The last three power supplies have been derived from the earlier ones. All of them are regulated except the filament supply. The 'power supply unit I' contains + 6 VDC, - 6 VDC & - 20 VDC supplies whereas + 180 VDC, + 230 VDC, 1.3 Amp. DC and 6.3 VAC supplies are housed in the "Power Supply Unit II". The "driver stage power supply unit" contains + 15 VDC and + 45 VDC supplies. Protecting fuses and indicating pilot lamps have been built-in at the appropriate places.

It is not intended here to discuss in detail the design of each and every supply as the designs are readily available elsewhere[19]. The detailed design procedure will be given for + 180 VDC supply and the salient features of others will be mentioned. The series regulator has been used throughout.

6.1 GENERAL DISCUSSION:

6.1.1. + 6 VDC & - 6 VDC Power Supplies (fig.6.1 & 6.2):

This designed is based upon Middlebrook's generalized power supply design[18]. The current capability of each is 1 Amp. although the acutal requirement is $<$ 250 mA. In - 6 VDC supply, D_{13} and D_{14} act as voltage doublers yielding an auxiliary supply for the zener D_{15}. The latter establishes a reference for a relatively constant current for the 'sense amplifier' Q_{32}. These supplies are needed in "Pulse generator", "Gated oscillator" and semiconductor version of the "receiver".

6.1.2. +230 VDC & + 180 VDC Power Supplies (Fig.6.3 & 6.8):

These two units have been designed on similar lines. Here the constant current to the 'sense amplifier' is supplied through transistors (Q_{33}, Q_{37}) instead of a resistor as in - 6 VDC supply (sec 6.1.1). The zener stack in + 230 VDC unit obviates the need for an input step down transformer. The diodes D25 & D40 protect the output series transistor against any transient voltage surges which otherwise may damage them. The current ratings are 100 mA each. + 230 VDC supply is needed in "Power Amplifier" 'driver stage power supply unit'. + 180 VDC supply is connected to the "tube-receiver".

6.1.3. 1.3 Amp. Supply (Fig. 6.4):

This supply is needed for providing variable regulated dc current to the gradient coils C', C" around the sample-coil (fig.2.1). Diode, D32 establishes the reference and the variable resistance R determines the various current values. The discrete variations in current (mA) are: 140, 240, 270, 300, 350, 410, 500, 660, 900, 1250.

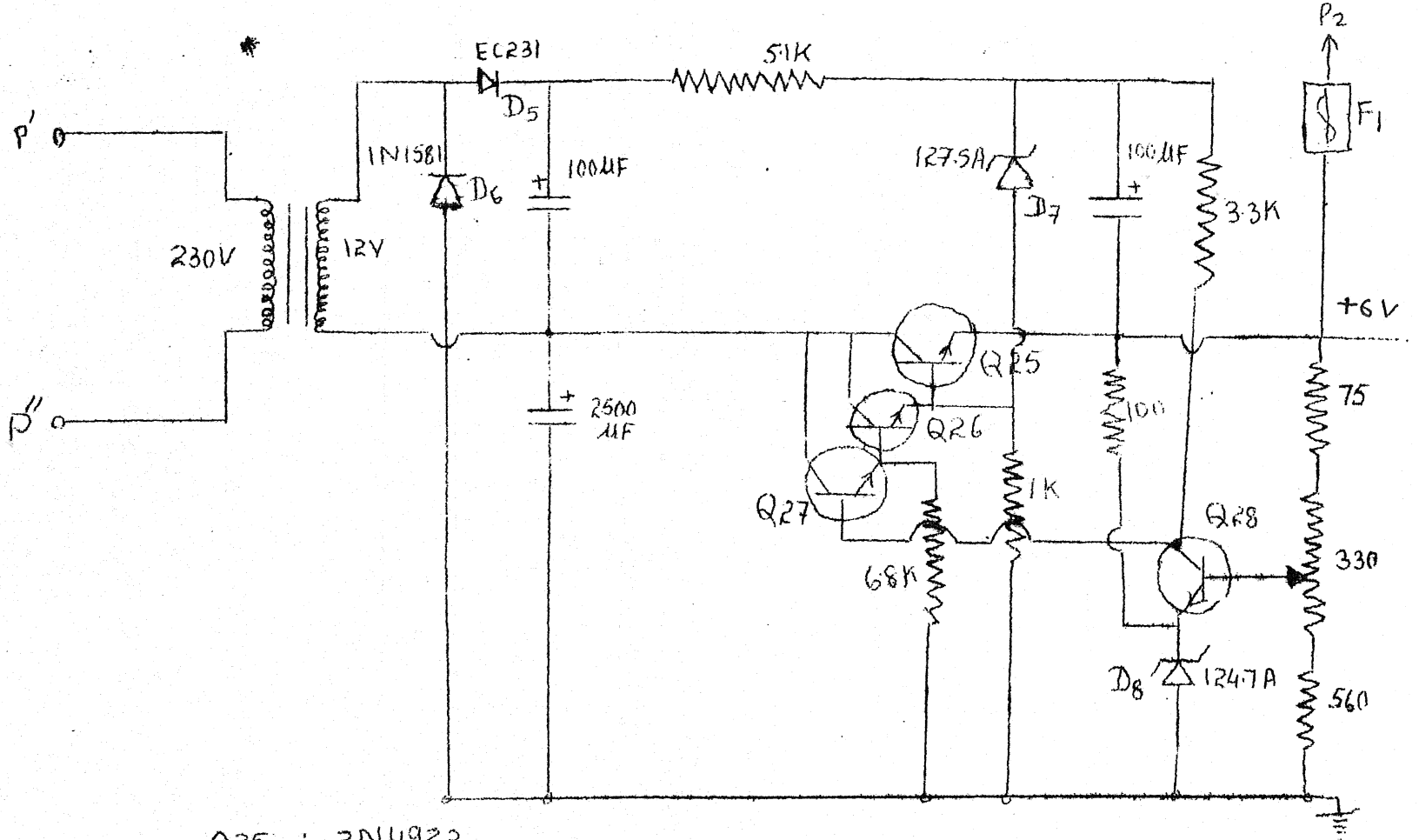

Q25 : 2N4922
Q26 : CIL461
Q27, Q28 : CIL473

F1 : 250 mA

FIG. 6·1: +6VDC SUPPLY

-6V AND -20V SUPPLIES

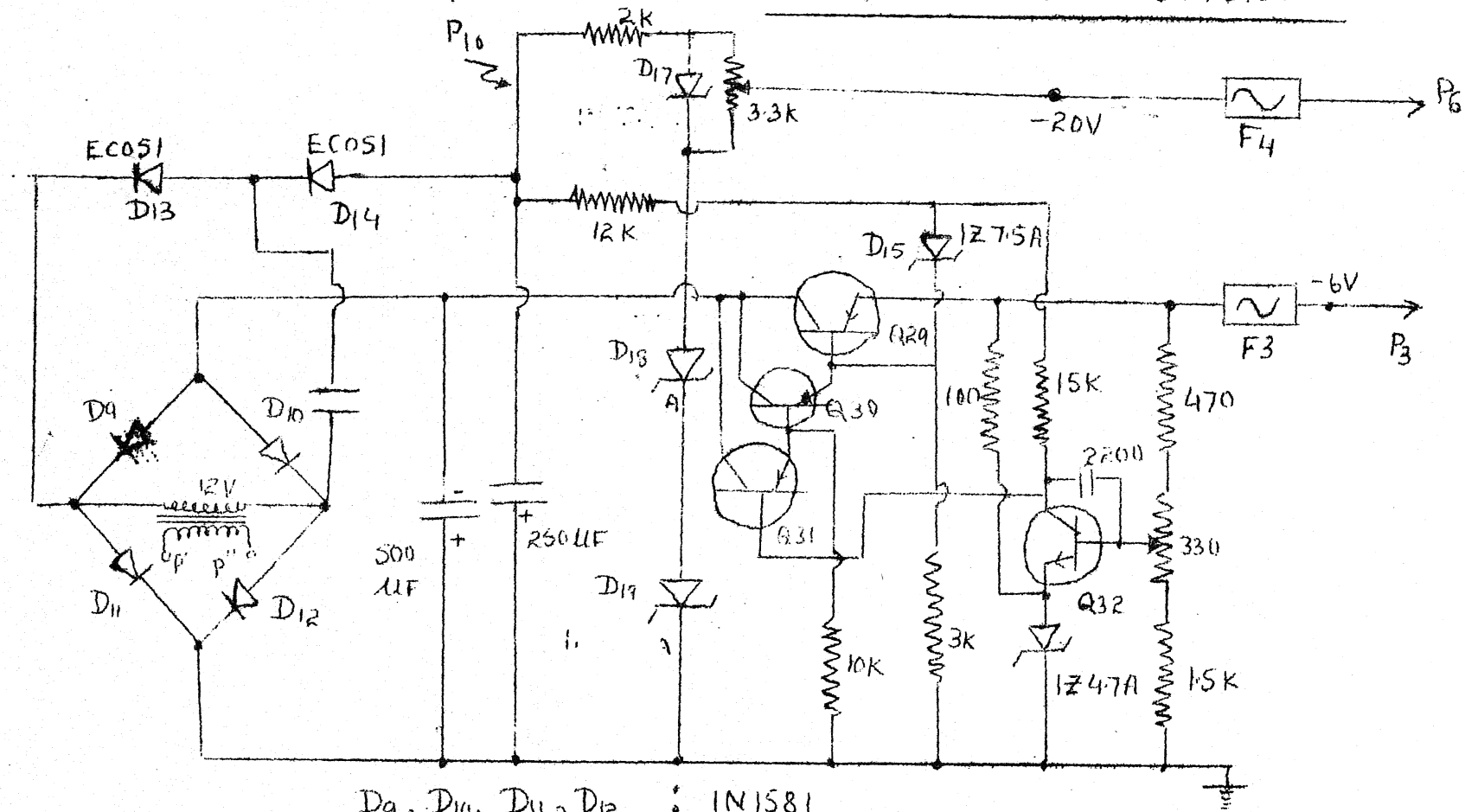

$D_9, D_{10}, D_{11}, D_{12}$: IN1581

D_{17} : IN522.6A

$D_{18,19}$: IN5240A

P6 : To Control Grid of $V_{1,2}$.

Q29 : 2N1905

Q30 : 2N1184

Q31 : 2N 321

Q32 : 2N599

F3 : 250 ma

F4 : 100 ma

FIG. 6.2.

FIG 6.3: + 230V DC SUPPLY

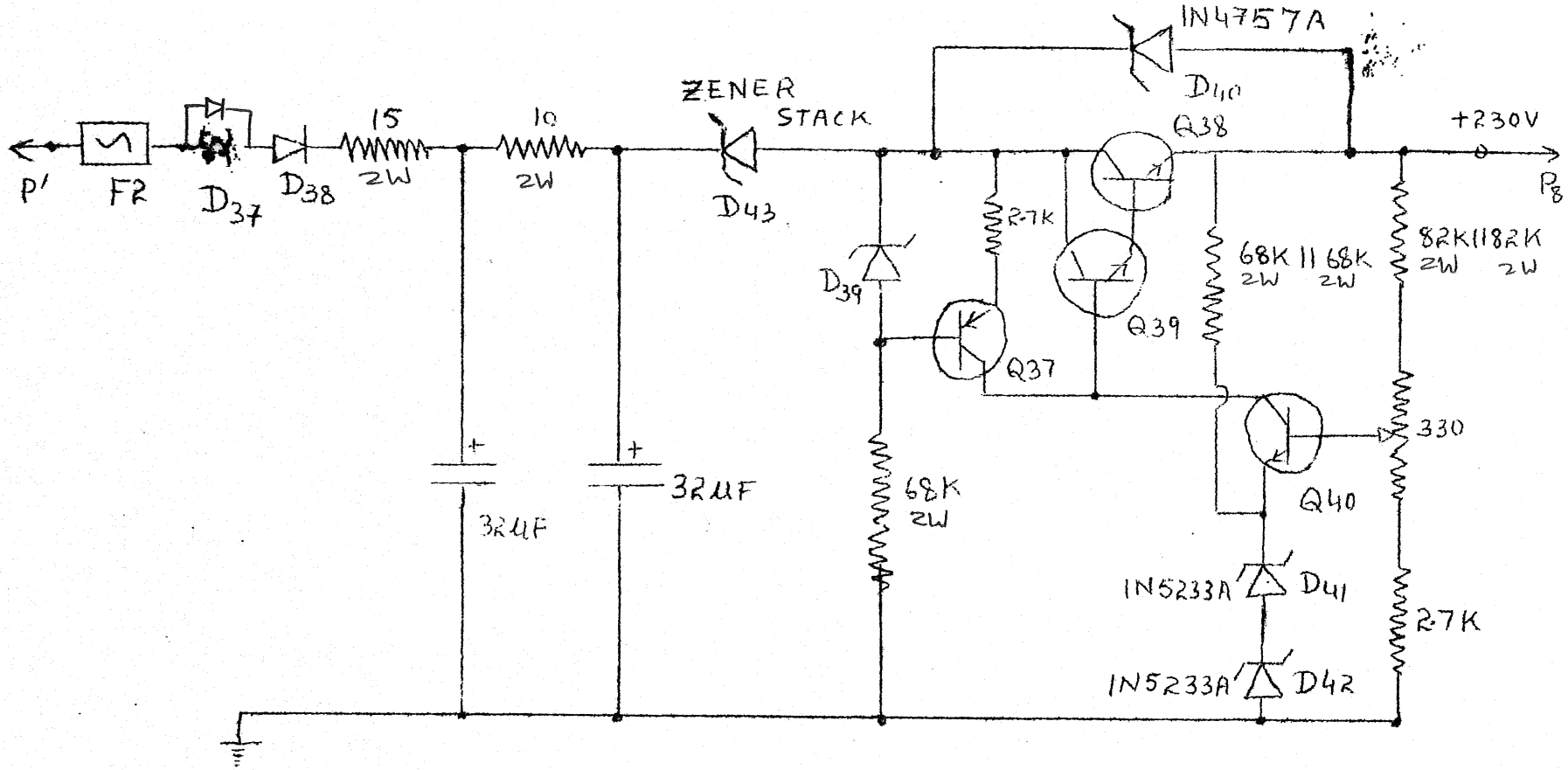

D_{37}, D_{38}	:	IN2071	Q38	:	2N4922
D_{43}	:	ZENER STACK	Q39	:	CIL621
D_{39}	:	SZ211	Q40	:	40426
Q37	:	2N2904	F2	:	500 ma

FIG 6.4: CURRENT SUPPLY

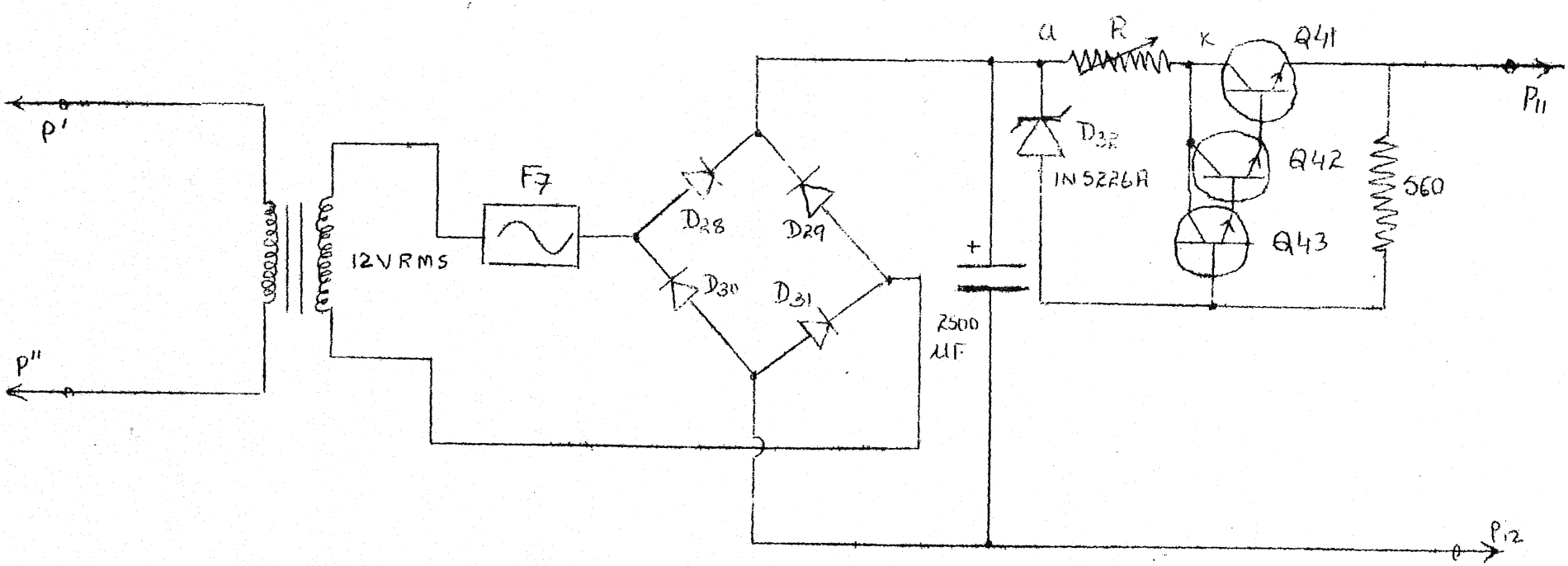

$D_{28}, D_{29}, D_{30}, D_{31}$: IN1581

Q41 : 2N297A

Q42 : 2N2904

Q43 : 2N363

F7 : 5A

$P_{11,12}$: To Gradient Coils

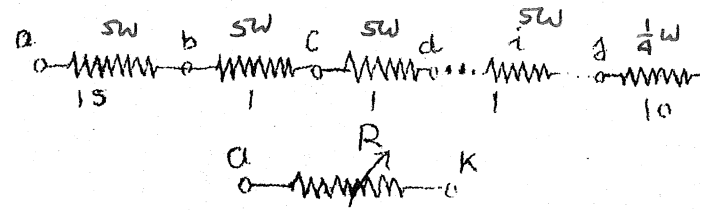

DETAILS OF R

6.1.4. The 6.3 VAC Supply:

This is just a step-down transformer of 5 Amp secondary rating. It is needed for tubes used in the "power Amplifier", (V_1, V_2) and the"tube-receiver" (V_3, V_4, V_5, V_6). The actual current required is (2 x .75 A + 4 x .175 A) = 2.2 Amp. AC (rms).

For keeping heater voltage constant, the input mains must also be regulated. Since this unit is readily available in laboratories, the separate regulator for the filament supply was not deemed necessary.

6.1.5. - 20 VDC Supply (Fig.6.2)

This unit supplies to the control grids of the transmitter tubes V_1 and V_2. The current requirement (as explained in the power-amplifier design, (sec 4.5)) is negligible and this makes it very easy to design from the doubler in the - 6 VDC supply (fig.6.2). Point P_{10} serves as the take off for this. The potentiometer across the reference zener, D_{17} allows this voltage to be varied from - 20 VDC to - 22.5 VDC.

6.1.6. Driver Stage Power Supply Unit: (Fig.6.5)

This provides two supplies of values + 15 VDC and + 45 VDC obtained from + 230 VDC regulated supply. It is needed for buffer, Q_{19} and driver stage transistors Q_{20}-Q_{22}. The current requirements are 4 mA and 5 mA respectively.

6.2 DETAILED DESIGN OF + 180 VDC SUPPLY[21]:

Output Voltage, V_o = + 180 VDC

Output Current, $I_o \leq$ 100 mA

Output transistor has to meet stringent requirements of high

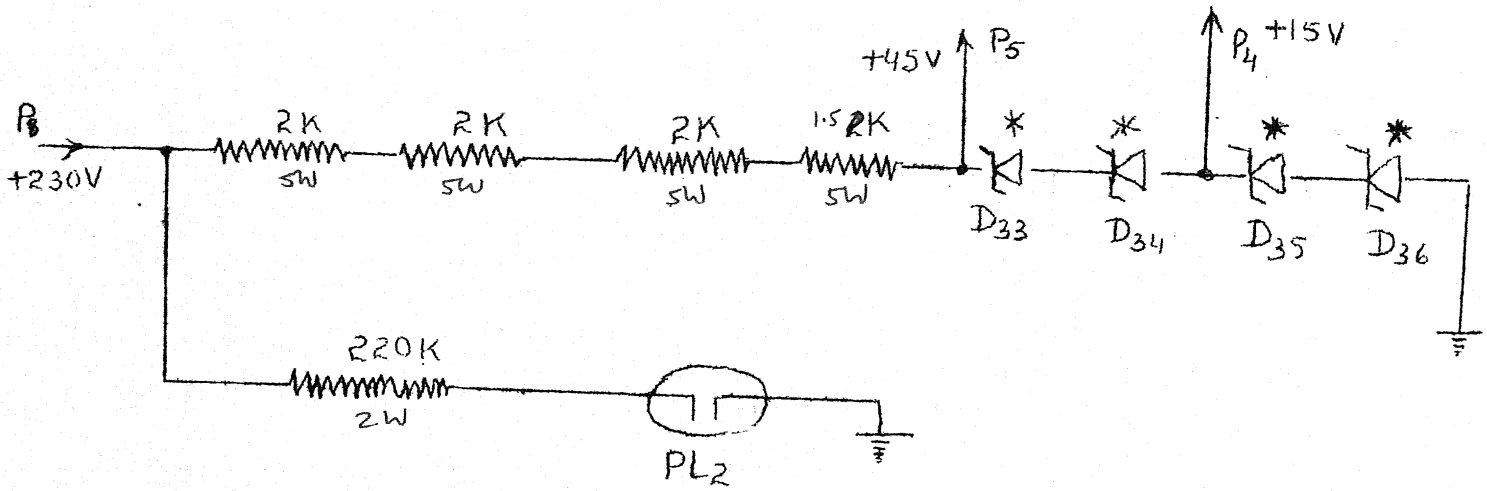

D_{33} , D_{34} : 3Z 15A

D_{35} , D_{36} : 3Z 10A & 3Z 4·7A

PL_2 : 65V NEON LAMP

P_5 : To DRIVER (Q20, 21, 22)

P_4 : To BOOSTER, (Q19)

FIG 6·5 DRIVER STAGE POWER SUPPLY

collector breakdown voltage and high collector dissipation. The availability of components dictates the suitable choice to be 2N4922 (BVCBO = 60 V and P_C = 30 W at 25° C case). Then, in fig.6.6

$$I_{B_1} \geq I_{E_1} / (h_{FE_1(min)} + 1) = 100/(20+1) \doteq 5 \text{ mA} = I_{E_2}.$$

The zener D_3' (fig.6.6) will limit $V_{CE_1} \doteq V_{CE_2} = 50$ V.

Then, $P_{C_1max} \leq 50 \times 0.1 = 5$ W

$P_{C_2max} \leq 50 \times 5 = 250$ mW.

Thus, heatsink for Q_1' should be designed to dissipate 5 W and still keep the temperature of the collector low enough to avoid thermal runaway. The two types of design are shown in fig.6.7. Table 6.1 gives information[11] regarding several transistor mounting materials.

Now, $I_{B_2} \leq I_{E_2}/(1+h_{FE_2})_{min} \doteq 5/40 = 0.175$ mA.

Let current source, I_{C_4} = 2 mA. Diode D_2' is chosen to have low breakdown voltage for small temperature variations[19], A breakdown voltage between 6 and 8 V will also cancel the -ve temperature coefficient of $\Delta V_{BE} / \Delta T$.

TABLE 6.1

THERMAL RESISTANCE OF SEVERAL TRANSISTOR MOUNTING MATERIALS

Insulating Washer Type	Typical Thermal Resistance θ_{CS} °C/W	
	Dry	with Silicone Grease
1. No insulator	0.20	0.10
2. Teflon	1.45	0.80
3. Mica	0.80	0.40
4. Anodized Aluminium	0.40	0.35

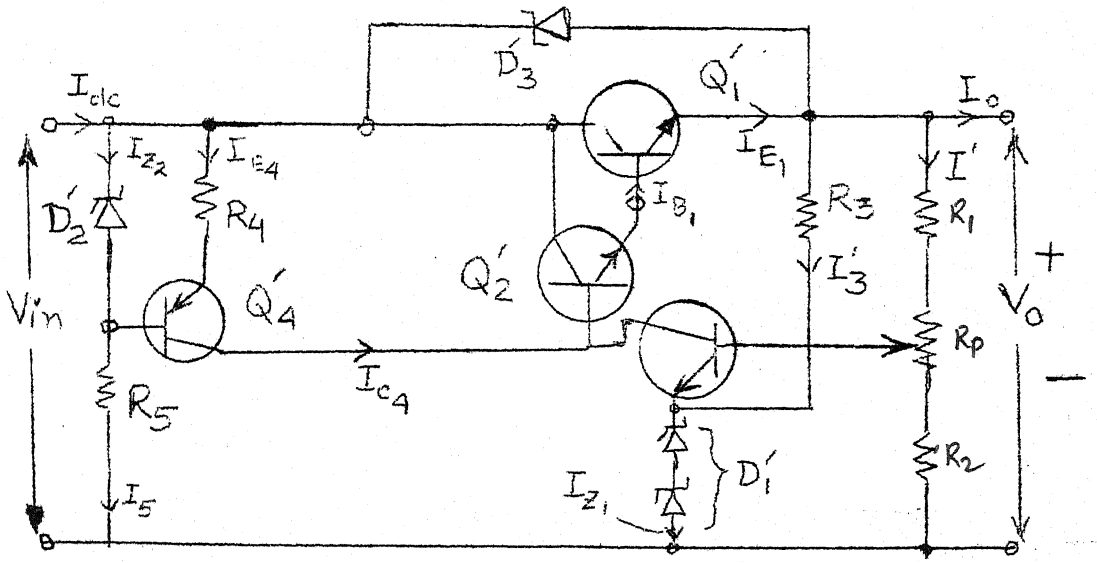

FIG 6.6 : REGULATOR CIRCUIT.

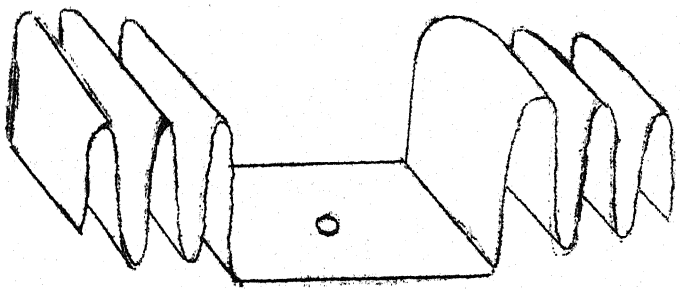

DESIGN I

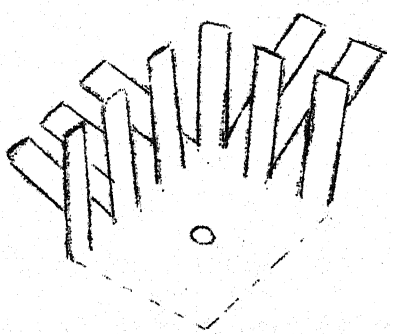

DESIGN II (ONLY HALF SHOWN)

FIG. 6.7 : HEAT SINK DESIGN.

Then, $R_4 = (V_{Z_2} - V_{EE}) / I_{E_4} = (6 - 0.6)/2 = 2.7$ K
and wattage is 6 x 2 = 12 mW. So use $\frac{1}{4}$ W.
Let 4 mA current flow through D_2', then assuming minimum drop of 10 volts across the output transistor,

$$R_5 \doteq (V_{in,(min)} - V_{Z_2}) / I_{Z_2} = ((10 + 180) - 6)/4$$
$$\doteq 45 \text{ K}.$$

The maximum current through R_5 will be:

$$I_{5\ max} = (V_{in,max} - V_{Z_2})/R_5 = ((50+180)-6)/45$$
$$\doteq 5 \text{ mA}.$$

The 'preregulator' transistor Q_4' must have BVCBO $\geq$ 60 V and collector dissipation $\geq$ 60 x 2 = 120 mW. The 2N2904 with BVCBO = 60 V and P_C = 600 mW (25°C) is suitable. The miniature heat sink is affixed to it.

The 'control transistor' should have BVCBO $\geq$ 180 V and $P_C \geq$ 180 x 2 = 360 mW. Either of the available transistors 2N3440 or 40426 is suitable.

The 'reference' for the high voltage supplies should consist of a stack of low voltage zeners instead of a single high voltage unit for small temperature variations. Two 6 V diodes in series have been used for this purpose. Resistor R_3 provides extra current (needed for the reference) which should be much large than the variations in current of the 'control transistor'. So, let I_3 = 5 mA, then

$$R_3 = (180 - 12)/5 = 33 \text{ K}.$$

The power dissipated = 168 x 5 = 840 mW. A parallel combination of two 2 W 47 K resistors has been used.

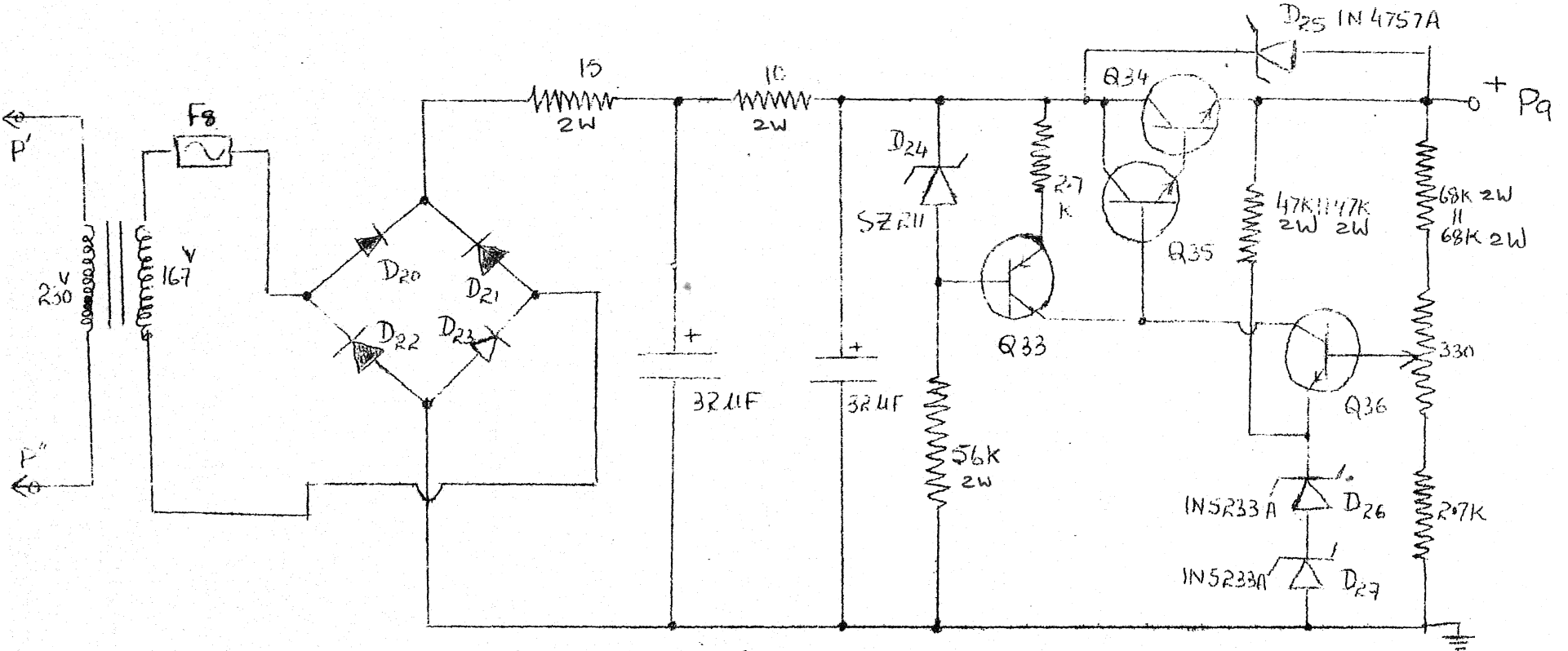

$D_{20}, D_{21}, D_{22}, D_{23}$: IN2071
Q33 : 2N2904
Q34 : 2 N 4922
Q35 : CIL 621
Q36 : 40426
F 8 : 500 mA

Pq : To Tube Receiver.

FIG. 6.8: + 180 VDC POWER SUPPLY

So, the current, $I_3 \doteq 168/24 = 7$ mA and therefore, $I_{Z_1} = 9$ mA. Hence power dissipation in each 1N5233A is $6 \times 9 = 54$ mW.

The 'comparison element' is designed to carry current of 5 mA, Thus

$$R_1 + R_2 + R_P = 180/5 = 36 \text{ K}.$$

Choosing $R_2 = 2.7$ K, $R_1 = 68\text{K}/2$ and $R_P = 330$ ohms satisfies the voltage drop requirement. Power dissipated in R_2, R_1 and R_P are 60 mW, 840 mW and 8 mW respectively. Resistors R_2 & R_P are $\frac{1}{4}$ W units and R_1 is parallel combination of two 2 W 68 K resistors. This completes the 'regulator' design.

The filter capacitors are 32 μF - 32 μF 450 VDC rating. The full wave rectifier comprises of four diodes which can be e.g. IN2071, IN4005 etc. (PIV = 600 V; $I_{dc,av} = \frac{3}{4}$ A & 1 A respectively). The rms value of the step down transformer is estimated as follows:

The output voltage of full wave rectifier (with capacitor) is approximated by[22]:

$$V_{dc} = V_m - (I_{dc}/4\,fC) \qquad (V_m = 2^{\frac{1}{2}}\, V_{rms}).$$

and peak to peak ripple is:

$$V_{PP} = I_{dc}/2\,fC.$$

Thus, for C = 64 μF, and current, $I_{dc} = (I_{Z_2} + I_{E_4} + I_3 + I' + I_o) =$ 120 mA. So,

$$V_{PP} = (120 \times 10^{-3})/(2 \times 50 \times 64 \times 10^{-6}) \doteq 18 \text{ V}.$$

and

$$V_m = V_{dc} + I_{dc}/4\,fC = (190 + 18) + 18/2 = 217 \text{ V}.$$

Thus, assuming no drop across diodes etc, the minimum rms output of transformer should be:

$$(V_{rms})_{min} = 217/2^{\frac{1}{2}} \doteq 155 \text{ V}.$$

The actual value is 165 V rms which was experimentally determined (by means of autotransformer) such that at full load current the output transistor never goes into saturation.

The conventional short circuit protection[23] afforded by two diodes across base to emitter junction of Q_1' is not needed because transistor 2N4922 can carry currents upto 1 Amp. The most crucial protection against voltage breakdown of Q_1' is provided by 51 V zener across collector and emitter terminals.

The 250 slow blo fuse F_8 at the input provides protection against overload. Another fuse of 100 mA (slow blow) rating can be connected at output for greater reliability. Some experimental data is given in table 6.2

The transformer design is outlined in Appendix C .

TABLE 6.2

I_o mA		0	50	60	77	100
For Q_1'	V_{CE} av volts	38	27	23	20	15
	P_C av W	0	1.4	1.8	1.5	1.5

o

CHAPTER VII

EXPERIMENTAL

The NMR experiment is perfouned using Varian Associates: V - 4502 - 12 system. This consists of a 9" rotating-base magnet, a V - 4501 console and the regulated power supply for the magnet.

7.1 PROCEDURE:

(1) The 'cooling water system' for the magnet is turned on.

(2) Power supply for the magnet is turned on. A minimum of half an hour should be allowed for the system to stabilize itself.

(3) The liquid to be investigated is poured in a test tube which is mounted inside the "sample coil".

(4) The gyromagnetic ratio for protons is 2.665×10^4 $gauss^{-1}$ sec^{-1}. Hence, the magnetic field required for oscillator frequency of 13 MHz is 3.06 K gauss. The field dial is set at this value.

The calibration of the magnet may be necessary to account for any error in the dial readings. This can be carried out by the fluxmeter, e.g. model F - 8A.

(5) The versatile C.R.O. Tek 454 is used for display. R.F. is connected to the channel A and the channel B is

used to monitor the NMR signal. Both the channels are used in DC mode. The "NORMAL" mode of triggering is employed, for which the synchronizing signal is taken from the output of the pulse programmer.

(6) The spectrometer is turned on by means of the switch S_1. (All the three pilot lamps must light at once). About one minute of warm up time is necessary for the tubes.

(7) The table 7.1 lists the various ranges of the time delay, period and pulse widths. The search for resonance is made as follows: The tuning knob is adjusted for maximum RF. The knobs T_D, T_R are put at position 1 with switch S_2 down. Then width of the $\pi/2$ pulse is gradually increased to observe the tail. If the signal is not observed, S_2 is switched to other position.

Now, it may be necessary to increase the delay between the pulses and repeat the previous procedure. Once the tail is observed, the $\pi/2$ width is adjusted to have the maximum signal. After this, the π pulse width is adjusted for maximizing the spin echo signal.

TABLE 7.1

Control of T_D, T_R, t_w

TIME DELAY		PERIOD		PULSE WIDTH		
Knob Position	T_D	Knob position	T_R secs.	Switch, S_2	t_w µs	2 t_w µs
1	70 - 230 µs	1	.10 - .425	S_2 "down	5-25	10-50
2	200 - 690 µs	2	.295-1.22			
3	.690 - 2.08ms	3	1.0 -4.05			
4	1.85 - 6.5 ms	4	2.8 -11.6			
5	5.6 - 19.4 ms	5	—	S_2"up"	25 - 50	50-100
6	13.6 -42.5 ms	6	—			
7	63 -200ms					
8	120 -355ms					

P.T.

In an experiment on water (with $MnSO_4$ added) the height of the spin echo pulse was 30 volts and it occupied a time slot of 0.2 m secs. The vertical and horizental sensitivities of channel B were at 20 V/cm and 0.2 ms/ cm respectiverly. The knobs T_D and T_R were at position numbers 2 and 1 respectively.

7.2 SIMULATION :

If the magnet is not available, the working of the instrument can be checked by a novel simulation technique. An RF signal generator is used to produce an induction signal in the coil by placing the signal lead end of the coaxial cable near the sample coil. The carrier is amplitude modulated internally and the detected sine wave is monitored on the CRO. The technique was extensively used for the actual testing of the spectrometer.

7.3 R.F. MONITORING:

A ceramic capacitor of value $\doteq$ 1.5 pf is soldered to the sample coil and the r.f. is detected at the other lead of the capacitor. This avoids loading of the tank circuit during monitoring.

———— o ————

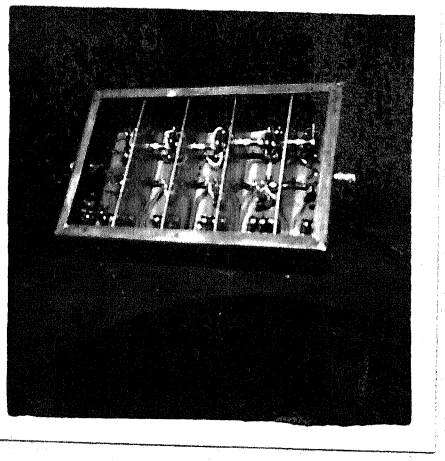

INSIDE VIEW OF THE TUBE - RECEIVER

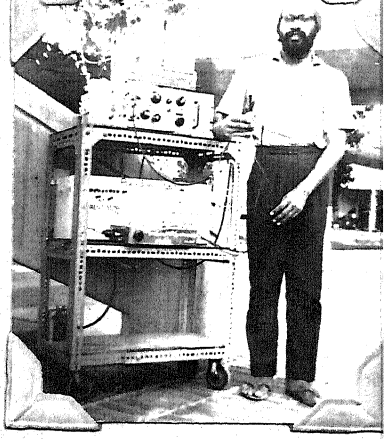

FULLY ASSEMBLED SPECTROMETER

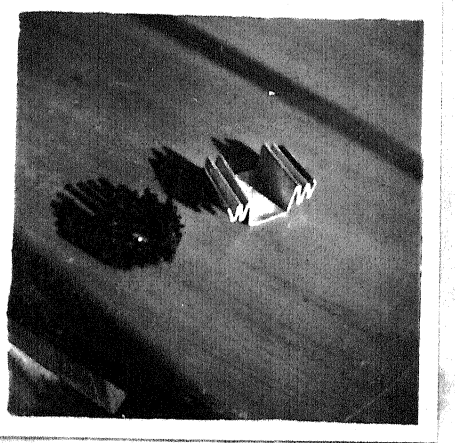

TWO TYPES OF HEAT-SINK DESIGNS USED

CHAPTER VIII

CONCLUSIONS

The previous chapters have described the design and performance of a 13 MHz Spin Echo NMR spectrometer. The most significant result of this design has been the achievement of infinite Carrier Suppression Ratio which is a major improvement over the existing instruments in terms of simplicity of circuit design & fabrication as well as the cost.

The gated oscillator configuration employed achieves two distinctive features. First, the rise and fall times of the pulsed waveform are independent of high Q of the crystal and second, the frequency-stability of the rf is controlled by the crystal itself.

Above advantages, are achieved at the cost of inability to employ the technique of "Coherent Detection". This, however, does not impose any limitation on the spin echo spectrometer to be used for liquid samples because neither the bandwidth of the signal is inconveniently large nor the signal to noise ratio at the input is less than unity.

A simple extension of the common emitter transistor amplifier circuit has allowed the design of the driver stage for class C power amplifier. Using the same concept, a solid state power amplifier has been proposed which utilizes

a recently discovered semiconductor device called as the 'overlay transistor'.

A new input coupling network to the receiver has been conceived in order to circumvent the compromises incurred upon by the single-coil technique. The band limited nature of the spin echo signal has been profitably exploited to achieve the acceptable output signal to noise ratio.

An important design limitation for the FET neutralized amplifier has been pointed out in the fabrication of the solid-state receiver.

The temperature stability of the individual blocks was constantly kept in mind during the design of the instrument. Adequate measures were taken to prevent the troubles arising due to the parasitic oscillations.

The flexibility of the instrument can be enhanced manifold by incorporating a few more digital modules into the pulse-programmer.

Reliability of the spectrometer has been given a major consideration during the design as well as the actual fabrication. More sophisticated protective mechanisms using thyristors can be provided.

Some analytical results and discussion about hardware aspects (with particular reference to the high frequency work) have been mentioned in the Appendices.

———— o ————

BIBLOGRAPHY

1. Valley, G.E., etal: vacuum tube amplifiers M.I.T. Radiation Laboratory Series, .18, chap 7 (Book). McGraw Hill, 1948.

2. Terman,F.E. Electronic and Radio Engineering, art 12.5. (Book) McGraw Hill, 1955.

3. Clark, W.G. "Pulsed Nuclear Resonance Apparatus". Rev. Sci.Instr. 35,316, 1964.

4. "Design of Inductors" Trans. A.I.E.E. 56, 1169, 1937.

5. Kitchlew, Anup & Rao, B.D.N. : A Spin Echo Spectrometer. Technical Rept No 1/70 Deptt. of Phys. I.I.T. Kanpur.

6. Manasse, F.K; etal : Modern Transister Electronics Analysis and Design. (Book) chap. 11. Prentic Hall, 1967.

7. Alley, C.L.; etal : Electronic Engineering (Book) Chap 12, John Wiley, 1966.

8. Chirlian, P.M. Electronic Circuits (Book) McGraw Hill, 1971.

9. Hunter, L.P. Handbook of Semiconductor Electronics. art 12.14, McGraw Hill, 1962.

10. RCA Transmitting Tubes. Technical manual TT - 5, p 46 - 50. R.C.A., 1962.

11. Sentz, R.E. Voltage and Power Amplifiers, Holt Rinehart & Winston Inc, chap 13, 11, 1968.

12. Pollak, V.L., etal : "Input Circuits for Pulsed NMR". Rev. Sci. Instr. 37, 268, March 1966.

13. Cobbold, R.S.C., Theory and Applications of F.E.T.'s. (Book) John Wiley., 1970.

14. Noll, E.M. F.E.T. principles, Expts & Projects. (Book) H.W Sams, Indiana-polis., 1968.

15. Singh, Ranjit and Viswanathan, T.R. "Bounds on Component values for neutralized F.E.T. amplifier" Electro Technology (India) 14, 171, Nov. 1970.

16. RCA Linear Integrated Circuits Technical Series I.C. - 42 (Book) p. 196, R.C.A., 1970.

18. Middle brook, R.D. : "Design of Transistor Regulated Power supplies". Proc I.R.E., 45, 1502, Nov 1957.

17. Gibbons, J.F. : Semiconductor Electronics (Book) McGraw Hill, 1966. art 7.6

19. Ashok, S. : Analysis and Design of Semiconductor Regulated Power Supplies. M.Tech Thesis : E.E. Deptt., IIT Kanpur, 1970.

20. Schwartz, S. : Selected Semiconductors Circuits Handbook., John Wiley, 1960.

21. Walston, J.A. etal. Transistor Circuit Design, Texas Instruments Inc. (Book) McGraw Hill, 1963, chap.9

22. Gibbons, J.F. : Semiconductor Electronics (Book) McGraw Hill, 1966. art 7.4.

23. Millman, J & Halkias, C.C. : Electronic Devices & Circuits (Book) McGraw Hill, 1967. chap.

———— o ————

GENERAL REFERENCES

The following list consists of references not cited in the thesis but were extremely helpful in the actual design and fabrication of the instrument.

1. Greenwood, I.A. Electronic Instruments. M.I.T. Rad. Lab. Series. 21. (Book) McGraw Hill, 1948.

2. Reference Data for Radio Engineers. 5th ed. International Telephone & Telegraph Corporation; 1969.

3. Hunter, L.P. : Handbook of Semiconductor Electronics, 3rd Ed., McGraw Hill, 1970.

4. Bloch, F.etal. : "The Nuclear Induction Experiment". Phys. Rev. 70, 474, 1946.

5. Hahn, E.L. : "Spin Echoes" Phys. Rev. 80, 780, Oct 1957.

6. CARR, H.Y. & PURCELL, E.M. : "Effects of Diffusion on Free Precession in NMR experiments". Phys. Rev. 94, 630, 1954.

7. Schwartz, J. "Spin Echo Apparatus" Rev. Sci, Instr. 28, 780, Oct 1957.

8. Pople, etal : High Resolution NMR (Book) Academic Press, 1969.

9. Luszczynski, K. etal : "Nuclear spin pulsed Apparatus". J. Sci. Instr. 36, 57, Feb 1959.

10. Blume, R.J. : "R.F. Gate with 10 carrier suppression". Rev. Sci. Instr. 32, 554, 1961.

11. Abragam, A. Principles of Nuclear Magnetism (Book) Oxford Univ. Press., U.K.,(1961).

12. Aubrun, J.N., etal : "Variable Frequency Spin Spectrograph". Electron. Lett. 2,214, June 1966.

13. Becker, E.D. High Resolution NMR (Book). Academic Press 1966.

14. Kitchlew, Anup : "Nuclear Spin Relaxation & Molecular Motion in Liquids". Ph.D Thesis, Dept. of Phys., IIT Kanpur., 1971.

Transmitter Design:

15. Tucker, D.G. : Transient Response of Tuned Circuits Cascades. Wireless Engg. 23, 250, Sep 1946.

16. Chance, B. etal : Waveforms. (Book) M.I.T. Rad. Lab. Series. 19. McGraw Hill, 1949.

17. Newhoff, H.R. Crystal Controlled MVBR Electronics 36, 60, Apr 12 (1963)

Componets:

18. Smith., J.R.G. : Elementary Telecommunications Practice: Chap 12 (Components used at Radio Frequencies). English Language Book Society, 1965.

19. A study of RF chokes, Electronics, 7, 121, Apr 1934.

20. Quartz Crystals. Lenkurt Demodulator, 13, July 1964.

Parasitic Oscillations & Shielding:

21. Venkateswaran, S, "Stability, Power Gain & Bandwidth of Linear active 4 pole networks, with particular reference to transistor amplifiers at high frequencies". Univ. of London, Ph.D. Thesis. June 1961.

22. Jorgensen, C.M. "Electromagnetic Interference Shielding Techniques". Electrotechnology May 1966, p 95.

23. E.W. & Wireless Engr. Jan 1931, p 18.

24. E.W. & Wireless Engr. Apr. 1934, p. 375.

25. E.W. & Wireless Engr. Dec. 1927, p 725.

26. Ferguson, J.G. : "Shielding in high frequency work". B.S.T.J., 8, 560 (1929).

27. FYLER, G.W.: "Parasitic & Instabilities in Radio Transmitters". Proc I.R.E. 23, 985, Sep 1935.

28. FYLER, G.W. : "Instabilities in Radio Transmitters", ibid, 24, 328, Feb 1936.

———— o ————

APPENDIX A

RELATION BETWEEN R.F. MAGNETIC FIELD AND R.F. VOLTAGE

The above relation forms the fundamental design equation for the spin echo apparatus. The derivation proceeds from calculation of magnetic field of a coil along its axis and then using the empirical inductance formula.

Consider the section of the sample coil of length b and radius r (All units mks unless specified) with turns per unit length = n. Then total number of turns is (Fig A.1)

$$N = nb \qquad \ldots \quad \ldots \quad (A.1)$$

Applying Biot and Savart low to a single turn coil, the expression for magnetic field at any point x on the axis is [**]

$$B = \mu_0 \, i \, r^2 \, / \, 2(r^2+x^2)^{3/2} \qquad \ldots \quad (A.2)$$

where i = total ampere turns.

The magnetic field contributed by an elemental length dx of the coil is then (fig.A.1):

$$dB = \mu_0 \, (i_0 \, n \, dx) \, r^2 \, / \, 2((r^2 + x^2)^{\frac{1}{2}})^3 \qquad \ldots \quad (A.3)$$

where, i_0 = rms ac current.

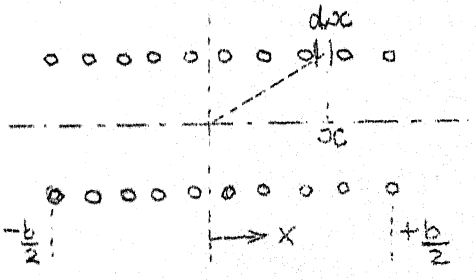

FIG A.1 COIL GEOMETRY

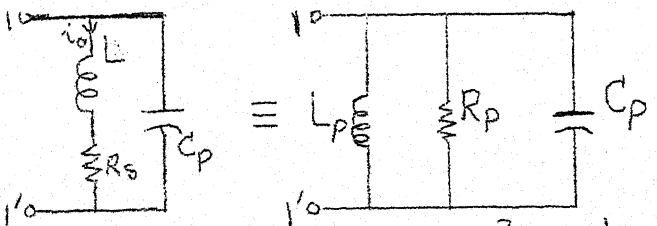

$R_p = R_s(1+Q^2)$, $L_p = L(1+Q^{-2}) \simeq L$

$Q = \omega_0 L / R_s = R_p / \omega_0 L = \omega_0 C_p R_p$

FIG A.2. SERIES- PARALLEL EQIVALENCE

** § 34.6 Halliday & Resnick. Vol.2.

APPENDIX B.1

USEFUL TUBE CHARACTERISTICS: 5763

Heater Volts	6V AC/DC
Heater Current	0.75 A
g_m	7000 $\mu\mho$
$\mu_{g_2g_1}$	16
C_{g_1p}	0.3 pf
C_{g_1k}	9.5 pf
C_{PK}	4.5 pf

Maximum Ratings	CCS	ICAS
Plate Input	10 W	15 W
Plate Dissipation	8 W	12 W
Plate voltage	250 V	300 V
Typical Operation (upto 30 MHz)		
grid resistor	39 K	18 K
grid 1 bias	-39 V	-42 V
Driving Power	0.05 W	0.15 W
useful power output	6.4 W	10.00 W

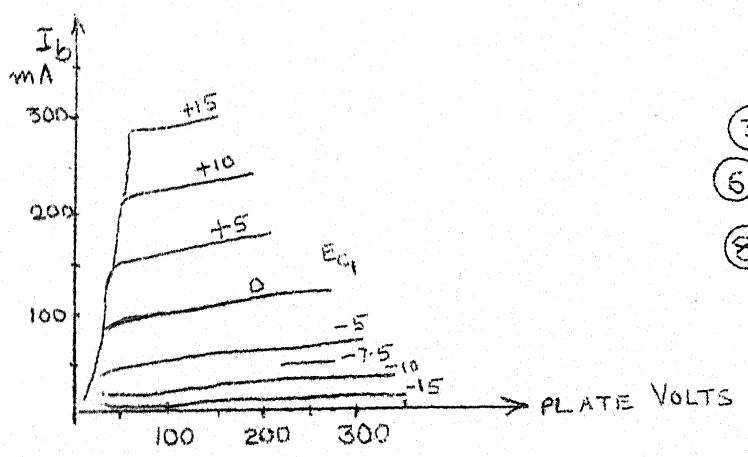

FIG B.1 : 5763 PLATE CHARACTERISTICS

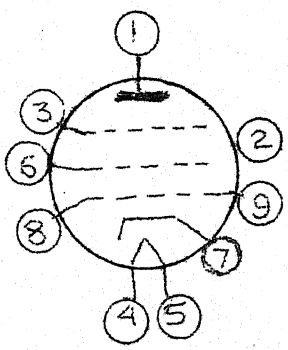

PIN CONNECTIONS

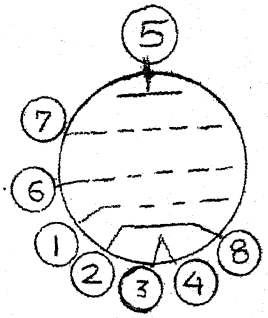

APPENDIX B.2

6AK5 CHARACTERISTICS

7 Pin miniature vaccum tube(pentode)
shorp cut off Pentode (upto 400 MHz).
Heater voltage = 6.3 VAC / dc.
Heater Current = 0.175 Amp.

C_{g_1p}	0.02 pf
C_{g1k}	4 pf
C_{pk}	4 pf

Characteristics Class A_1 Amplifiers:

E_b	120	180	V
E_{c_2}	120	120	V
R_K	180	180	Ohms
r_P	0.3	0.5	M Ω
g_m	5	5.1	m ℧
I_P	7.5	7.7	ma
I_{C_2}	2.5	2.4	ma
E_{c_1}	-8.5	-8.5	V (for I_b = 10 ua)

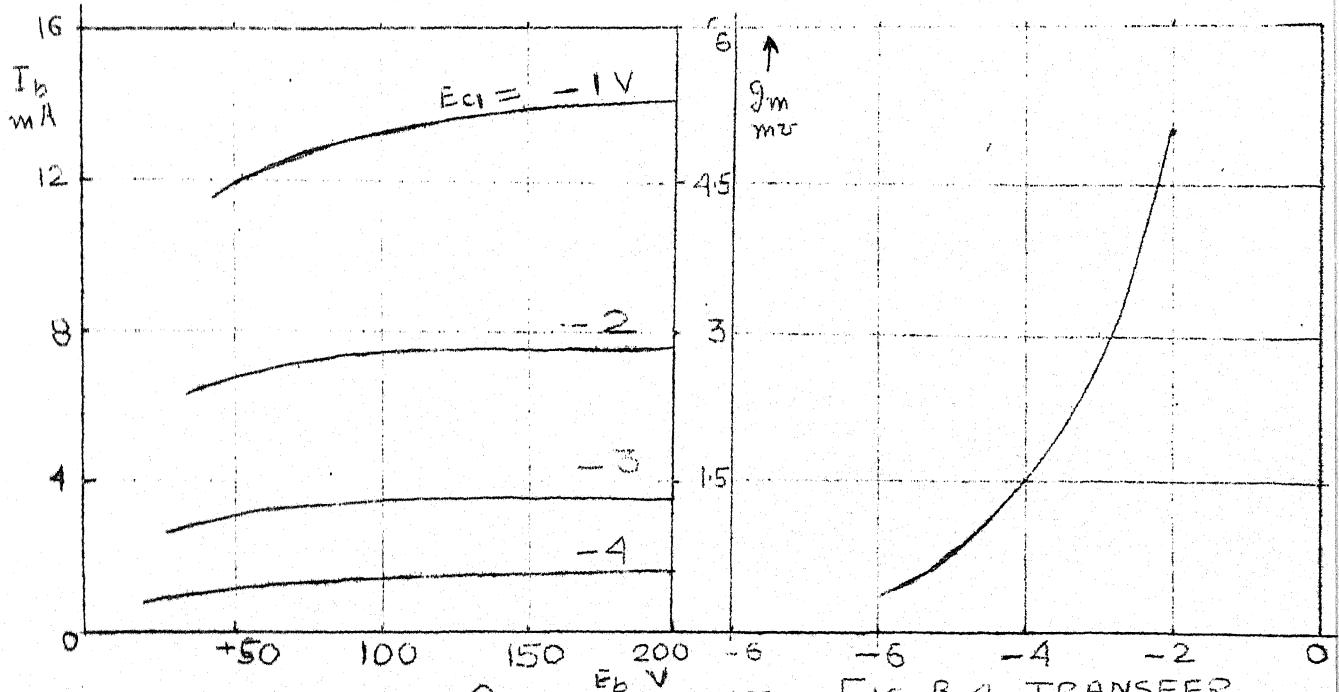

FIG. B-3 : PLATE CHARACTERISTICS.

FIG B.4 TRANSFER CHARACTERISTICS

APPENDIX B.3

TIS 59 FET CHARACTERISTICS. (N channel Junction Type)

FIG B.6
TIS59 - OUTLINE

At 13 MHz,

$y_{11} = \rho_{11} + j\,\sigma_{11} = 0 + j\,490\ \mu\mho$

$y_{12} = \rho_{12} + j\,\sigma_{12} = 0 - j\,245\ \mu\mho$

$y_{21} = \rho_{21} + j\,\sigma_{21} = 2 - j\,0.245\ \text{m}\mho$

$y_{22} = \rho_{22} + j\,\sigma_{22} = 50 + j\,245\ \mu\mho$

Maximum device dissipation in free air at 25° C = 200 mW.

Pinch off voltage $(V_P)_{max}$ = 9 V.

V_{DS} = 15 V

Absolute maximum ratings:

BVDSS = 25 V

BVGSS = 25 V

$I_{D(on)}$ = 25 mA

I_{GSS} = 4 nA

Parameters at 25°C, V_{GS} = 0V, V_{DS} = 15 V

g_{fs} = 2.3 to 5 m$\mho$

y_{os} = 50 $\mu\mho$

C_{is} = 6 pf max.

Derate in free air: 2 mW / °C.

APPENDIX B.4

CA 3023 CHARACTERISTICS

Frequency Range DC to 40 MHz.
Maximum input Signal ± 3 V.
Maxm ambient temperature range: - 55° to 125°C.

Device dissipation	35 mW		
Input Impedance	300	13 pf	) 4.7 K = R_β
Output Impedance	100		)
Noise figure	6.5 - 8.5 dB		

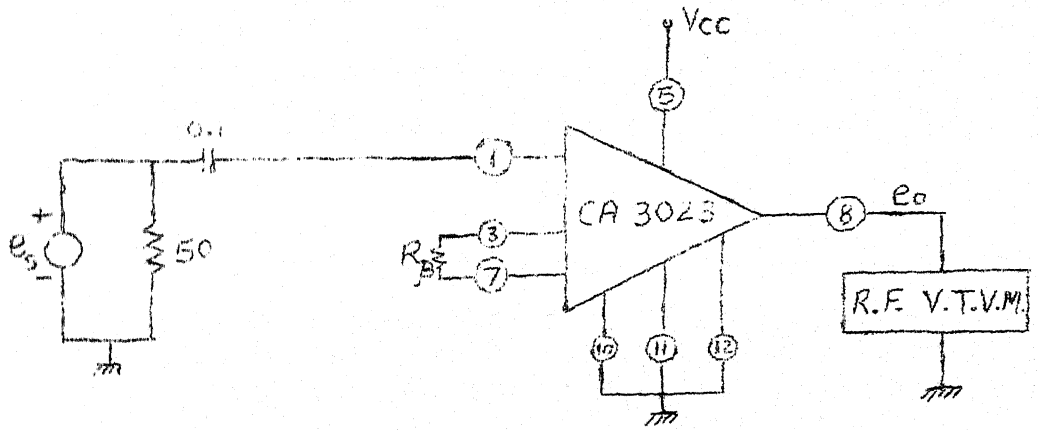

Fig. B.6 Amplifier Voltage Gain Test Setup

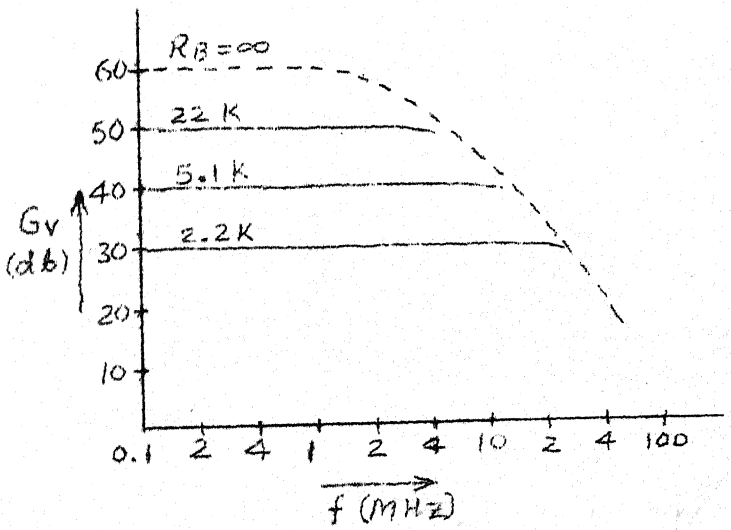

Fig.B.7 Frequency Response

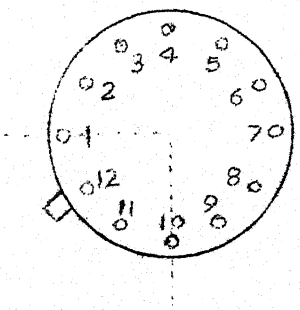

Fig.B.8 Outline

APPENDIX C

TRANSFORMER DESIGN

Ratings: + 165 V, $\frac{3}{4}$ A. (Secondary) (Fig 6-8)

(a) Volts/Turn $E_t = c\ (KVA)^{\frac{1}{2}}$, $c \doteq 1$, $KVA \doteq 0.13$

$\therefore E_t = 0.36$ V/Turn

(b) $\phi_{max} = E_t/4.44f = 0.00162$ Wb, f = frequency.

Let $B_{max} = 1$ Wb/m^2. Thus net sectional area of core is, $A_i = 0.00162$ m^2 = 16.2 cm^2

Therefore, gross sectional area, $A_g = 16.2/0.9$

$= 18$ cm^2

(c) Window Area, $A_w = (KVA)10^3/2.22\ f\ B_{max}\ A_i\ K_w$

where, K_w = winding factor $\doteq 0.5$

= Current density in Cu = 2.2 Mega Amp/m^2.

Thus, $A_w = 8.2.x\ 10^{-6}\ KVA/A_i = 6$ cm^2

(d) LT design

Turns, $N_2 = 165/.36 = 457$

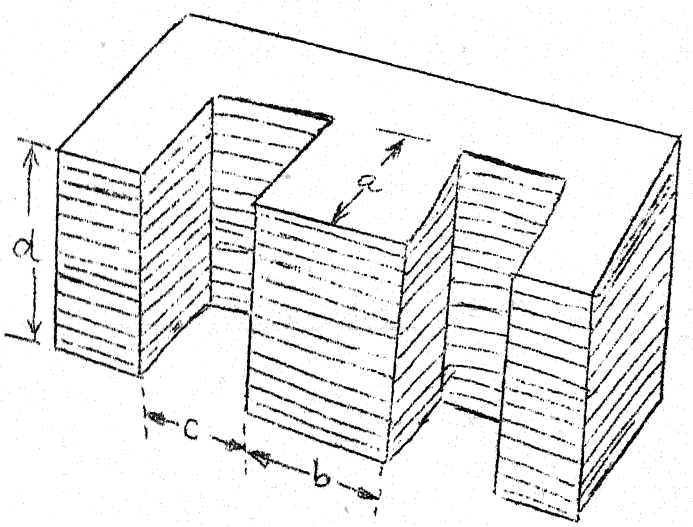

$A_w = a \times c$

$A_i = b \times d$

Fig. C.1 Window Area and Stacked depth of a Transformer Core

Current, $I_2 = \frac{3}{4} A$. Therefore, Cross Section,

$a_2 = \frac{3}{4}/2.2 \times 10^6 \quad m^2 = 0.34 \text{ mm}^2$.

From (Table C.1) wire gauge = 22.

(e) HT Design

Turns, $N_1 = 230 / .36 = 639$

Current, I_1 = KVA x 1000/V_1 x Efficiency = 0.66 Amp.

Therefore, Cross Section, $a_1 = 0.3 \text{ mm}^2$.

Hence, gauge = 23

For T_{13} stampings (fig.C.1), the stack depth $A_1/b = 18/3.15$ = 5.7 cm. The actual window area = a x c = 6.3 x 2.25 = 14.2 cm^2

TABLE C.1

WIRE GAUGE DATA

Gauge	14	15	16	17	18	19	20	21	22	23	24
Area mm2	3.24	2.63	2.07	1.59	1.17	0.811	0.66	0.52	0.397	0.29	0.245

12 V_{rms} 8 Amp Transformer Design Fig 6.4

(i) LT Design

Turns : 40

Gauge : 14

(ii) HT Design

Turns : 743

Gauge : 24

(iii) Stack depth = 5 cm (for T_{13} stampings)

APPENDIX D.1

PULSED RESPONSE OF TUNED CIRCUITS

Consider the parallel tuned circuit of Fig.D.1. Switch S is initially closed and opened at t = 0.

$$\therefore \quad V(s) = I(s)/\underline{Y}(s) = I(s)/(sC + 1/R + 1/sL)$$

$$= sRL\ I(s)/(s^2LCR + SL + R) \qquad \ldots (D.1)$$

Roots of the characteristic equation,

$$s^2LCR + sL + R = 0 \qquad \ldots (D.2)$$

are :

$$s_{1,2} = -(1/2RC) \pm j\,(1/LC - 1/4R^2C^2)^{\frac{1}{2}} \qquad \ldots (D.3)$$

The output voltage,

$$v(t) = L\ di/dt \qquad \ldots (D.4)$$

The current in inductor i(t) is

$$i(t) = A(\exp(-t/2RC))\ \cos\ (wt + \emptyset) \qquad \ldots (D.5)$$

The initial conditions are:

$$i(0+) = E/R' \qquad \ldots (D.6)$$

and

$$(di/dt)_{t\,=\,0} = 0 \qquad \ldots (D.7)$$

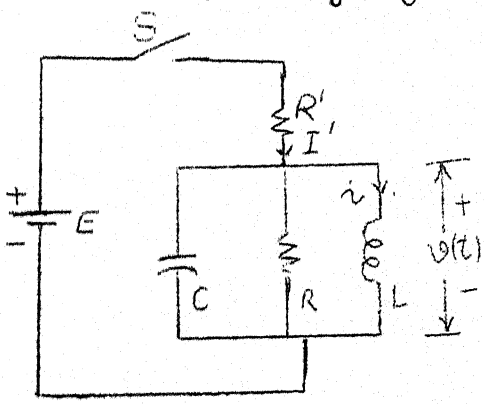

Fig. D.1 Parallel Tuned Circuit excited by a pulse.

This gives value of A & $\emptyset$ as:

$$A = (E/R^1)(1+(1/4w^2o^2R^2))^{\frac{1}{2}} \qquad \ldots (D.8)$$

$$\text{and } \emptyset = \tan^{-1}(-1/2wRC) \qquad \ldots (D.9)$$

Hence Eq(D.4) reduces to:

$$v(t) \doteq -(E/R')wL(\exp(-wt/2\ )).\sin wt \qquad \ldots (D.10)$$

$$\text{where, } Q \equiv wCR \qquad \ldots (D.11)$$

Thus, output is a damped sinusoid, the rate of damping being such that the amplitude is reduced to (1/e) of its initial value in Q/π cycles.

The relative amplitude can be expressed in terms of the number of cycles N as $\exp(-\pi N/Q)$. Let N be the number of cycles elapsed for the amplitude to be reduced by P%, then

$$\exp(-\pi N/Q) = 1 - (P/100) \quad \ldots (D.12)$$

or $$\ln(1 - P/100) = -N\pi/Q \doteq -P/100 \quad \ldots (D.13)$$

Hence, $$N \doteq PQ/100\pi \quad \ldots (D.14)$$

Thus with a crystal oscillator the oscillations cannot be quenched abruptly. This is because Q is so high that when gating waveform is applied the oscillation continue with any small decrements in amplitude. Consequently the conventional crystal oscillators are not suitable for gated oscillator synthesis.

APPENDIX D .2

ON THE USE OF CRYSTAL IN PULSED OSCILLATOR

The electrical equivalent circuit of a piezoelectric crystal is shown in fig.D.2a together with the impedance as a function of frequency.

The series and parallel resonance frequencies are related by

$$f_p/f_s \doteq (1 + C/C_h)^{\frac{1}{2}} \qquad \ldots \qquad (D.15)$$

For $f_s < f < f_p$, the impedance is inductive but capacitive else-where. The Quartz crystal can oscillate in any or all of the several modes, each of which has its characteristic frequency. There will in general be one mode that is more easily excitable than any of the others. However, it is possible for a coupling between the modes to exist so that excitation of one mode induces excitation of the other. This condition can be very troublesome in a pulsed crystal oscillator since it leads to an output voltage containing two or more frequencies

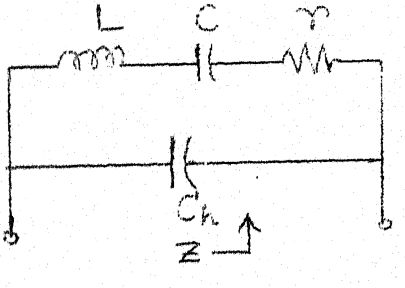

Fig. D.2a Equivalent Circuit of Crystal

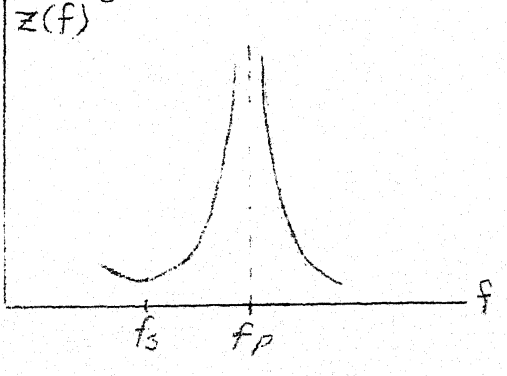

Fig. D.2b Impedance Function

which are <u>not</u> harmonically related.

The shifting of modes has been observed in the gated oscillator also. This phenomena however occurs only if the amplitude of gating pulses drops below the threshold value of 1.5 volts. Since the pulse-programmer gives pulses of fixed amplitude 4.5 V, this undesirable behaviour is of no concern.

APPENDIX D.3

OSCILLATOR BUILDUP ANALYSIS

It is instructive to examine the oscillator build up phenomena as takes place in the R.F. pulsed oscillators. The oscillator can be viewed as a feedback amplifier with special restrictions on A and β . Equivalently, it can be analyzed from negative resistance point of view. Fig. D.3 depicts the equivalent circuit suitable for analysis.

Now

$$V(s) = I(s)\, Z(s) = I(s)/Y(s)$$

$$= I(s)/(G_s + G + sC + (1/sL)) \qquad \ldots(D.16)$$

or $$V(s)/I(s) = (s/C)/(s^2 + s(G_s+G)/C + (1/LC)) \qquad \ldots(D.17)$$

The poles are located at

$$s_{1,2} = -(G_s+G)/2C \pm j\,(1/LC - (G_s + G)^2/4C^2)^{\frac{1}{2}} \qquad \ldots(D.18)$$

$$= -\alpha \pm j\, w_o'$$

Here $\alpha \cong (G_s + G)/2C$ is independent of inductance value but depends on the losses and hence on Q of the coil. The

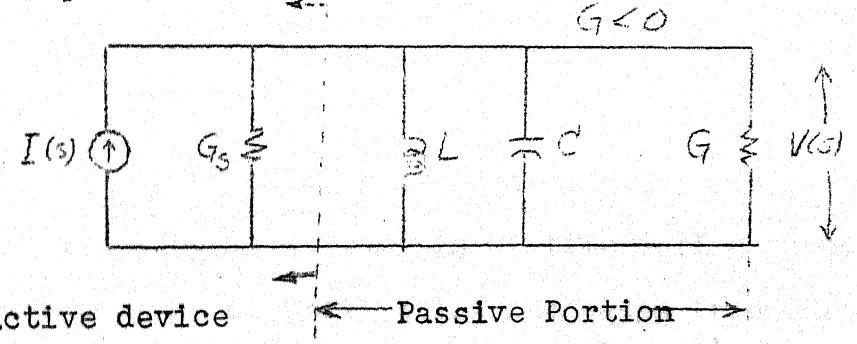

Fig. D.3 Model for Oscillator build up analysis.

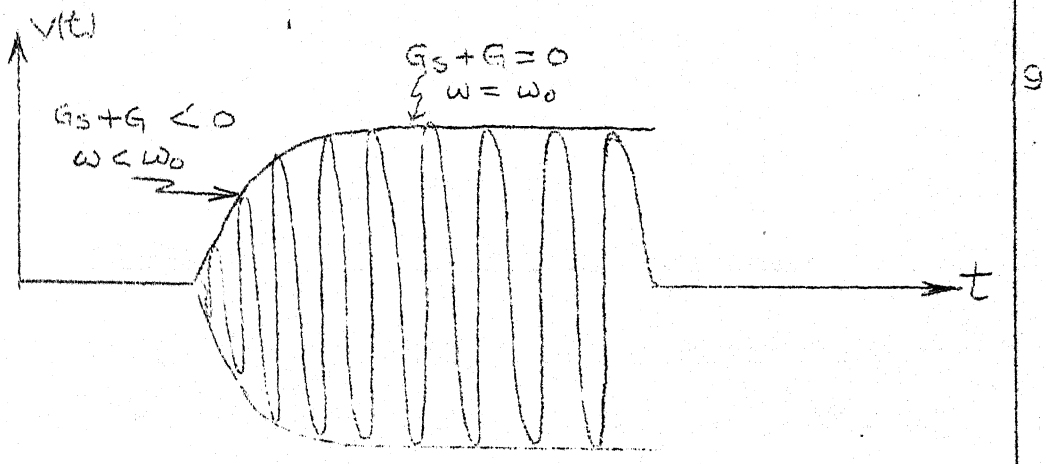

Fig. D.4 Oscillator buildup.

solution v(t) will be of the form:

$$v(t) = e^{-\alpha t}\,(A_1 \exp(jw_o' t) + A_2 \exp(-jw_o' t)) \qquad \ldots(D.19)$$

Hence for oscillations to build up $-\alpha > 0$.

or $\quad G_s + G < 0 \qquad \ldots (D.20)$

Thus $\quad G < -G_s \qquad \ldots(D.21)$

Now, the conductance G represents coil-losses and any external resistance. Eq (D.20) states the necessary condition that oscillations will build up if sum of the conductances in the parallel circuit is less than zero.

As the amplitude grows, the gain of the amplifier falls due to inherent nonlinearity. Physically, $(G_s + G)$ starts increasing from its initial negative value. The steady state is reached when

$$G_s + G = 0 \qquad \ldots (D.22)$$

This means G_s is a function of time during transients. Also the frequency of oscillation increases from initial value,

$$f = (1/2\pi)(1/LC - (G_s + G)^2/4C^2)^{\frac{1}{2}} \qquad \ldots (D.23)$$

to a steady state value,

$$f_o = (1/2\pi)(1/LC)^{\frac{1}{2}} \qquad \ldots(D.24)$$

This behaviour is summarized in Fig.(D.4).

APPENDIX E

SOME CONDLUSIONS ABOUT RF CHOKE DESIGN.

RF chokes are frequently needed in high frequency amplifiers for decoupling purpose. It is not immediately obvious which design will be optimum e.g. value of inductance, number of turns and physical layout of the winding all have remarkable effect on RF choke performance as an effective decoupler.

Q of the RFC should be large enough to avoid any significant RF losses. Ignoring the losses, the simplified equivalent circuit consists of an inductor in parallel with the parasitic capacitor. The self resonant frequency of this circuit should be larger than the operating signal frequency in order that the effective impedance is inductive. This implies that beyond a certain value it is no longer useful to increase the choke value. Mathematically:

$$w_o L C_{ex} < 1 \quad \ldots \quad (E.1)$$

and $$w_r L C_{ex} = 1 \quad \ldots \quad (E.2)$$

or $$w_r > w_o \quad \ldots \quad (E.3)$$

where w_r and w_o are selfresonant frequency of coil and the signal frequency respectively.

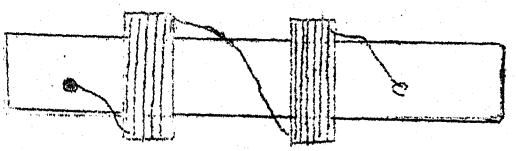

Fig. (E.1) π Winding

must have self capacitance $<$ 3 pf. This becomes particularly very importants for power amplifier where cables add their own capacitance. Thus the fundamental problem is to design RFC with as high an inductance as possible with small parasitic capacitance such that self resonant frequency of the combination is much larger than operating frequency.

Now inductance of a single layer winding is given as:

$$L = \mu n^2 r^2/(9r + 10l) \quad \text{microhenry} \qquad \ldots(E.4)$$

Where μ is the permeability of core, n the no of turns of winding, r and l are radius and length of core in inches. A larger inductance can be achieved by (i) increasing n (ii) increasing μ. Method (i) increases parasitic capacitance also. Method (ii) introduces some losses but a good quality powdered core is satisfactory for most applications. Also multilayer windings increase parasitic capacitance remarkably. π type winding as shown in fig. E.1 avoids this difficulty to some extent since now the parasitic capacitances are series.

The Q meter can conveniently be used to measure parasitic capacitance as small as 1 pf:-

The resonance is observed at two frequencies f_1 and f_2 :

$$w_1^2 L C_1 = 1, \; w_2^2 L C_2 = 1 \qquad \ldots.(E.5)$$

where $C_1 = C_{ex} + C_{d_1}$

$C_2 = C_{ex} + C_{d_2}$

where C_{d_1} and C_{d_2} are dial readings. If $w_2 = 2\ w_1$,

Then

$$w_2^2/w_1^2 = 4 = C_1/C_2 = (C_{ex}+C_{d_1})/(C_{ex} + C_{d_2}) \quad \ldots (E.6)$$

Hence,

$$C_{ex} = (C_{d_1} - 4\ C_{d_2})/3 \quad \ldots (E.7)$$

Here it has been tacitly assumed that over the frequency range $w_1 < w < w_2$ the parasitic capacitance is a constant quantity. This may not be true strictly. However the error incurred upon will not be too great if $(w_1+w_2) / 2 \doteq w_o$. Using single layer winding winding of gauge 30 wound on formers with ferrite cores, the author has been able to fabricate chokes as high as 75, μH with parasitic capacitance as less as 2 pf.

———— o ————

APPENDIX F

F.E.T. PREAMPLIFIER ANALYSIS:

BOUNDS ON COMPONENT VALUES OF NEUTRALIZING NETWORK

(Modified Approach)

Fig.(F.1) shows the basic FET amplifier configuration used in the preamplifier. Fig. F.2 depicts the equivalent circuit pertinent for analysis. Here, range of values permissible for the condenser C_1 used to develop the neutralizing voltage are deduced.

The neutralizing condenser C_n sends current i_n to

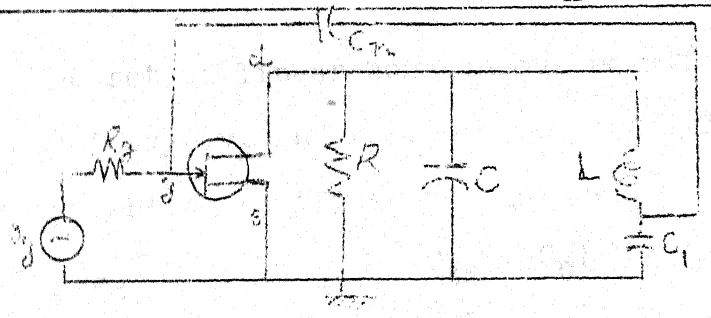

Fig(F.1) FET Neutralization scheme.

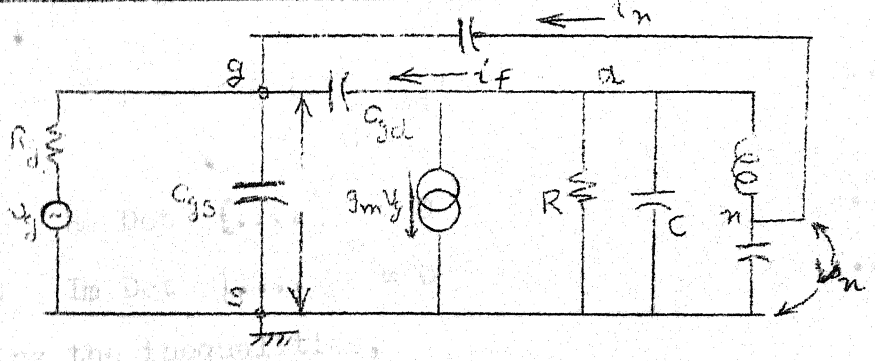

Fig.(F. 2) Equivalent Circuit.

cancel the undesired feedback through miller capacitor C_{g_d}.

Thus $i_f + i_n = 0$ ....(F.1)

These currents by ohm's law are evaluated to be:

$$i_f = (v_d - v_g)\ j\ w\ C_{gd} \qquad \ldots(F.2)$$

and $$i_n = (v_n - v_g)\ j\ w\ C_n \qquad \ldots(F.3)$$

Eliminating i_f, i_n from (F.1), (F.2) and (F.3),

$$C_{gd}\ v_d - (C_{gd} + C_n)v_g + C_n\ v_n = 0 \qquad \ldots(F.3a)$$

At node n and node d the KCL gives:

$$(v_d - v_n)/j\ wL = v_n\ j\ w\ C_1 + (v_n - v_g)\ jwC_n \quad \ldots\ldots\ (F.4)$$

$$i_f + g_m v_g + (v_d/R) + jwC\ v_d + (v_d - v_n)/jwL = 0 \qquad \ldots(F.5)$$

On simplification the result is:

$$v_d - w^2L\ C_n v_g + (-1 + w^2L(C_1 + C_n))\ v_n = 0 \qquad ..(F.4a)$$

$$v_d(1-w^2LC - w^2L\ C_{gd} + jwL/R) + (w^2LC_{gd} + jwL\ g_m)v_g - v_n = 0$$

$$..(F.5a)$$

The set of linear homogeneous equations (F.3a), (F.4a) and (F.5a) in v_d, v_g and v_n can have nontrivial solution iff the determinant of coefficients vanishes, i.e.

$$\begin{vmatrix} C_{gd} & -(C_{gd} + C_n) & C_n \\ 1 & -w^2\ L\ C_n & -1+w^2L(C_1+C_n) \\ u+jwL/R & w^2LC_{gd} + jwLg_m & -1 \end{vmatrix} = 0 \qquad \ldots(F.6)$$

where $u \triangleq 1 - w^2\ L\ (C + C_{gd})$ ... (F.7)

Also,

$$\text{Re Det } [\ldots] = 0 \qquad \ldots\ (F.8)$$

and $$\text{Im Det } [\ldots] = 0 \qquad \ldots\ (F.9)$$

On using the inequalities,

$$1 >> w_o^2\ L\ C_{gd} \qquad \ldots\ (F.10)$$

and $$1 << w_o^2\ L\ C_1 \qquad \ldots\ (F.11)$$

The equation (F.8) after simplification reduces to:

$$C_n \doteq \frac{w_o^4 L^2 C_{g_d}^2 C_1 + C_{g_d} (1 + u w_o^2 L C_1)}{2 w_o^2 L C_{g_d} - 1 - u w_o^2 L C_1} \quad ..(F.12)$$

For realizable values of C_n we have from (F.12):

$$2 w_o^2 L C_{g_d} > 1 + u w_o^2 L C_1 \quad ... (F.13)$$

which simplifies to

$$w_o^2 L C > 1 \quad .. (F.14)$$

and is true since the effective inductance is now reduced due to presence of C_1. Next, Eq(F.9) yields on using (F.10) and (F.11), another expression for C_n :

$$C_n \doteq w_o^2 L C_1 C_{g_d} / (1 - (w_o^2 L C_1 / g_m R)) \quad ... (F.15)$$

Consequently,

$$1 > w_o^2 L C_1 / g_m R \quad ... (F.16)$$

Eq(F.16) yields the upper bound on C_1 as

$$C_1 \lesssim g_m RC \quad .. (F.17)$$

The lower bound is evident from fig. (F.1) to be:

$$1/jw_oC << jw_oL$$

or

$$C >> 1/w_o^2 L \quad .. (F.18)$$

Combining (F.17) & (F.18) the allowable set of values for C_1 is found to be

$$\boxed{(1/w_o^2 L) << C_1 < g_m RC} \quad ... (F.19)$$

This result is identical to the one reported by author using a simplified model. [Ref 15, p 82]

APPENDIX G.1

COMPONENTS USED AT HIGH FREQUENCY

The proper choice of components is very essential for the successful high frequency work.

G.1.1. RESISTORS:

Wire wound resistors are very stable with respect to changes with temperature than composition type resistors but unless the special winding method have been used (e.g. Ayrton-Perry, fishline) they contribute appreciable self inductance and self capacitance which makes them unsuitable for high frequency work. Hence, wherever the resistance of power rating $\leq$ 1W is required composition Type are suitable. It is to be kept in mind that composition type resistors are subject to noise due to variations in resistance from intermittent contact between particles.

G.1.2. CAPACITORS:

Electrolytic and paper condensers are unsuitable because they became inductive at high frequencies. Ceramic, mylar, polyster, mica are of low loss, high breakdown strengh and stability. But mica can become self resonant at about 10 MHz (depending on capacitance value) whereas some special ceramic condensers are usable even upto 1 GHz. One of the most desirable types is the silvered mica. It has low temperature coefficient of capacity, low power factor, and very low parasitic inductance. However, ceramic condensers, owing to large dielectric constant are very compact, small sized units for even as large a value as 0.1 μF. Also due to negative temperature coefficient of

ceramic capacitors, some compensation can be made for the positive coefficient of coil inductance. Also, the high secular stability of ceramic is a very desirable property.

The condensers with air as dielectric became necessary for tuning purposes.

Colour bands are used for pin-up type ceramic capacitors, whereas 6 coloured dots in 2 rows are employed for silvered mica capacitors. The former is decoded in the usual way as is for resistors, with the first significant figure away from the leads whereas latter is read with arrow to the right.

G.1.3 INDUCTORS:

Since the capacitors used are of very small losses, the unloaded Q of a resonator depends almost entirely on the Q of the coil. The coil must have low parasitic capacitance and a high unloaded Q.

The form of inductance coil most frequently used in RF circuitry is the single layer solenoid, although powdered iron cores are sometimes necessary for a larger inductance or variable inductance. The self inductance and the resistivity vary with frequency because of proximity and skin effects. Since the resistivity of a conductor varies rapidly with temperature, the inductance of a coil may be very sensitive to temperature changes even though no appreciable change occurs in its dimensions.(This may be as high on 100 ppm/°C). For reducing skin-effect two methods used are: (i) Silvered surface. (ii) use of sheet copper straps. A thick copper

wire (e.g. 18 gauge) is necessary for high Q. These thick wire coils can be made self-supporting also.

R.F. Chokes necessitate the use of multilayer winding. Wave winding and Bank winding can be profitably employed for minimizing self capacitance.

G.1.4. CONNECTING LEADS:

Connecting wires should be as short as possible. The thicker wire has less inductance. 16 gauge bare copper wire is used for making an effective "ground" running in the chasis. It is not desirable to worry about the layout-apperance as one does at low frequencies.

G.1.5. COAXIAL CABLES:

The coaxial cables are used to transfer energy from one point to the other which are physically separated. The reactance for lengths less than quarter wave length is capacitive . This can become troublesome at some places in the circuit. Hence out of the available kinds, the lower capacitance per feet type is selected:

TABLE G.1

Cable Type -RG-	Capacitance pf/ft	Z_0 (Ω)
58/U	28.5	53.5
8/U	26	50
59/U	21	73
62A/U	13.5	93
71/U	13.5	93
63/U	10	125
79B/U	10	125
73B/U	10	125

RG62A/U has been used instead of RG79B/U because latter is too thick and stiff.

———— o ————

APPENDIX G.2

CHASIS LAYOUT & OTHER IMPORTANT FABRICATION ASPECTS

The justification for including this note is as follows: the success of the high frequency circuits is almost entirely dependent on how much care has been observed in the chasis layout. The important points are summarized:-

(i) Chasis material must be highly conductive. Copper chasis is the best, if available. Aluminium does not lend itself on any soldered "ground" on the chasis. Mild steel chasis with cadmium electroplating is satisfactory for most applications.

(ii) No unnecessary holes should be drilled into the chasis. The different stages should be shielded against one another by dividing the chasis into compartments. (e.g. see tube receiver photograph)

(iii) Effective grounds are made by first scratching the chasis (to make it rough and expose clean surface) heating it for a minute by solder iron (at least 125 W) and then touching the heated portion by the solder wire.**

(iv) Proper soldering is very essential: avoid dry joints. For this, the parts to be soldered must be sandpapered before the process. External flux is not necessary since solder wire contains it already. Any residual flux must be cleaned by Trichloroethyleve (or any organic solvent) since otherwise the dust deposited in course of time introduces noise.

** OR in case of Aluminium chasis, a thick copper wire is run as a bus bar.

(v) Tubes must be used with the shields (preferably spring type) to avoid undesirable RF coupling to other parts in the circuit.

(vi) If two or more coils are mounted on the some card, their axis should be held mutually perpendicular.

(vii) The power supply leads must enter or leave the chasis by means of ceramic feed through capacitors to decouple the finite, nonzero power supply impedance.

(viii) Use of Multipin plugs is very convenient for the connections to and fro for the various boxes.

(ix) 19" rack and panel arrangement is suitable for power supply units. (Fig.G.1)

(x) Ground lead and power supply leads are elegantly fabricated using 14 or 16 gauge bare Copper wire. The thick wire is more reliable than ordinary 22 gauge wire which may break off easily.

(xi) Adequate protection should be provided against vibration by using rubber feet or hard sponges.

(xii) Printed circuits should be used as far as possible because of their numerous advantages.

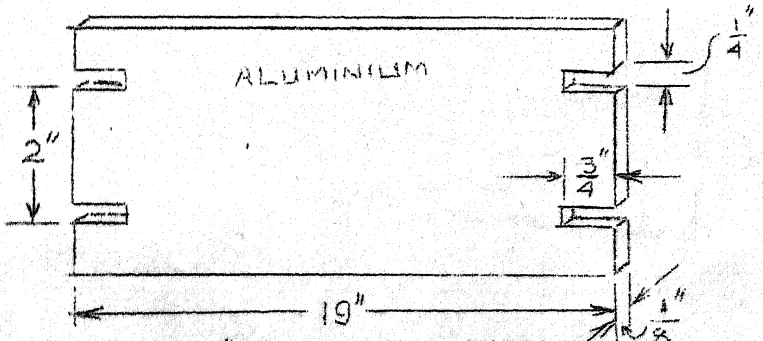

FIG. G-1 : 19" RACK & PANEL DESIGN FOR FRONT SIDE.

13 MHz SPIN ECHO NMR SPECTROMETER

PULSE PROGRAMMER

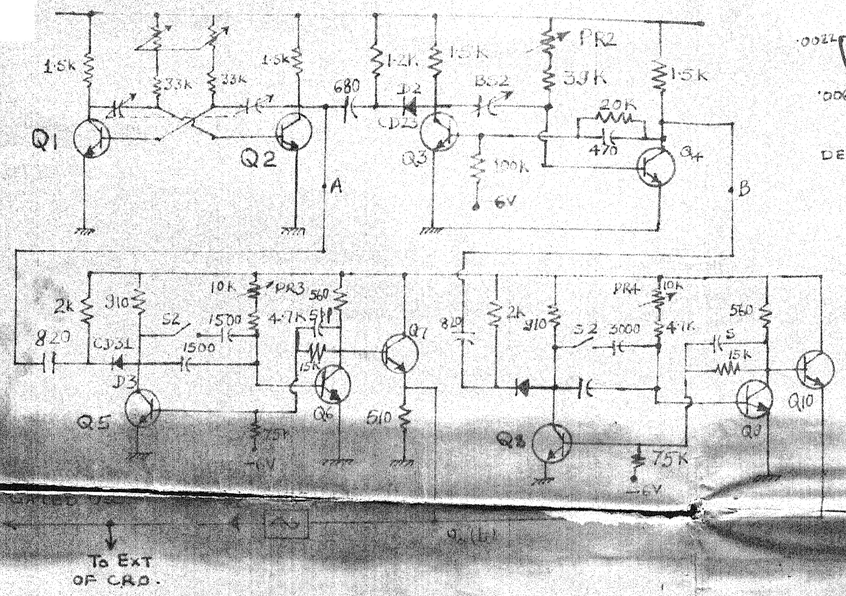

$Q_1 - Q_4$: CIL 523
$Q_5 - Q_{10}$: CIL 732

NOTE
RESISTORS IN OHMS UNLESS SPECIFIED.
CAPACITORS : < 1 in μF
> 1 in pf

POWER SUPPLY UNIT I

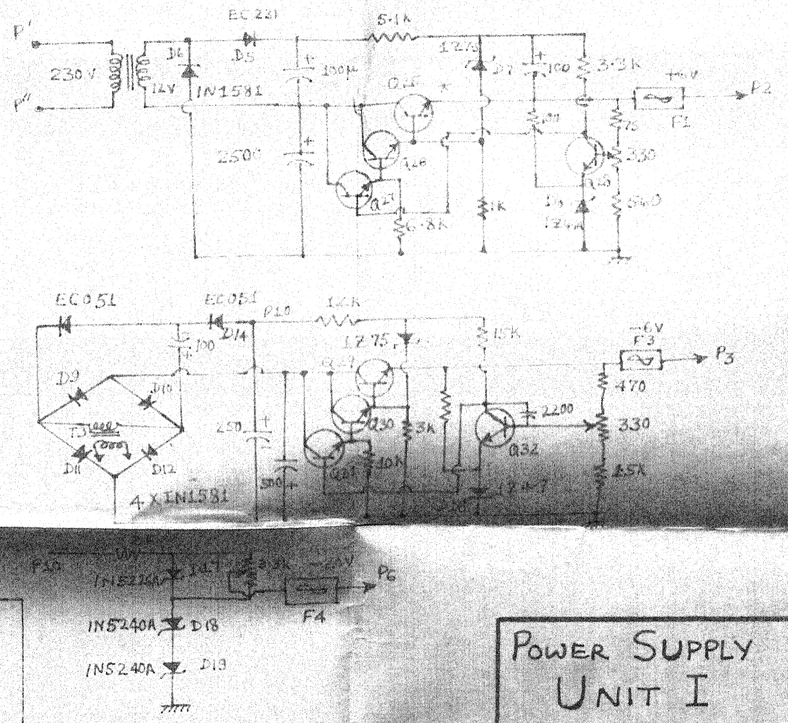

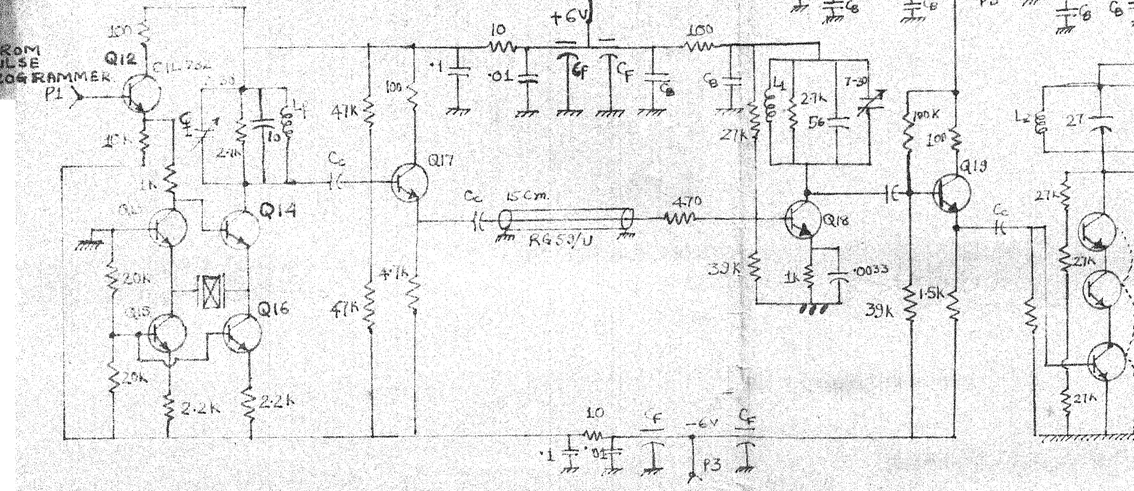

$V_{1,2}$: 5763
$V_3 - V_6$: 6AK5

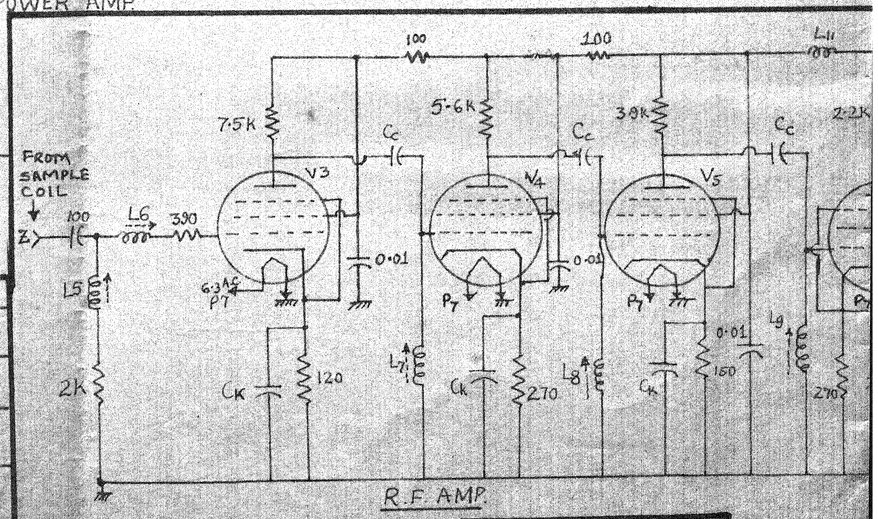

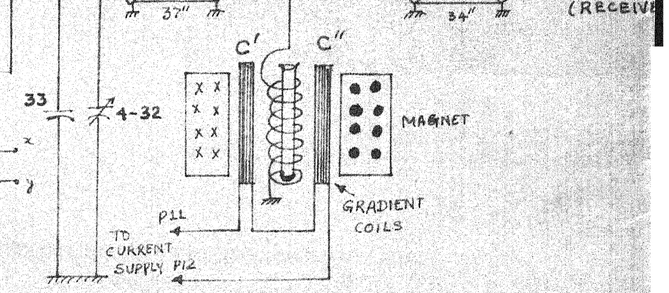

Q12, Q13, Q14, Q17, Q18 :— CIL 732
Q15, Q16 :— CIL 701
Q19 :— CIL 769
Q20, Q21, Q22 :— 2N 918
Q23, Q24 :— 2N 1990

C_F = 2300 PF = 0·0023 μ
C_B = 0·0033
C_C = 0·0033

FOR Q25 TO Q43 see back.

FUSE DATA	
F1	1/4 A
F2	1/2 A
F3	1/4 A
F4	1/10 A
F5	1/10 A
F6	2 A
F7	5 A
F8	1/2 A

COIL DATA

S.N.	L_f	L_1	L_2	L_3	L_4	L_5	L_6	$L_{7,8,9,10}$	$L_{11,12}$
VALUE μH.	2·8-5	1·58	1·78	14·1	1	65	70	9·5	5-9
Q	60	200	210	33	200	55	55	60	60
REMARKS	MILLER #4504	11 TURNS	12 TURNS	RFC	8 TURNS	—	—	NOMINAL VALUE	MILLER #4505

DEPTT OF
M.TECH TH
SEP. 19

POWER SUPPLY UNIT I

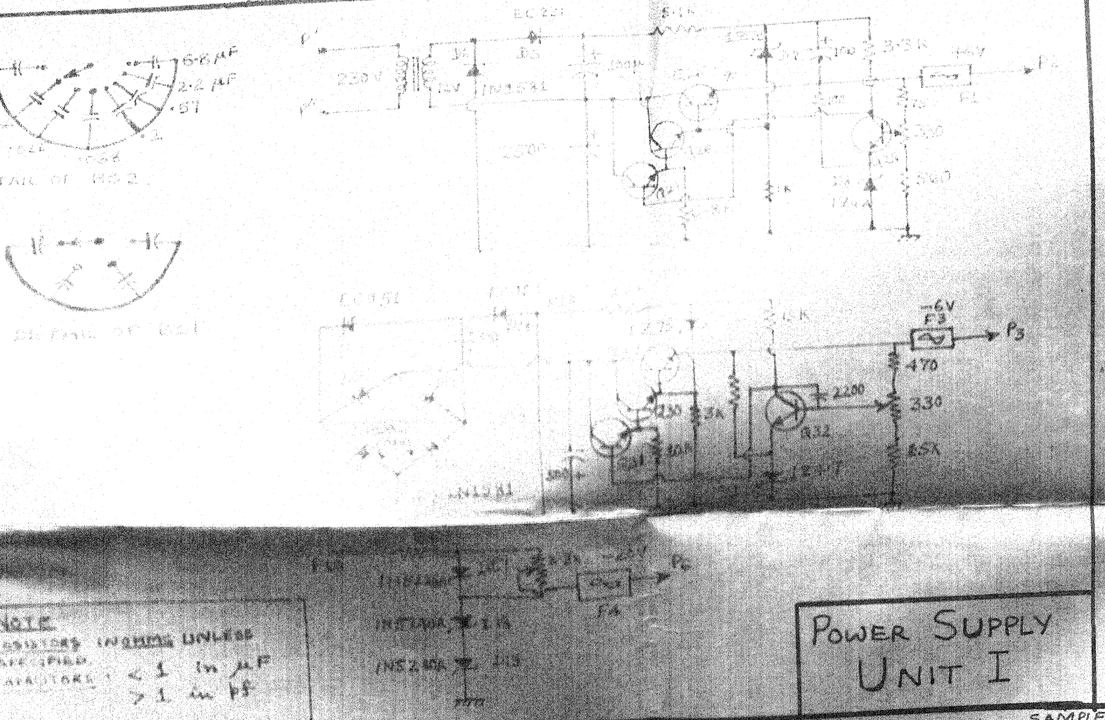

POWER SUPPLY UNIT II

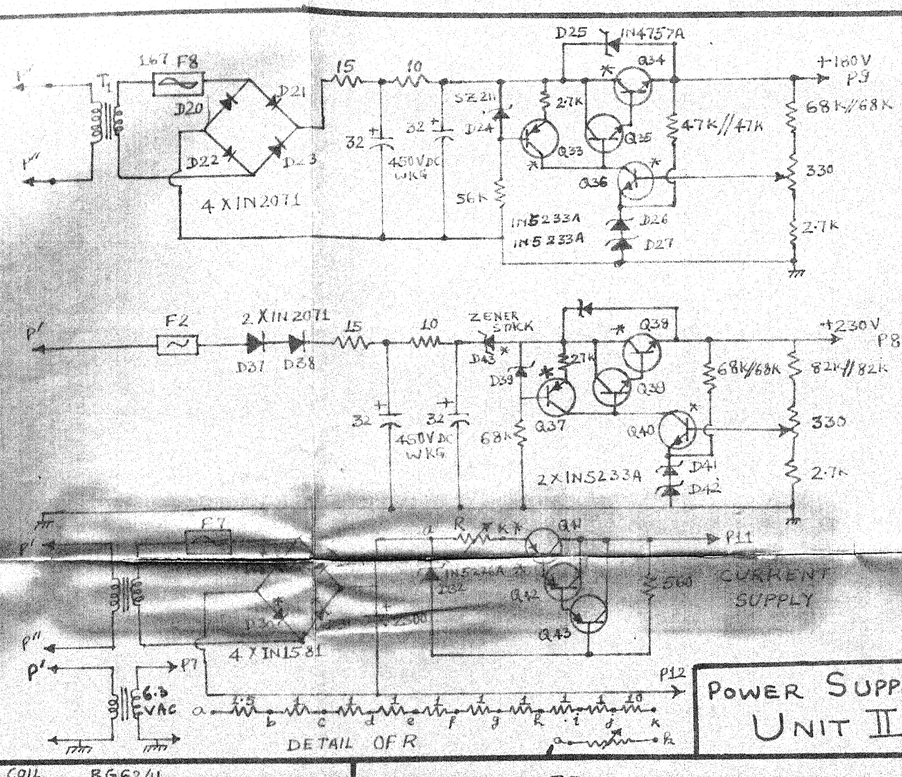

DRIVER STAGE POWER SUPPLY

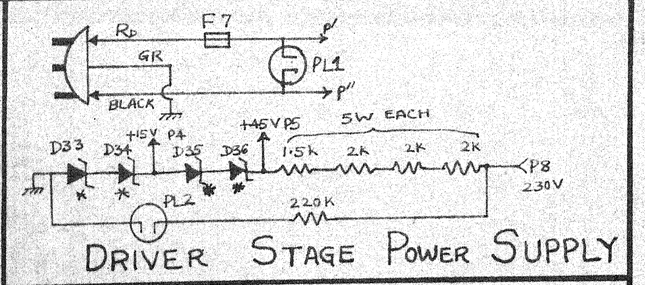

POWER AMP

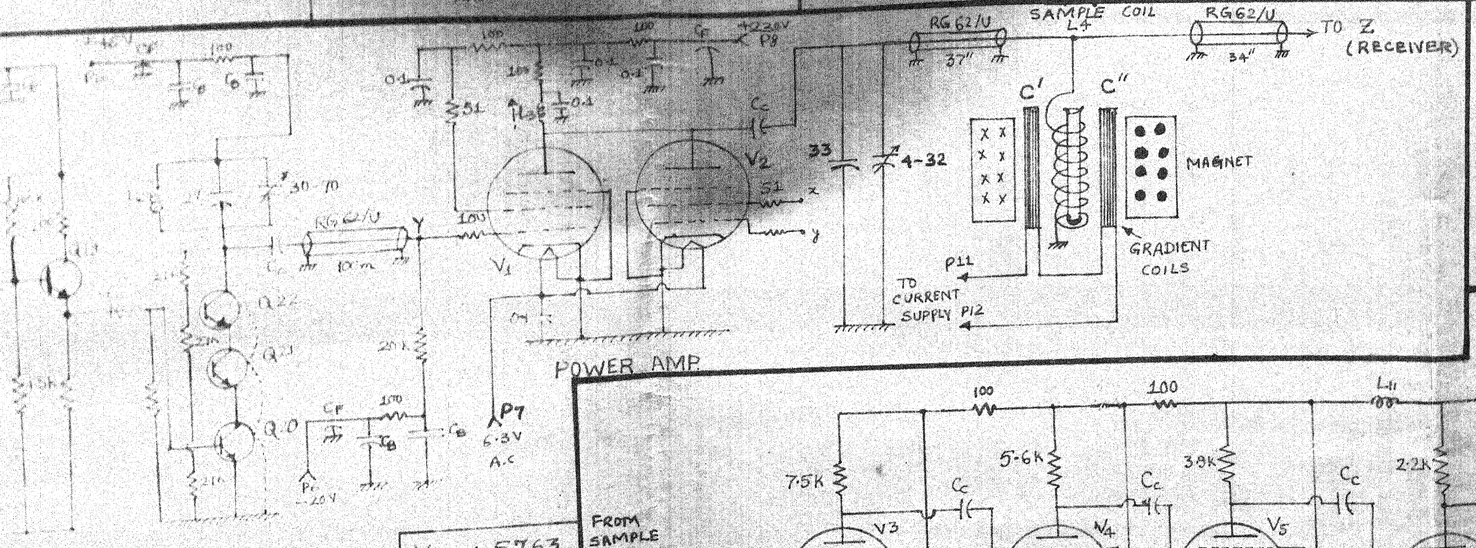

R.F. AMP

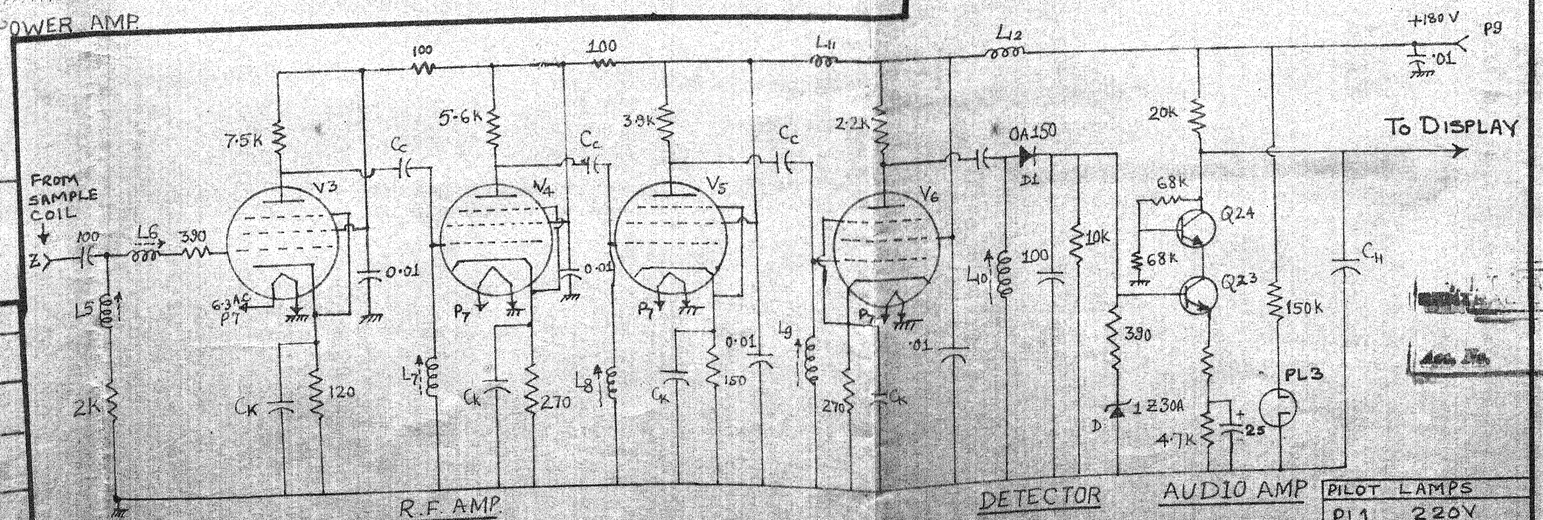

COIL DATA						
L2	L3	L4	L5	L6	L7,8,9,10	L11,12
78	14·1	1	65	70	9·5	5–9
210	33	200	55	55	60	60
12 TURNS	RFC	8 TURNS	–	–	NOMINAL VALUE	MILLER #4505

V1,2 : 5763
V3–V6 : 6AK5

PILOT LAMPS	
PL1	220V
PL2	65V
PL3	65V

RECEIVER

DEPTT OF E.E. IIT/K
M.TECH THESIS
SEP. 1971.

GRINECHO NMR SPECTROMETER